1989

Synthetic approaches to rigid square pyramidal pnictogens and synthesis of new trinuclear cobalt(II) complexes

Ronald Verne Davis
Iowa State University

Recommended Citation

Davis, Ronald Verne, "Synthetic approaches to rigid square pyramidal pnictogens and synthesis of new trinuclear cobalt(II) complexes " (1989). *Retrospective Theses and Dissertations*. 9116.
https://lib.dr.iastate.edu/rtd/9116

INFORMATION TO USERS

The most advanced technology has been used to photograph and reproduce this manuscript from the microfilm master. UMI films the text directly from the original or copy submitted. Thus, some thesis and dissertation copies are in typewriter face, while others may be from any type of computer printer.

The quality of this reproduction is dependent upon the quality of the copy submitted. Broken or indistinct print, colored or poor quality illustrations and photographs, print bleedthrough, substandard margins, and improper alignment can adversely affect reproduction.

In the unlikely event that the author did not send UMI a complete manuscript and there are missing pages, these will be noted. Also, if unauthorized copyright material had to be removed, a note will indicate the deletion.

Oversize materials (e.g., maps, drawings, charts) are reproduced by sectioning the original, beginning at the upper left-hand corner and continuing from left to right in equal sections with small overlaps. Each original is also photographed in one exposure and is included in reduced form at the back of the book. These are also available as one exposure on a standard 35mm slide or as a 17" x 23" black and white photographic print for an additional charge.

Photographs included in the original manuscript have been reproduced xerographically in this copy. Higher quality 6" x 9" black and white photographic prints are available for any photographs or illustrations appearing in this copy for an additional charge. Contact UMI directly to order.

U·M·I

University Microfilms International
A Bell & Howell Information Company
300 North Zeeb Road, Ann Arbor, MI 48106-1346 USA
313/761-4700 800/521-0600

Order Number 9014891

Synthetic approaches to rigid square pyramidal pnictogens and synthesis of new trinuclear cobalt(II) complexes

Davis, Ronald Verne, Ph.D.

Iowa State University, 1989

U·M·I
300 N. Zeeb Rd.
Ann Arbor, MI 48106

Synthetic approaches to rigid square pyramidal pnictogens and synthesis of new trinuclear cobalt(II) complexes

by

Ronald Verne Davis

A Dissertation Submitted to the
Graduate Faculty in Partial Fulfillment of the
Requirements for the Degree of
DOCTOR OF PHILOSOPHY

Department: Chemistry
Major: Inorganic Chemistry

Approved:

In Charge of Major Work

For the Major Department

For the Graduate College

Iowa State University
Ames, Iowa

1989

TABLE OF CONTENTS

DEDICATION

To my Grandpa Van Ness

EXPLANATION OF DISSERTATION FORMAT

This thesis consists of three sections. Each section represents research as it was, or will be, submitted for journal publication. Literature citations, tables and figures pertain only to the sections in which they are included. Preceding the first section is a brief introduction. Following the last section is a general summary.

INTRODUCTION: STATEMENT OF RESEARCH PROJECT

The investigation of species of novel geometry is particularly interesting to chemists. Such systems have the potential to be reaction intermediates or to give insight to little understood reaction pathways. In addition, the preparation of compounds with less common geometries poses a synthetic challenge which may result in the discovery of previously unknown reaction chemistry.

The first goal of this research was to characterize the new trinuclear complexes of the type $[CpCo[P(O)(OMe)_2]_2I]_2Co$ which we had seredipitously discovered. In these complexes the small energy difference between tetrahedral and octahedral cobalt(II) could allow both of these geometries to be present. The weak donor abilities of the iodine could make the formation of tetrahedral species containing uncoordinated iodines more likely.

The second goal of this research was to synthesize new pnictogen species $\underline{1}$ using the carbon backbone of 1,1,2,2-(tetrahydroxymethyl)ethane and its derivatives. In these compounds the restraints placed on the system by the carbon backbone limit the geometries possible for the central pnictogen and make the formation of square pyramidal species more likely.

The general chemistry of the pnictogens predicts that there are two possible coordination types for $\underline{1}$, namely, tricoordinate and pentacoordinate. In the case of

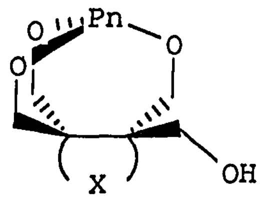

1a

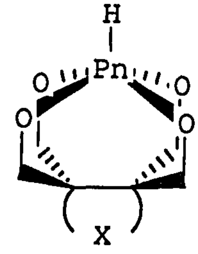

1b

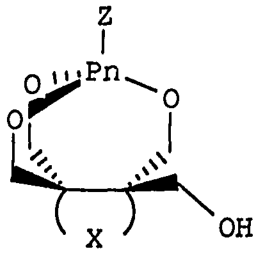

1c

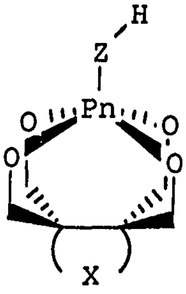

1d

Figure 1. Tricoordinate, tetracoordinate and pentacoordinate pnictogen derivatives of 1,1,2,2-(tetrahydroxymethyl)ethane

tricoordination, the compound contains a pendant alcohol function and the geometry around the pnictogen is tetrahedral (1a). Pentacoordinate pnictogen species normally contain a trigonal bipyrimidal geometry. The carbon backbone of 1, however, precludes the formation of this geometry and square pyrimidal compounds could be formed (1b). The presence of additional substituents on the pnictogen would make it more susceptible to nucleophilic attack, and thus perhaps more readily able to form pentacoordinate species 1d, rather than tetracoordinate compounds 1c. This effect could be enhanced by using electron withdrawing groups to derivatize 1a. Also, the deprotonation of 1a and 1c might also lead to the formation of anionic square pyrimidal pentacoordinate species.

SECTION I. SYNTHESIS OF NEW TRINUCLEAR COBALT(II) COMPLEXES

INTRODUCTION

During the past 15 years much effort has been devoted to investigating the chemistry of tridentate ligands of Type 1 (Cp = C_5H_5, Cp* = C_5Me_5, R = MeO, EtO, PrO, BuO, Me, Et, Pr, Bu).[1] Though these anions are known to react with many main-group reagents,[2] primary interest has centered on their use as ligands in metal complexes because of the unusual ability of 1 to form a variety of essentially substitutionally inert complexes, in spite of the "hard" nature of their ligating oxygens. These ligands act as six-electron donors and form complexes analogous to those formed by cyclopentadienyl derivatives. As with cyclopentadienyls, the potential number of complexes of 1 is large and nearly every transition metal has been shown to form highly stable complexes containing such ligands. In an attempt to prepare more reactive species utilizing a labile halide donor as part of the tridentate framework, Klaui and Buchholz have reported the preparation of metal complexes of anion 2.[3] This anion forms metal complexes that tend to be

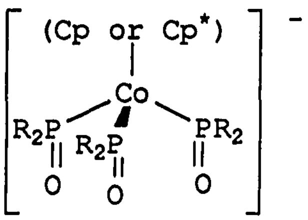

1

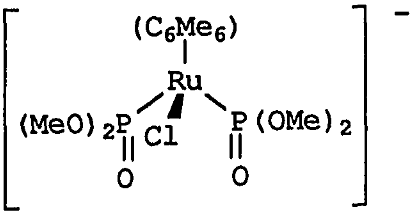

2

more reactive than their anion 1 analogs, but thus far they have shown no sign of any lability of the bridging halide.[4]

Stable complexes of ligands 1 can be broken down into four categories: metal bis-arene analogs, metal carbonyls, oxo metal complexes and organometallic compounds. Many complexes of the first type (i.e., $(\underline{1})_2M^x$) are known (M = Bi^{3+}, Cd^{2+}, Co^{2+}, Cu^{2+}, Fe^{2+}, Fe^{3+}, Ga^{3+}, Mg^{2+}, Ni^{2+}, Pb^{2+}, Sn^{2+})[5] and several have been structurally characterized.[1,5b,6] Here ligand 1 acts as a tris-chelating six-electron donor, in most instances forming an octahedron of phosphoryl oxygens around the central metal atom as shown below. Local octahedral symmetry is not always present in these complexes and, similar to the analogous

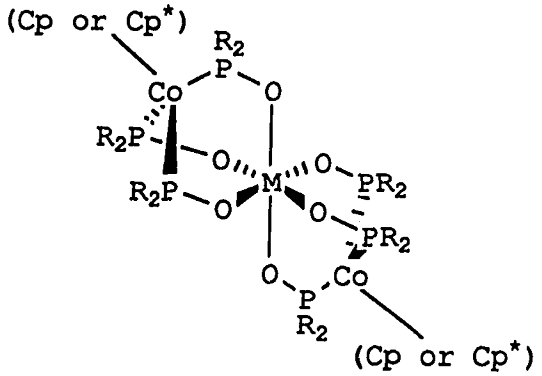

cyclopentadienyl complexes, X-ray structural analysis of both $[CpCo[P(O)(OEt)_2]_3]_2Sn$ and $[CpCo[P(O)(OEt)_2]_3]_2Pb$[5b] indicates the presence of a stereochemically active lone electron pair on the central metal. Metal carbonyl complexes with the formula $[(\underline{1})M(CO)_3]^n$ have been prepared for the Group 6 and Group 7 metals (n = +1, M = Cr, Mo, W; n = 0, M = Mn, Re)[7] and reactions of $[(\underline{1})M(CO)_3]^+$ (M = Cr, Mo, W) with nitrosyl, hydride and trimethyl phosphine demonstrate that, analogously to the cyclopentadienyl analogs, displacement of CO rather than $\underline{1}$ occurs yielding, for example, $[(\underline{1})M(CO)_2(NO)]$, $[(\underline{1})M(CO)(PMe_3)(NO)]$, $[(\underline{1})M(CO)_3H]$, $[(\underline{1})M(CO)_2(PMe_3)H]$ and $[(\underline{1})M(CO)(PMe_3)_2H]$ (M = Cr, Mo, W).[7a] Other stable carbonyl complexes containing $\underline{1}$ include $[(\underline{1})Mo(CO)_3]_2$,[7a] $[(\underline{1})Cu(CO)]$,[1] $[(\underline{1})Rh(\mu\text{-}CO)_3Rh(\underline{1})]$[8] and $[(\underline{1})W(CO)_2]_2$.[9] The last of these compounds contains the W-W quadruply bonded $W_2(CO)_4$ fragment which was previously known only for cyclopentadienyl derivatives. An example of an oxo metal complex of $\underline{1}$ can be found in the recently reported $[CpCo[P(O)(OEt)_2]_3V(O)(acac)]$.[6e] Only a few examples of organometallic complexes containing $\underline{1}$ have been described. Copper alkene and alkyne complexes of $\underline{1}$ have been reported as well as $\eta^5\text{-}C_5H_5Rh(\underline{1})$ and $\eta^6\text{-}C_6H_6Ru(\underline{1})$ but relatively little is known about them.[1] The structure of a metal alkyl complex of $\underline{1}$, $[CpCo[P(O)(OEt)_2]_3PtMe_3]$, has recently appeared in the literature along with a study of this compound's reactivity with $[CPh_3]^+$ and with HCl.[6d] Though rhodium, iridium, ruthenium and osmium cyclopentadienyl analogs of this compound react with $[CPh_3]^+$ to give $[(\eta\text{-}C_nH_n)MH(C_2H_4)(L)]^+$ (n = 5, M = Rh, Ir; n = 6, M = Ru, Os; L = PR_3, CO),[10] the platinum complex of 1 is unreactive to $[Ph_3C^+]$ over long periods of time.

The inert nature of the complexes discussed above has led to the preparation of compounds containing anion 2. Although investigations of the complex chemistry of 2 have been reported only recently, a substantial number of metal compounds containing this ligand have been characterized. Complexes of the type $(2)_2M$ (M = Mg, Zn, Cd, Pb, Al) containing two coordinated 2 anions bound octahedrally to the central metal atom with the halides trans have been isolated from the reaction of the sodium salt of 2 (Na^+2^-) with the appropriate metal halide, sulfate or acetate.[4] Also, the four metal carbonyl complexes (2)CuCO, $(2)Re(CO)_3$, $(2)Mo(CO)_3H$ and $(2)W(CO)_3H$ have been prepared.[4] These complexes are analogous to compounds described above for 1 with the exception that unlike 1, the latter two hydrides of 2 are prepared by oxidative addition reactions of $(\text{solvent})_3M(CO)_3$ with the protonated form of 2. Anion 2 has also been found to form organometallic complexes containing the $Ru(C_6Me_6)$, $Rh(C_5Me_5)$ and Ru(p-cymene) fragments by reaction of Na^+2^- with the appropriate organometallic dihalide dimer.[14] Although these complexes have the potential of containing an uncoordinated halide ligand, no evidence of complexes of this type was detected.

We recently reported the first published example of a structurally characterized complex containing tridentate $[CpCo[P(O)(OMe)_2]_2I]^-$, namely, $[CpCo[P(O)(OMe)_2]_2I]_2Co$ (3).[11] An interesting feature of 3 is that it is in equilibrium with an isolable isomer (4) which contains uncoordinated iodines and a tetrahedral central cobalt(II). As described here, these complexes can be prepared by

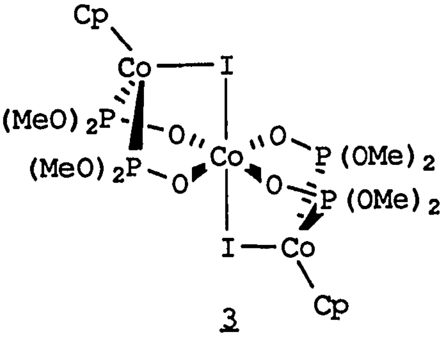

3

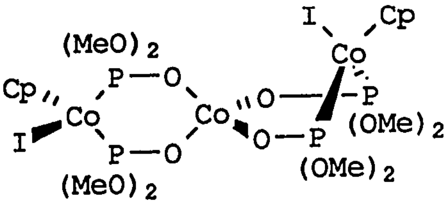

4

several different methods. Also presented here are the synthesis and characterization of the new pentamethylcyclopentadienyl cobalt complexes 5 and 6. These two complexes are the Cp* analogs of the octahedral and tetrahedral complexes 3 and 4, respectively.

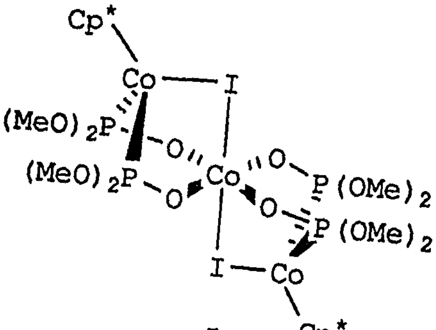

5

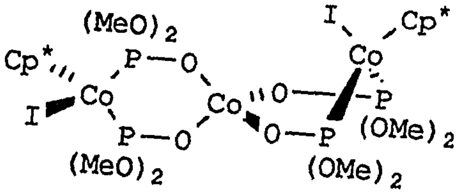

6

EXPERIMENTAL SECTION

Infrared spectra were obtained with NaCl plates on a Perkin-Elmer 681 spectrometer, which was calibrated with polystyrene. Pertinent infrared data for the compounds discussed below are presented in Table 1. Electron paramagnetic resonance (EPR) spectra were recorded on a Bruker ER-200D spectrometer with diphenylpicrylhydrazyl radical as g marker (g = 2.0037) using cylindrical quartz tubes for both microcrystalline samples and for frozen solutions. The EPR data for compounds 3-6 are presented in Table 2. NMR spectra were obtained on Nicolet NT- 300 (^{1}H), Bruker WM-200 (^{13}C) and Bruker WM-300 (^{31}P) instruments at room temperature. Chemical shifts are given in ppm (positive downfield) relative to internal Me_4Si (^{1}H, ^{13}C), and external 85% H_3PO_4 (^{31}P) standards. The ^{1}H NMR, ^{13}C NMR and ^{31}P NMR data for the compounds described below are presented in Tables 3, 4 and 5, respectively. High resolution mass spectra were obtained on a Kratos MS-50 mass spectrometer using electron impact ionization (70 eV).

Magnetic susceptibility measurements on solid samples were performed with a Faraday balance with the use of Bruker Research B-E15 B8 Magnet, a Cahn RG Electrobalance, and a Hewlett-Packard 3465A Digital Multimeter; measurements in solution were obtained on a Nicolet NT-300 spectrometer using concentric NMR tubes.[12]

Preparation of Compounds

Complexes $CpCo(CO)I_2$ (7)[13] and $Cp^*Co(CO)I_2$ (8)[14] were prepared as previously described. All reactions were carried out with strict exclusion of moisture. Solvents were dried by standard methods and distilled before use. Trimethyl phosphite was distilled from sodium and stored under nitrogen. All other chemicals were used as received.

$CpCo[P(OMe)_3]I_2$ (9)

This complex was prepared as previously described.[15] The ^1H NMR spectrum of the crude reaction mixture indicated the presence of a small amount of unreacted purple 7 which was removed by silica gel chromatography using ethyl acetate as the eluent. Complex 9 eluted as the second purple band which gave a dark purple solid upon removal of the solvent under vacuum (m.p. 161-163°C; yield 2.61 g., 68.7%).

$CpCo[P(O)(OMe)_2][P(OMe)_3]I$ (10)

This complex was prepared as described previously,[15] though all attempts to isolate and purify it according to the literature procedure resulted in the decomposition of 10 to 3 and 4 as described below.

$CpCo[P(O)(OMe)_2]_2[P(OMe)_3]$ (11)

Complex 11 was prepared in the manner described by Brill[15] with the exception that it was isolated by silica gel chromatography of the crude reaction mixture using ethyl acetate as the eluent. Pure 11 was isolated upon solvent removal from the brown fraction (yield 0.856 g, 43.8%).

$[CpCo[P(O)(OMe)_2]_2I]_2Co$ (4)

Three routes were found to afford complex 4: a) A solution reported to give 10,[15] prepared from 7 (0.4328 g, 1.066 mmoles) and $P(OMe)_3$ (0.2621 g, 1.056 mmoles), in $CHCl_3$ (15 mL) was immediately placed under dynamic vacuum and the solvent removed. After an additional hour under vacuum the flask was flushed with N_2. This procedure resulted in nearly pure brown solid 4 (yield 0.2791 g, 79.3% based on cobalt). b) A solution of 10, prepared from 7 (0.2832 g, 0.6978 mmoles) and $P(OMe)_3$ (0.1728 g, 1.392 mmoles) in $CHCl_3$ (20 mL) was chromatographed on silica gel using ethyl acetate as the eluent. The brown band was collected and the solvent removed. The resulting brown solid proved to be pure 4 (yield 0.1481 g, 64.0% based on cobalt). c) To a fresh solution of 10, prepared from 7 (1.2576 g, 3.0987 mmoles) and $P(OMe)_3$ (0.7678 g, 6.188 mmoles) in acetone (15 mL), was added CoI_2 (0.4735 g, 1.514 mmoles) under N_2 in one portion. The solution was stirred for one hour and chromatographed on silica gel using ethyl acetate as the eluent. The solvent was removed from the eluate containing the brown band, yielding a brown solid mixture containing 3 and 4 as demonstrated by ^1H and ^{31}P NMR spectroscopy. In all three preparations, recrystallization of the product from CH_2Cl_2/hexane (70/30) produced dark purple crystals of 3 and a small amount of crystalline 4. A typical yield of 4 upon recrystallization and separation from 3 by the Pasteur method was less than 5.0% (m.p. 207-209°C; high resolution MS (EI, 70 eV) m/e Calcd. 996.70859, Found 996.70861(1)).

$[CpCo[P(O)(OMe)_2]_2I]_2Co$ (3)

As described above, complex 3 was isolated from attempts at the recrystallization of 4. A typical yield of 3 from these recrystallizations is 85.9% based on ^1H NMR integration of the products (m.p. 184-186°C; high resolution MS (EI, 70 eV) m/e Calcd. 996.70859, Found 996.70912(5)).

$Cp^*Co[P(OMe)_3]I_2$ (12)

To a stirred solution of $CHCl_3$ (35 mL) containing 8 (1.6693 g, 3.5071 mmoles) was added dropwise under N_2 over a period of 1 hour $P(OMe)_3$ (0.4346 g, 3.502 mmoles). ^1H NMR and ^{31}P NMR spectroscopy of the crude reaction mixture showed the presence of 12 as well as 13 (vide infra). The crude mixture was subjected to silica gel chromatography using ethyl acetate as the eluent. The first fraction was a purple band which was collected and the solvent removed under vacuum. The resulting shiny purple solid proved to be 12 (m.p. 167-168°C; yield 0.727 g, 36.3%; MS (EI, 70 eV) m/e (relative intensity, fragment) 572 (4, M^+), 448 (16, $M^+ - P(OMe)_3$), 445 (29, $M^+ - I$), 321 (100, Cp^*CoI^+)).

$[Cp^*Co[P(O)(OMe)_2]I_2]_2Co$ (13)

In the preparation of complex 12 described above, a second cobalt-containing product, 13, was isolated upon silica gel chromatography using ethyl acetate as the eluent. This complex eluted very slowly with ethyl acetate but was found to elute more easily with ethanol. Upon solvent removal from the brown solution, brown solid 13 was obtained (m.p. 55-57°C; yield 0.853 g, 62.2% based on cobalt; high resolution MS (EI, 70 eV) m/e Calcd. 1172.6639 Found 1172.6659(1.7)).

$Cp^*Co[P(O)(OMe)_2][P(OMe)_3]I$ (14)

This complex could be prepared by two routes: a) To a stirred solution containing $CHCl_3$ (35 mL) and 8 (1.9256 g, 4.0455 mmoles) was added $P(OMe)_3$ (1.0019 g, 8.0749 mmoles) under N_2 over a period of one hour. A ^1H NMR spectrum of the crude reaction mixture contained signals assigned to 12, 13 and 14 as well as unreacted $P(OMe)_3$. The reaction was followed by ^1H NMR spectroscopy and was found to require 120 hours for completion. Silica gel chromatography of the resulting mixture of 13 and 14 with ethyl acetate gave two fractions with the first corresponding to brown 13 and the second corresponding to purple 6. b) $P(OMe)_3$ (0.4545 g, 3.663 mmoles) was added dropwise over a period of one hour to a solution of $CHCl_3$ (35 mL) and 12 (2.0968 g, 3.6654 mmoles) under N_2. The reaction was followed by ^1H NMR spectroscopy and was found to require 48 hours to reach completion. Removal of the solvent under vacuum gave essentially pure brown 14 based on its ^1H and ^{31}P NMR spectra (yield 2.016 g, 99.3%).

$Cp^*Co[P(O)(OMe)_2]_2[P(OMe)_2]$ (15)

This complex was prepared by three routes: a) To a stirred solution of 8 (2.7130 g, 5.6998 mmoles) in $CHCl_3$ (30 mL) was added $P(OMe)_3$ (2.1152 g, 17.047 mmoles) under N_2 over a period of one hour. The reaction was followed by ^1H NMR spectroscopy and was found to require 120 hours to reach completion. The resulting mixture of 13 and 15 was subjected to silica gel chromatography using ethyl acetate as the eluent. The first brown fraction was collected and the solvent removed under vacuum giving brown solid 15 (yield 0.688 g, 22.6%). b) To a solution of 12 (5.3393 g, 9.3337 mmoles) in $CHCl_3$ (35 mL) was added $P(OMe)_3$ (2.3149 g, 18.657 mmoles) over a period of one hour under N_2 with stirring. The reaction was followed by ^1H NMR spectroscopy and was found to require 120 hours to reach completion. The crude product was purified by silica gel chromatography using ethyl acetate as the eluent. The resulting brown fraction was placed under vacuum to remove the solvent giving brown solid 15 (yield 2.111 g, 42.2%). c) To a fresh solution of 14, prepared from 12 (3.2231 g, 5.6343 mmoles) and $P(OMe)_3$ (0.6984 g, 5.629 mmoles), in $CHCl_3$ (35 mL) was added $P(OMe)_3$ (0.6970 g, 5.617 mmoles) dropwise under N_2 with stirring over a period of one hour. The reaction was followed by ^1H NMR spectroscopy and was found to require 120 hours to reach completion. The crude reaction mixture was then subjected to silica gel chromatography using ethyl acetate as the eluent. The solvent was removed under vacuum from the brown fraction yielding solid 15 (yield 1.198 g, 39.7%).

$[Cp^*Co[P(O)(OMe)_2]_2I]_2Co$ (6)

Passage of a solution of pure 14 (2.0118 g, 3.6301 mmoles) in ethyl acetate down a silica gel column using ethyl acetate as the eluent gave a single brown fraction. Removal of the solvent from this fraction under vacuum gave 6 (m.p. > 300°C; yield 1.177 g, 85.5% based on cobalt; high resolution MS (EI, 70 eV) m/e Calcd. 1136.86509, Found 1136.86589(70)).

$[Cp^*Co[P(O)(OMe)_2]_2I]_2Co$ (5)

Recrystallization of complex 6 from CH_2Cl_2/hexane (70/30) produced crystals consisting only of 5 (m.p. 286-88°C; typical yield 96.2%; high resolution MS (EI, 70 eV) m/e Calcd. 1136.86509, Found 1136.86574(60)).

X-ray Diffraction Data for 3, 4, 5 and 9

The same general procedure was used in all four structure determinations. A crystal was mounted on a glass fiber and centered on an Enraf-Nonuis CAD4 diffractometer. Cell dimensions and the orientation matrix were obtained from least-squares refinement using setting angles of 25 reflections in the range 25 < two-theta < 34°. During data collection, three representative reflections were checked every 60 min. as orientation and intensity standards. Since the change in intensity was less than the error in the measurements, no decay correction was applied. Lorentz and polarization corrections were applied to the data, and empirical absorbtion corrections, based on a series of psi-scans, were initially applied to the data. Refinement of the structure was carried out using the SHELX76 package.[16] Scattering factors were obtained from the usual sources.[17]

In all four structures 25 reflections chosen from a rotation photograph were indexed to give the approximate unit cell which subsequent solution of the structure showed to be of a specific symmetry. The structure was solved with the use of over 3000 unique reflections in each case with $I > 2\sigma(I)$.

Structure Solution and Refinement

The positions of the cobalt and iodine atoms were given by direct methods. Following the isotropic refinement of these atoms, the remainder of the nonhydrogen atoms appeared in a difference Fourier map. The hydrogen atoms were not refined individually, but were included in ideal positions "riding" on the appropriate carbon atoms. A common isotropic temperature factor was refined for the methyl hydrogen atoms, and another for the cyclopentadienyl hydrogen atoms. In 4 the hydrogen atoms were not refined. All four structures were refined by use of block-cascade least-squares methods, with anisotropic temperature factors for all nonhydrogen atoms. The crystal data for all four structures are summarized in Table 6. The final positional parameters for the four structures are given in Tables 7, 8, 9 and 10. Selected bond lengths and angles are given in Tables 11, 12, 13 and 14. The ORTEP diagrams of the four structures are presented in Figures 1-4.

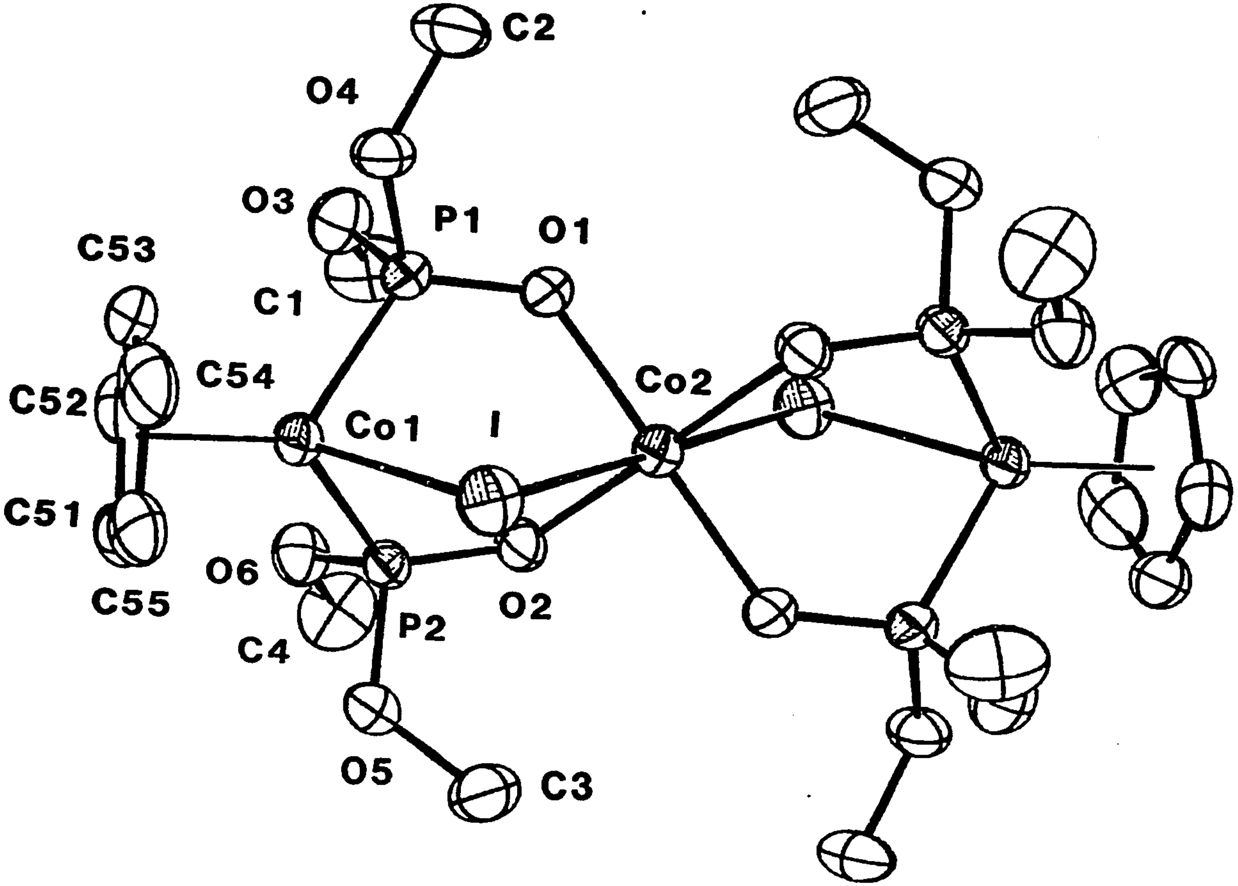

Figure 1. ORTEP drawing of 3, with ellipsoids at the 50% probability level

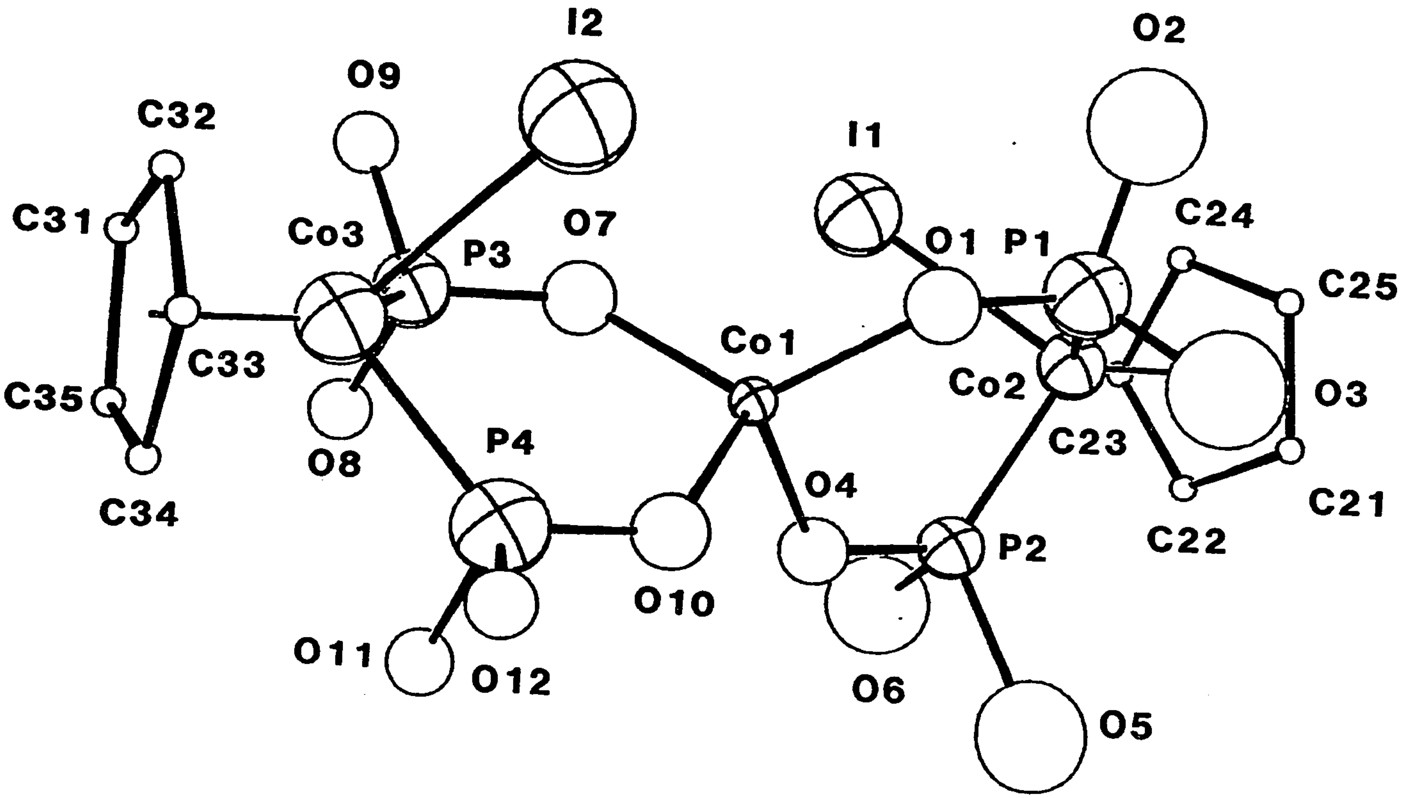

Figure 2. ORTEP drawing of 4, with ellipsoids at the 50% probability level

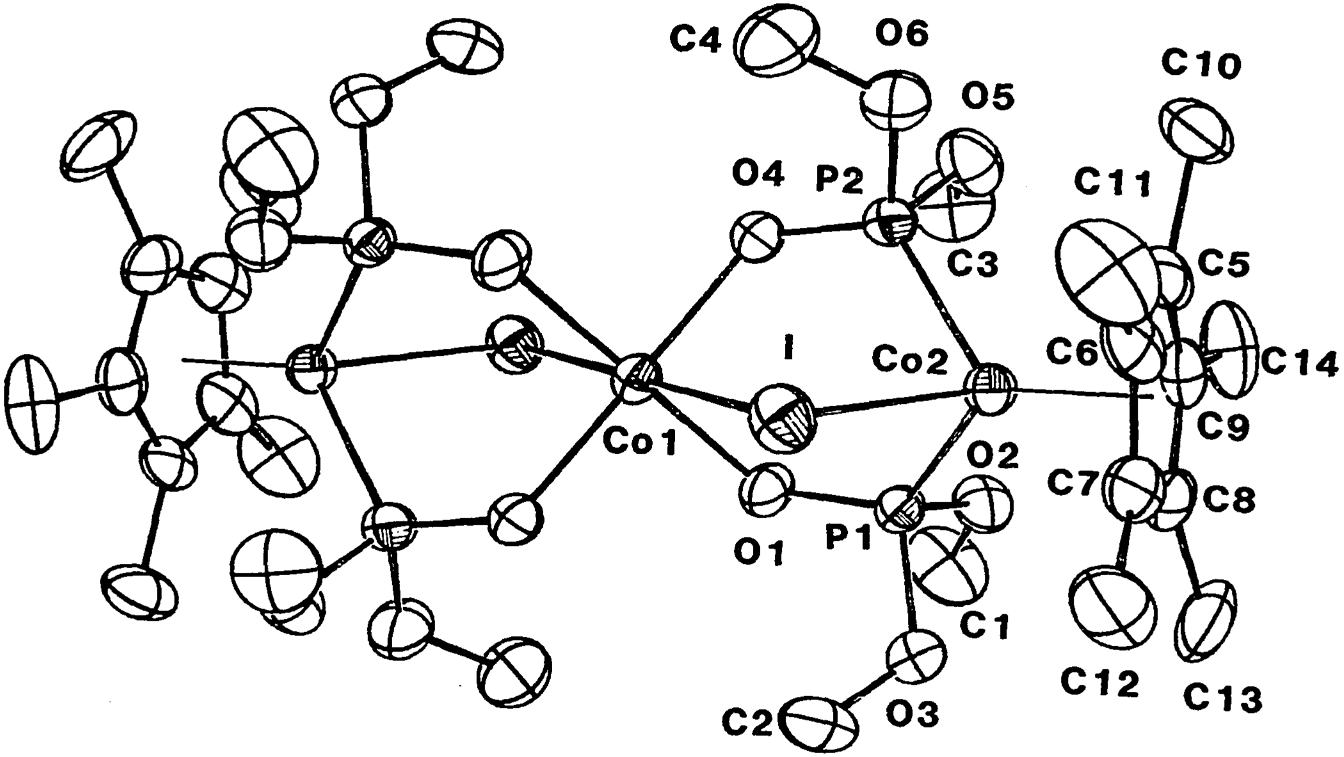

Figure 3. ORTEP drawing of 5, with ellipsoids at the 50% probability level

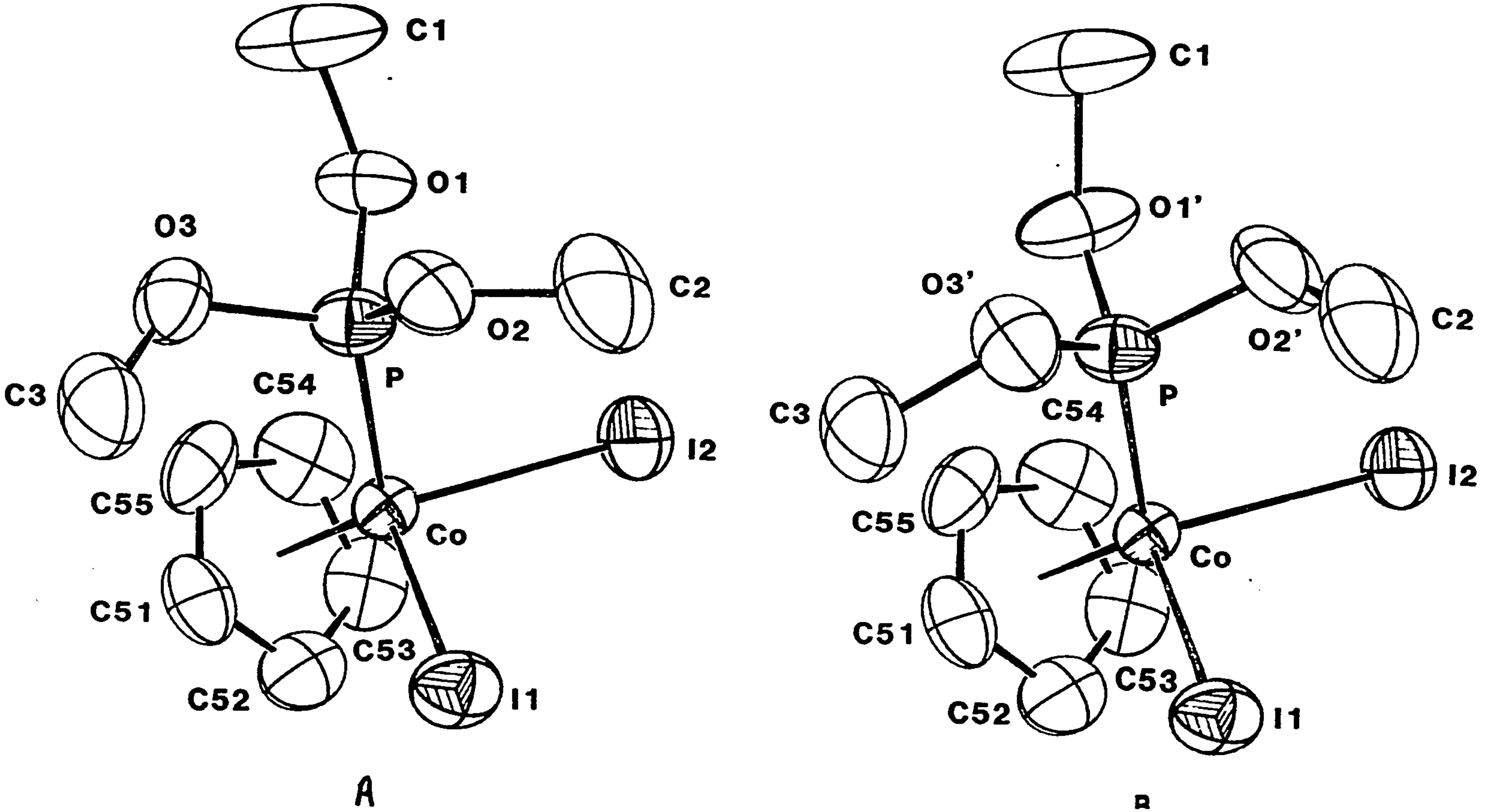

Figure 4. ORTEP drawing of 9, with ellipsoids at the 50% probability level (orientations A and B)

RESULTS AND DISCUSSION

Synthetic Pathways

The reaction of trialkyl phosphites with metal halide complexes to give metal phosphonates has been known for 45 years. This pseudo-Arbuzov reaction, so called because of its similarity to the well-known Michaelis-Arbuzov reaction of organophosphorus chemistry (reaction 1), has been the

$$P(OR)_3 + R'X \longrightarrow P(O)(R')(OR)_2 + RX \qquad (1)$$

subject of study by many investigators. In one such study, Brill found that reaction of $CpCo(CO)I_2$ (7) with one equivalent of $P(OMe)_3$ yields $CpCo[P(OMe)_3]I_2$ (9) (reaction 2) whereas reaction of two equivalents of phosphite with 7

$$\underset{\underline{7}}{CpCo(CO)I_2} + 1P(OMe)_3 \longrightarrow \underset{\underline{9}}{CpCo[P(OMe)_3]I_2} + CO \qquad (2)$$

produces the mixed phosphite-phosphonate complex $CpCo[P(O)(OMe)_2][P(OMe)_3]I$ 10 (reaction 3).[18] Reaction 3 is believed to proceed through the bis-phosphite intermediate

$$\underset{\underline{7}}{\mathrm{CpCo(CO)I_2}} + 2\mathrm{P(OMe)_3} \longrightarrow \underset{\underline{16}}{[\mathrm{CpCo[P(OMe)_3]_2I]^+I^-}}$$

$$\underset{\underline{16}}{[\mathrm{CpCo[P(OMe)_3]_2I]^+I^-}} \xrightarrow{-\mathrm{MeI}} \underset{\underline{10}}{\mathrm{CpCo[P(O)(OMe)_2][P(OMe)_3]I}} \qquad (3)$$

(16) first observed by Klaui and Neukomm.[19] Reaction of three equivalents of trimethyl phosphite with 7 gives the bis-phosphonate complex 11 in reaction 4.[15] The latter

$$\underset{\underline{7}}{\mathrm{CpCo(CO)I_2}} + 3\mathrm{P(OMe)_3} \xrightarrow{-2\mathrm{MeI}} \underset{\underline{11}}{\mathrm{CpCo[P(O)(OMe)_2]_2[P(OMe)_3]}} \qquad (4)$$

complex reacts with $\mathrm{CoCl_2}$ to give the high-spin cobalt(II) complex 17 in reaction 5.[15] Complex 17 contains two

$$\underset{\underline{11}}{\mathrm{CpCo[P(O)(OMe)_2]_2[P(OMe)_3]}} + \mathrm{CoI_2} \xrightarrow{-2\mathrm{MeI}} \underset{\underline{17}}{\mathrm{[CpCo[P(O)(OMe)_2]_3]_2Co}} \qquad (5)$$

tridentate units of 1 facially coordinated to a central cobalt(II).[6a]

In connection with some of our studies of metal phosphite complexes, we had occasion to reexamine the reactions of 7 with $P(OMe)_3$ and found them to be more complicated than previously reported. In agreement with the results of Brill, reaction 2 gives 9 in high yield by a fast reaction which proceeds via displacement of CO. Reaction 3, or reaction of 9 with one equivalent of $P(OMe)_3$, gives 16 which has been isolated from the reaction of $CpCo[P(OMe)_3]_2$ (18)[20] with I_2 at low temperature by Klaui and Neukomm

$$\underset{\underline{18}}{CpCo[P(OMe)_3]_2} + I_2 \longrightarrow \underline{16} \xrightarrow{-MeI} \underline{10} \qquad (6)$$

(reaction 6).[19] This cationic intermediate to 10 was initially detected by us in the reactions reported by Brill, though after a few minutes it quickly disappeared. Complex 16, in which one of the phosphite ligands has displaced an iodide, undergoes nucleophilic attack by I^- on one of the phosphite methyl groups to produce MeI and 10. Klaui and Neukomm[19] succeeded in isolating crystalline 10 at low temperature and Brill reported obtaining essentially pure 10 from the crude reaction mixtures at room temperature by solvent removal.[18] We have been unable to repeat the latter at room temperature either by removal of the solvent under vacuum or by column chromatography of the crude reaction material. In our hands 10 appears to be unstable at room temperature under these conditions and undergoes decomposition to form the trinuclear complex 4 (reaction 7).

$$\underset{\underline{10}}{\mathrm{CpCo[P(O)(OMe)_2][P(OMe)_3]I}} \longrightarrow \underset{\underline{4}}{\mathrm{[CpCo[P(O)(OMe)_2]_2I]_2Co}} \qquad (7)$$

Though the decomposition of complex 10 in solution is slow, we find that a sample of 10 subjected to solvent removal under dynamic vacuum gives the brown air stable complex 4 containing a tetrahedral central cobalt(II). We have also isolated MeI from the reaction mixture, though other products remain unidentified. Our attempts to isolate 10 by chromatography proved ineffective, also producing complex 4 in addition to several organophosphorus product bands. The organophosphorus products $HP(O)(OMe)_2$, $OP(OMe)_3$ and $OP(C_5H_5)(OMe)_2$[21] were isolated chromatographically and identified by their characteristic ^1H and ^{31}P NMR spectra. Studies of the decomposition of 10 to 4 thus far have not proven to be informative since conditions under which intermediates in this decomposition can be observed have not been found. In solution complex 10 slowly forms 4, but only these two species have been detected during the process. In solution the intermediate species are apparently too low in concentration to be seen, possibly because their formation may be very slow in comparison to their reaction to give 4. All attempts to recrystallize 4 gave mainly 3, an isomer of 4 containing an octahedral central cobalt(II), and only a small amount of crystalline 4.

In an attempt to prepare 4 by a different route, reaction of 10 with CoI_2 was found, via ^{31}P NMR spectroscopy, to produce a mixture of trinuclear species including 3 and 4. Chromatography proved inadequate for the separation of these isomers and recrystallization of the mixture gave mainly complex 3 and only a small quantity of 4.

Octahedral complex 3 is a common product in this chemistry and it appears to be the preferred isomer when tetrahedral 4 is recrystallized. Crystals of 3 have also been obtained in the recrystallization of 9. We have studied this slow reaction and believe it proceeds through the pathway presented in Scheme 1. As seen in this scheme, the initial step is phosphite dissociation (perhaps facilitated by substitution of the phosphite ligand by a solvent molecule). The dissociation is necessary since ligand transfer to a second metal atom leads to a product (10) in which two phosphonate groups are bound through their phosphorus atoms to the same cobalt atom (10). Thus the eventual appearance of complex 10 over time in solutions of 9 is a good indication that the initial dissociation occurs.

Scheme 1

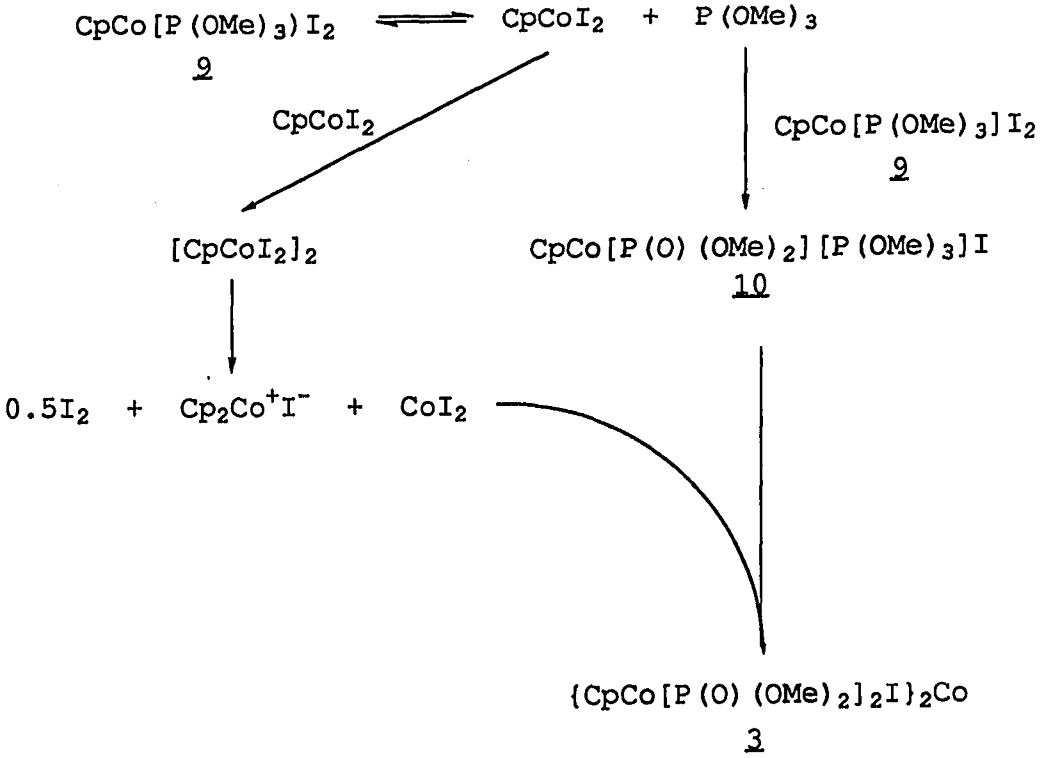
CpCo[P(OMe)3)I2
9
CpCoI2 + P(OMe)3
CpCoI2
CpCo[P(OMe)3]I2
9
[CpCoI2]2
CpCo[P(O)(OMe)2][P(OMe)3]I
10
0.5I2 + Cp2Co+I- + CoI2
{CpCo[P(O)(OMe)2]2I}2Co
3

Similar dissociation reactions are known for a number of metal phosphine complexes.[22] Although such reactions are known to occur in phosphite complexes,[23] free phosphite has not been detected in the decomposition of 9. This is not surprising, though, since the reaction of free P(OMe)$_3$ with 9 proceeds rapidly. The dimeric complex [CpCoI$_2$]$_2$, which may be the other product of the initial step, readily disproportionates in solution to give Cp$_2$Co$^+$I$^-$, I$_2$ and CoI$_2$.[24] Although this dimer was not detected in solution, we did observe its disproportionation product, Cp$_2$Co$^+$I$^-$, in the ^{1}H NMR spectrum of the reaction mixture. As we have shown, the decomposition of complex 10, or its reaction with CoI$_2$ in solution, leads to the formation of crystalline 3 in the final step in Scheme 1.

Reactions of Cp*Co(CO)I$_2$ (8) with P(OMe)$_3$ in most instances give results that parallel those of the Cp complexes. Reaction of 8 with one equivalent of phosphite yields a mixture of 12 as well as 13 in reaction 8. These two compounds can be separated by chromatography to give

Cp*Co(CO)I$_2$ + 1P(OMe)$_3$ ----------
8

Cp*Co[P(OMe)$_3$]I$_2$ + [Cp*Co[P(O)(OMe)$_2$]I$_2$]$_2$Co (8)
12 13

dark purple 12 and brown 13. Attempts to prepare pure 12 under a variety of conditions failed to exclude complex 13 from the products. The new complex 13 is surprisingly unreactive towards $P(OMe)_3$. A mixture of 12 and 13 in the presence of one equivalent of $P(OMe)_3$ gives a mixture containing free phosphite, unreacted 13 and the new complexes 14 and 15 in reaction 9. Integration of the Cp* signals in the ^1H NMR spectrum monitored during the reaction

$$\underline{12} + \underline{13} + 1P(OMe)_3 \longrightarrow \underline{13} + \underset{\underline{14}}{Cp^*Co[P(O)(OMe)_2][P(OMe)_3]I} + \underset{\underline{15}}{Cp^*Co[P(O)(OMe)_2]_2[P(OMe)_3]} \qquad (9)$$

showed that the amount of 13 remained unchanged. The products 14 and 15 of this reaction are also produced by reacting one or two equivalents of phosphite, respectively, with pure 12 (reactions 10 and 11). These

$$\underline{12} + 1P(OMe)_3 \xrightarrow{-MeI} \underline{14} \qquad (10)$$

$$\underline{12} + 2P(OMe)_3 \xrightarrow{-MeI} \underline{15} \qquad (11)$$

syntheses can also be accomplished by the reaction of the carbonyl complex 8 with $P(OMe)_3$, although 13 is always present as a contaminant.

A comparison of the reactivities of the Cp and Cp* complexes described herein is of interest. Similar to 7, displacement of the single carbonyl of 8 with a $P(OMe)_3$ takes only a few minutes. However, though the reaction of $P(OMe)_3$ with 9 is complete within five minutes, the same reaction with 12 takes about two days to reach completion. Reaction times of several days are also found for the reaction of 12 with more than one equivalent of $P(OMe)_3$ (reaction 11) and the reaction of 14 with one equivalent of $P(OMe)_3$ (reaction 12). Complex 14 is apparently much more

$$\underset{\underline{14}}{Cp^*Co[P(O)(OMe)_2][P(OMe)_3]I} + P(OMe)_3 \xrightarrow{-MeI} \underset{\underline{15}}{Cp^*Co[P(O)(OMe)_2]_2[P(OMe)_3]} \tag{12}$$

stable than its Cp analog 10, since we have succeeded in isolating 14 at room temperature. Complex 14 does not decompose under reduced pressure, and removal of solvent from a solution of 14 prepared from pure 12 yields essentially pure 14. Silica gel chromatography of the complex, however, does give the Cp* analog of <u>4</u>, the brown tetrahedral complex $[\mathrm{Cp^*Co[P(O)(OMe)_2]_2I]_2Co}$ (<u>6</u>) (reaction

$$\underset{\underline{14}}{\mathrm{Cp^*Co[P(O)(OMe)_2][P(OMe)_3]I}} \longrightarrow \underset{\underline{6}}{\mathrm{[Cp^*Co[P(O)(OMe)_2]_2I]_2Co}} \qquad (13)$$

13). In this chromatographic treatment the organophosphorus products $\mathrm{OP(OMe)_3}$, $\mathrm{HP(O)(OMe)_2}$, and $\mathrm{(C_5Me_5)P(O)(OMe)_2}$[21] were also eluted and were identified by ^{1}H NMR, ^{13}C NMR and ^{31}P NMR spectroscopy. Attempts to recrystallize <u>6</u> gave only the dark brown octahedral complex <u>5</u>, a structural isomer of <u>6</u>.

The relative stability of complex <u>14</u> compared with <u>10</u> made the study of the decomposition of <u>12</u> to complex <u>6</u> attractive. Since some reactions of the Cp* compounds were found to be much slower and their products more stable towards decomposition than the Cp complexes, it was possible that intermediates in the decomposition of <u>12</u> to <u>6</u> might be observed. Recall that the Cp analog of <u>12</u>, namely <u>9</u>, was observed to decompose to <u>4</u> (Scheme 1). In addition, the stability of $\mathrm{[Cp^*CoI_2]_2}$ (the Cp* analog of $\mathrm{[CpCoI_2]_2}$ in Scheme 1) towards disproportionation made the isolation of this intermediate and a determination of its role in the mechanism a possibility. However, the reaction of complex

12 to form 6 was not observed. This may be due to greater stability of 12 towards dissociation of a phosphite ligand, or to the very slow reaction of free phosphite to displace iodide as might be expected from the slow reactions of 8, 12 and 14 with $P(OMe)_3$.

Spectroscopic Results

The protons of the Cp ligand appear as a singlet at ca. 5.5 ppm. The 15 Cp* protons give rise to a singlet, doublet or triplet at ca. 2 ppm, depending on the number of phosphorus groups bound to the metal. These patterns are found even when chemically inequivalent phosphorus atoms are present, indicating coincidentally equivalent couplings. In some cases such $^4J(PCoCCH)$ couplings are undetectably small. In all of the complexes the OCH_3 protons give rise to signals in the range of 3.5-3.9 ppm and contain $^3J(POCH)$ values of ca. 10 Hz for both phosphite and phosphonate groups. These results parallel those of complexes of 2, for which a series of compounds including the salt $[(C_6Me_6)Ru[P(O)(OMe)_2]_2Cl]^-Na^+$ have recently been reported.[3] In the ruthenium complexes $^4J(PRuCCH)$ is on the order of 2 Hz and $^3J(POCH)$ is ca. 10 Hz for both phosphite and phosphonate-containing compounds. The ^1H NMR spectra of the ruthenium complexes also display "virtual" coupling similar to that found in the cobalt complexes discussed herein. The latter complexes exhibit "virtual" coupling in the OCH_3

signals due to the presence of phosphorus atoms which are strongly coupled to each other as well as to the protons. This is most noticible in the spectra of compounds 3, 4, 5 and 6. As expected, the strength of this type of coupling is dependent on the difference between the chemical shifts of the two phosphorus groups and on the magnitude of their coupling constant.[25] When the ^{31}P NMR signals are widely separated, as in 10 and 14, no virtual coupling is evident and first-order spectra are observed. However, when the two phosphorus atoms are chemically equivalent, as in complexes 3 and 5, the OCH_3 protons appear as "virtually" coupled triplets because of the magnetic inequivalence of the phosphorus atoms. The values of the OCH_3 proton-phosphorus couplings are independent of whether Cp or Cp* is the arene present in the complex, and this is also true of the phosphorus-phosphorus couplings. The ^{31}P NMR data reveal $^{2}J(PCoP)$ values approximately 50 Hz higher for complexes 10 and 14 compared with 11 and 15.

In the IR spectra of the cobalt compounds, the most useful feature is the P==O stretching vibration. This band is very intense and is easily identified in the range of 1260-1070 cm^{-1}. In organic phosphonates the P==O stretch tends to be found toward the high frequency end of this region while coordination of the phosphorus to a metal lowers the stretching frequency considerably.[26] The $_{\nu}$(P==O) values are summarized in Table 1. As is seen in this table, bridging of the phosphonate oxygens to a cobalt atom lowers the stretching frequency even further. Thus in complexes 10 and 14 the P==O stretches appear at 1183 and 1172 cm^{-1}, while in complexes 3, 4, 5, 6 and 13 this band is shifted to 1094-1064 cm^{-1}, nearer to the range of P-O-C stretches (~1025 cm^{-1}).[25] As in the ruthenium complexes mentioned above, this decrease in ν(P==O) represents a lowering of the P-O bond order from two to nearly one in these compounds.

Electron paramagnetic resonance data for compounds 3-6, summarized in Table 2, are indicative of the spin states present in these complexes. For the tetrahedral compound 4, the liquid helium temperature solid state EPR contains resonance band at g = 4.9 showing the eight line hyperfine splitting expected in a (I = 7/2) ^{59}Co system. The additional feature at g = ca. 2.1 is characteristic of tetrahedral high spin Co(II) compounds.[27] In the case of the octahedral complexes, solid state EPR spectra at liquid helium temperatures display resonance bands at g = ca. 4.6 containing the same type of eight-line hyperfine splitting present in the spectra of the tetrahedral complexes discussed above. In the spectra of these octahedral complexes the characteristic resonance band at g = 2.6 is indicative of the octahedral nature of these species.[27] In frozen solution samples of the octahedral species, features of both of these isomers are present in the EPR spectra. The presence of two overlapping eight-line hyperfine splitting patterns is clear in the low field region of the spectra while the resonance bands at $g = 2.6$ and $g = 2.1$ are characteristic of each of the two isomers. These measurements indicate that the tetrahedral form may be favored at lower temperatures.

Magnetic Measurements

Both solid state and $CHCl_3$ solution magnetic susceptibility measurements on the new trinuclear complexes support the conclusions drawn above. Both 4 and 6 have magnetic moments consistent with high-spin tetrahedral cobalt(II). Room temperature magnetic measurements in solution of 4 and 6 yield μ values of 4.85 and 5.01 B.M., respectively. Complex 13 could well be a tetrahedral cobalt(II) complex since its solution magnetic moment was found to be 5.45 B.M. In the case of complexes 3 and 5 the solution magnetic moments are 4.5 and 4.7 B.M. These values are consistent with high-spin octahedrality. This is confirmed by variable temperature solid state measurements in which $\mu = 4.35$ and 4.54 B.M. for 3 and 5, respectively, are observed.

Description of the Structures

In the structure of complex 9, shown in Figure 4, the most notable feature is the disorder of the $P(OMe)_3$ ligand. This ligand exists in two different orientations (A and B) which differ in the relative positions of the oxygen atoms. The two orientations are nearly equally populated (A = 59.4% and B = 40.6%). The conformations of the methoxy groups are the most common found in metal complexes of $P(OMe)_3$.[28] Although there is a great deal of variation among the P-O bond lengths in 9, the two conformations A and B contain similar mean P-O bond distances (1.586(22) Å in A and 1.581(33) Å in B) (Table 14). These values compare well with the similarly oriented $P(OMe)_3$ in the structure of 11, which contains a mean P-O bond length of 1.584(3) Å.[15] The geometry around the metal atom in 9 can be considered pseudo-octahedral with the two iodides and the phosphite ligand occupying one face of the octahedron and the Cp ring the other face. This geometry is common for cobalt(III) cyclopentadienyl complexes and it is supported by the P-Co-I and I-Co-I bond angles which are close to 90° (92.4-96.3°). The Co(III)-I bond lengths (2.5704(6) Å and 2.5717(6) Å) in 9 are in agreement with other cobalt(III) iodide complexes which have been structurally characterized. Thus the cationic complex $[CpCo(dppm)I]^+I^-$ contains a Co(III)-I distance of 2.556(4) Å, slightly shorter than 9, while in

$CpCo[dppm(O)]I_2$ the Co(III)-I distances (2.598(1) Å and 2.572(1) Å) are very similar to those in 9.[29] The Co(III)-I bond lengths in 9 are of particular interest in the examination of the structures of 3, 4 and 5 which follows.

The structure of complex 4, seen in Figure 2, contains two $[CpCo[P(O)(OMe)_2]_2I]^-$ units bound to a central cobalt(II) through four phosphoryl oxygens. The geometry around the central cobalt(II) in this complex is tetrahedral with the two iodines exhibiting no bonding interactions with the central metal atom. The Co(II)-I distances (3.65(1) Å and 3.75(1) Å) are greater than the sum of the van der Waals radii for I^- and Co(II) (~3.5 Å[30]), indicating negligible interaction between these two atoms. The mean Co(II)-O (1.96(12) Å) and P==O (1.53(10) Å) bond lengths are similar to those found in coordinated tridentate phosphonate ligand systems. For example, in the complex $[CpCo[P(O)(OMe)_2]_3]_2Co$ (17), containing two tridentate 1 anions bound facially to a central octahedral cobalt(II), the mean Co(II)-O bond distance is 2.091(28) Å and the mean P==O distance is 1.53 Å.[6b] The central cobalt(II) atom in 4 is in a highly distorted tetrahedron of oxygens as can be seen in the O-Co(II)-O angles and distances in Table 12. Comparison of the Co(III)-I bond lengths of 4 (2.55(2) Å and 2.63(2) Å) with those of 9 shows they are similar to those of 9 and to that in the cationic complex $[CpCo(dppm)I]^+I^-$ (2.556(4)

Å).[28] All other distances found in the structure are normal and compare well with those in the Co(III) complexes mentioned above.

As seen in Figures 3 and 5, complexes 3 and 5 respectively, contain two $[(C_5R_5)Co[P(O)(OMe)_2]_2I]^-$ anions (R = H, Me, respectively) bound to a central cobalt(II), forming an octahedral coordination sphere made up of four phosphoryl oxygens and two trans iodines. In both structures the octahedron around the central cobalt(II) inversion center is distorted owing to a lengthening of the Co(II)-I bonds. The Co(II)-I distances in 3 and 5 (3.0232(2) Å and 3.0241(2) Å, respectively) are midway between the sum of the van der Waals radii (~3.5 Å)[30] and a normal Co(II)-I bond distance (2.76 Å).[30] Despite this elongation, the deviation from octahedral coordination in these compounds is only slight and the angles around the central cobalt(II) in 3 are all within 2.5° of 90°. Complex 5 is somewhat more distorted than 3, although the bond angles around the central cobalt(II) are all within 5° of 90°. This coordination is similar to the unpublished structure of the complex $[Cp^*Ir[P(O)(OMe)_2]_2Cl]_2Cu$ prepared by Werner.[31] Although the interaction of the iodines with the central cobalt(II) atoms of 3 and 5 might be expected to cause some lengthening of the Co(III)-I bonds, this is not significant. The Co(III)-I bond length in 3 (2.5571(5) Å) is shorter than that in 9 while in complex 5 the Co(III)-I length (2.5769(4) Å) is comparable. A comparison of the P==O distances in 3 (1.501(3) Å and 1.506(2) Å) with those of 11 (1.487(2) Å and 1.492(3) Å)[15] shows that the P==O bond lengths are similar within experimental error. This should not necessarily be taken to mean that the P==O bond does not elongate upon coordination to the cobalt(II) because 11 contains water molecules in the crystal which hydrogen bond to the phosphoryl oxygens, probably making them longer than the expected non-coordinated P==O distance. Complex 5 contains slightly longer P==O distances (1.510(2) Å and 1.512(2) Å) than those in 11. An examination of the bond lengths and angles in 3 and 5 shows that in going from the Cp to Cp* analogs no change (within experimental error) occurs around the Co(II). However, in 5 the Co(III)-I bond and both of the Co(III)-P bonds are longer than their counterparts in 3. This is consistent with other complexes such as $(C_5R_5)Co(CO)_2$ wherein a substantial lengthening in the Co-CO bond takes place in going from R = H[32] to R = Me.[33] In 5 this slight distortion probably minimizes steric interactions between the methyl groups of the Cp* and the other three ligands bound to the cobalt(III).

Although 4 could exist as a pair of entantiomers, only one entantiomer appears in the X-ray structure we have determined. Complex 3, on the other hand, can exist as a pair of diastereomers (Figure 5) which differ in the orientation of the $[CpCo[P(O)(OMe)_2]_2I]^-$ chelating units surrounding the central cobalt(II). Only the trans di-iodo octahedral isomer (a in Figure 5) is present in the structure and none of the spectroscopic evidence suggests the presence of the cis di-iodo form in any of the reactions studied.

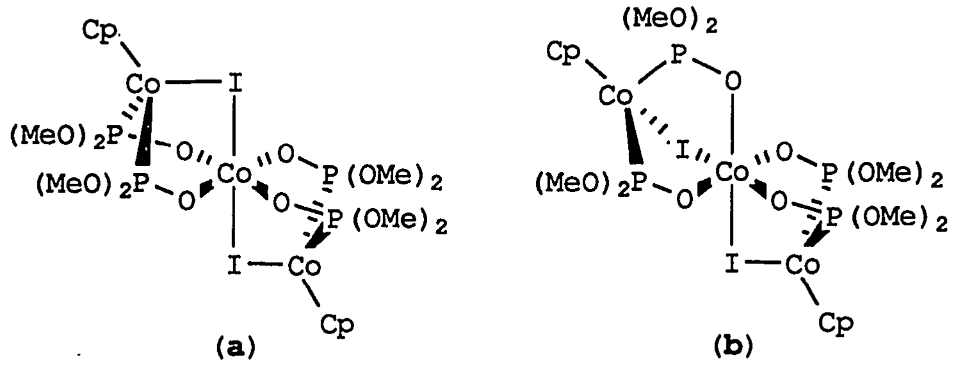

Figure 5. Representation of the two possible diastereomers of <u>3</u>

CONCLUSIONS

It has been shown that several cobalt-phosphonate and cobalt-phosphite complexes readily undergo disproportionation to form stable isomeric trinuclear complexes containing either a tetrahedral or octahedral central cobalt(II). The tetrahedral complexes isomerize to the octahedral form upon recrystallization, allowing the isolation of the first truly isomeric complexes containing octahedral or tetrahedral cobalt(II). Similar results are obtained for both Cp and Cp* complexes. In addition, the octahedral form appears to be more stable in room temperature solutions whereas the tetrahedral form is preferred at low temperatures.

Table 1. IR P==O stretching frequencies (cm^{-1}) for complexes containing complexed phosphoryl groups[a,b]

Compound	ν (P==O)	Reference
$[(C_6H_6)Ru[P(O)(OMe)_2]_2I]^-Na^+$ (2)	1127	4
$[CpCo[P(O)(OMe)_2]_2I]_2Co$ (3)	1070	c
$[CpCo[P(O)(OMe)_2]_2I]_2Co$ (4)	1064	c
$[Cp^*Co[P(O)(OMe)_2]_2I]_2Co$ (5)	1094	c
$[Cp^*Co[P(O)(OMe)_2]_2I]_2Co$ (6)	1081	c
$CpCo[P(O)(OMe)_2][P(OMe)_3]I$ (10)	1183	15
$CpCo[P(O)(OMe)_2]_2[P(OMe)_3]$ (11)	1186	15
$[Cp^*Co[P(O)(OMe)_2]I_2]_2Co$ (13)	1175	c
$Cp^*Co[P(O)(OMe)_2][P(OMe)_3]I$ (14)	1172	c
$Cp^*Co[P(O)(OMe)_2]_2[P(OMe)_3]$ (15)	1176	c
$[CpCo[P(O)(OMe)_2]_3]_2Co$ (17)	1171	6a

[a] Spectra taken in $CHCl_3$ solution.

[b] By comparison, ν(P=O) for $HP(O)(OMe)_2$ is 1260 cm^{-1}.

[c] This work.

Table 2. Electron paramagmetic resonance data for 3-6

	g value	
Compound	Frozen solution[a]	Solid
$[CpCo[P(O)(OMe)_2]_2I]_2Co$ (3)	5.0, 4.6, 2.6, 2.1	4.6, 2.6
$[CpCo[P(O)(OMe)_2]_2I]_2CO$ (4)	5.0, 4.6, 2.6, 2.1	4.9, 2.1
$[Cp^*Co[P(O)(OMe)_2]_2I]_2CO$ (5)		4.6, 2.6
$[Cp^*Co[P(O)(OMe)_2]_2I]_2CO$ (6)		4.9, 2.1

[a] Ethylbenzene.

Table 3. ^1H NMR spectral data (chemical shifts (ppm) and coupling constants (Hz)) for compounds 3-16, 18

Compound	$C_5\underline{H}_5$	$C_5(C\underline{H}_3)_5$ [^4J(PCoCCH)]	$P(O)(OC\underline{H}_3)_2$ [^3J(POCH)]	$P(OC\underline{H}_3)_3$ [^3J (POCH)]	Ref.
$[CpCo[P(O)(OMe)_2]_2I]_2Co$ (3)[a]	5.10s		3.72t[9.50]		b
$[CpCo[P(O)(OMe)_2]_2I]_2Co$ (4)[a]	5.27s		3.83m, 3.74m		b
$[Cp^*Co[P(O)(OMe)_2]_2I]_2Co$ (5)[a]		1.90d[2.59]	3.79t[9.62] 3.55t[10.63]		b
$[Cp^*Co[P(O)(OMe)_2]_2I]_2Co$ (6)[a]		1.74s	3.65t[9.24] 3.57t[10.60]		b
$CpCo(CO)I_2$ (7)	5.65s				13
$Cp^*Co(CO)I_2$ (8)		2.01s			14
$CpCo[P(OMe)_3]I_2$ (9)	5.27s			3.84d[10.49]	15
$CpCo[P(O)(OMe)_2]_2[P(OMe)_3]I$ (10)	5.24s		3.70d[10.54]	3.83d[10.81]	15
$CpCo[P(O)(OMe)_2]_2[P(OMe)_3]$ (11)	5.27s		3.62t[2.10]	3.79d[11.34]	15
$Cp^*Co[P(OMe)_3]I_2$ (12)[a]		1.94d[2.54]		3.81d[9.78]	b
$[Cp^*Co[P(O)(OMe)_2]I_2]_2Co$ (13)[a]		1.98d[1.63]	3.68d[10.48] 3.67d[11.27]		b

---

[a] $CHCl_3$. [b] This work.

Table 3. Continued

Compound	$C_5\underline{H}_5$	$C_5(C\underline{H}_3)_5$ [^4J(PCoCCH)]	$P(O)(OC\underline{H}_3)_2$ [^3J(POCH)]	$P(OC\underline{H}_3)_3$ [^3J (POCH)]	Ref.
Cp*Co[P(O)(OMe)2][P(OMe)$_3$]I (14)[a]		1.95t[2.66]	3.81t[9.87]	3.83d[9.77]	b
Cp*Co[P(O)(OMe)$_2$]$_2$[P(OMe)$_3$] (15)[a]		1.98q[2.57]	3.65t[9.91]	3.81d[9.71]	b
[CpCo[P(OMe)$_3$]$_2$I]$^+$I$^-$ (16)	5.74s			3.96t[11.3]	19
CpCo[P(OMe)$_3$]$_2$ (18)	4.65s			3.50t[11.89]	20

Table 4. ^{13}C NMR spectral data (chemical shifts (ppm) and coupling constants (Hz)) for compounds 3-6, 9-15

Compound	$\underline{C}_5H_5$	$\underline{C}_5(CH_3)_5$	$C_5(\underline{C}H_3)_5$	$P(O\underline{C}H_3)$ $[^2J(POC)]$	$P(O)(O\underline{C}H_3)$ $(^2J(POC)]$
$[CpCo[P(O)(OMe)_2]_2I]_2Co$ (3)[a,c]	89.72s				56.50d[7.07] 55.86d[8.90]
$[CpCo[P(O)(OMe)_2]_2I]_2Co$ (4)[a,c]	88.36s				56.69d[7.23]
$[Cp^*Co[P(O)(OMe)_2]_2I]_2Co$ (5)[a,c]		110.51s	11.11s		54.38d[7.29] 51.24d[8.94]
$[Cp^*Co[P(O)(OMe)_2]_2I]_2Co$ (6)[a,c]		114.72s	11.31s		54.10bs 50.44bs
$CpCo[P(OMe)_3]I_2$ (9)[b]	87.17s			56.53d [8.23]	
$CpCo[P(O)(OMe)_2]_2[P(OMe)_3]I$[b] (10)	89.20s			55.24d [7.61]	52.68d [4.41]
$CpCo[P(O)(OMe)_2]_2[P(OMe)_3]$[b] (11)	90.51s			54.22d [7.86]	51.41 [4.15]
$Cp^*Co[P(OMe)_3]I_2$ (12)[a,c]		91.51s	27.27s	61.70d [9.40]	

---

[a] $CHCl_3$. [b] See reference 18. [c] This work.

Table 4. Continued

Compound	$\underline{C}_5H_5$	$\underline{C}_5(CH_3)_5$	$C_5(\underline{C}H_3)_5$	$P(O\underline{C}H_3)$ $[^2J(POC)]$	$P(O)(O\underline{C}H_3)$ $(^2J(POC)]$
$[Cp^*Co[P(O)(OMe)_2]I_2[_2Co$ (13)^{a,c}		103.07s	10.10s		54.55d[6.93] 52.00d[9.03]
$Cp^*Co[\underline{P}(\underline{O})(OMe)2][P(OMe)_3]I$ (14)^{a,c}		91.17s	10.75s	55.84d [9.01]	52.32d [4.30]
$Cp^*Co[\underline{P}(\underline{O})(OMe)_2]_2[P(OMe)_3]$ (15)^{a,c}		92.06s	11.30s	55.19d [8.86]	51.93d [4.25]

Table 5. ^{31}P NMR spectral data (chemical shifts (ppm) and coupling constants (Hz)) for compounds 3-6, 9-16

Compound	$\underline{P}(OMe)_3$	$\underline{P}(O)(OMe)_2$	$^2J(PCoP)$
$[CpCo[P(O)(OMe)_2]_2I]_2Co$ (3)[a,b]		113.5s	
$[CpCo[P(O)(OMe)_2]_2I]_2Co$ (4)[a,b]		115.1s 111.7s	
$[Cp^*Co[P(O)(OMe)_2]_2I]_2Co$ (5)[a,b]		114.7s	
$[Cp^*Co[P(O)(OMe)_2]_2I]_2Co$ (6)[a,b]		117.8s 111.5s	
$CpCo[P(OMe)_3]I_2$ (9)[c]	132.3s		
$CpCo[P(O)(OMe)_2][P(OMe)_3]I$ (10)[c]	146.1d	89.5d	184.1
$CpCo[P(O)(OMe)_2]_2[P(OMe)_3]$ (11)[c]	149.0t	94.5d	137.5
$Cp^*Co[P(OMe)_3]I_2$ (12)[a]	135.4s		
$[Cp^*Co[P(O)(OMe)_2]I_2]_2Co$ (13)[a,b]		91.3	
$Cp^*Co[P(O)(OMe)_2][P(OMe)_3]I$ (14)[a,b]	147.9d	97.9d	184.7
$Cp^*Co[P(O)(OMe)_2]_2[P(OMe)_3]$ (15)[a,b]	148.7t	96.3d	135.6
$[CpCo[P(OMe)_3]_2I]^+I^-$ (16)[d]	136.0s		

[a] $CHCl_3$.

[b] This work.

[c] See reference 15.

[d] See reference 19.

Table 6. Crystallographic data for (3), (4), (5) and (9)

Compound	(3)	(4)	(5)	(9)
mol wt	996.97	996.97	1137.24	501.91
space group	$P2_{1/n}$	F2dd(no.43)	P1- (no. 2)	$P2_{1/c}$
a, A	8.868(1)	45.877(4)	8.857(2)	7.2025(8)
b, A	15.409(2)	33.046(5)	14.324(2)	25.656(2)
c, A	11.391(1)	8.617(3)	8.829(1)	7.8560(8)
a, deg		90.	100.25(1)	
b, deg	91.92(1)	90.	106.37(1)	105.55(1)
c, deg		90.	98.49(1)	
vol, A_3	1555.7(5)	13064(7)	1034.1(5)	1398.5(5)
d_{calcd}, g/cm^3	2.13	2.027	1.826	2.384
Z	2	16	1	4
lambda	MoK_a	MoK_a	MoK_a	MoK_a
mu, cm^{-1}	37.99	36.189	28.689	56.95
cryst. size,mm	0.2 x 0.3 x 0.5	0.3 x 0.3 x 0.3	0.27 x 0.38 x 0.30	0.2 x 0.4 x 0.5
refl. coll.	+h,±k,±l	+h,±k,±l	+h,±k,±l	+h,±k,±l
no. of refl. coll.	3555	2307	3636	3206
unique data with $F_2 > 2\sigma(F_2)^2$	3128	924	3328	2481

Table 6. Continued

Compound	(3)	(4)	(5)	(9)
2theta range, deg	0-55°	3-45°	4-50°	0-55°
final R, %	2.83	13.7	3.07	2.78
final R_w, %	4.98	18.2	5.37	3.78
GOF[a]	2.86	3.7	1.67	1.149
no. of var.	180	89	227	175
temp	22±1	23±1	22±1	22±1
max. trans factor	0.999	0.9997	1.00	0.999
min. trans factor	0.826	0.7656	0.803	0.721

---

[a] The goodness of fit is defined as $[w(F_o - F_c)^2/(n_o - n_v)]^{1/2}$, where n_o and n_v denote the number of data and variables, respectively.

Table 7. Table of positional parameters for $[CpCo[P(O)(OMe)_2]_2I]_2Co$, <u>3</u>, and their estimated standard deviations

Atom	x	y	z	$B(A^2)^a$
I(1)	0.12808(3)	0.56811(1)	0.27527(2)	3.161(6)
Co(1)	0.15010(5)	0.40767(3)	0.22112(3)	2.292(9)
Co(2)	0.0000	0.5000	0.5000	2.57(1)
P(1)	0.24348(9)	0.37626(5)	0.39544(7)	2.32(1)
P(2)	-0.07864(9)	0.38658(5)	0.27660(6)	2.22(1)
O(1)	0.1737(3)	0.4156(2)	0.5012(2)	2.95(5)
O(2)	-0.1183(3)	0.4126(2)	0.3993(2)	2.61(4)
O(3)	0.2579(3)	0.2736(2)	0.4177(2)	3.59(6)
O(4)	0.4189(3)	0.3996(2)	0.3956(2)	3.02(5)
O(5)	-0.1989(3)	0.4317(2)	0.1867(2)	3.20(5)
O(6)	-0.1157(3)	0.2863(2)	0.2560(2)	3.19(5)
C(1)	0.1373(6)	0.2240(3)	0.4631(5)	5.1(1)
C(2)	0.5088(4)	0.3893(3)	0.5042(4)	3.95(8)
C(3)	-0.2982(5)	0.4983(3)	0.2268(3)	3.92(8)
C(4)	-0.2561(6)	0.2506(3)	0.2930(5)	5.2(1)
C(51)	0.0934(4)	0.3506(3)	0.0591(3)	3.50(8)
C(52)	0.1900(5)	0.2962(3)	0.1298(3)	3.94(8)
C(53)	0.3284(5)	0.3417(4)	0.1479(4)	4.6(1)
C(54)	0.3144(5)	0.4230(4)	0.0956(4)	4.8(1)
C(55)	0.1676(5)	0.4289(3)	0.0386(3)	4.00(9)

[a] Anisotropically refined atoms are given in the form of the isotropic equivalent displacement parameter defined as: $(4/3) * [a2*B(1,1) + bc*B(2,2) + c^2*B(3,3) + ab(\cos \gamma)*B(1,2) + ac(\cos \beta)*B(1,3) + bc(\cos \alpha)*B(2,3)]$.

Table 8. Table of positional parameters for [CpCo[P(O)(OMe)$_2$]$_2$I]$_2$Co, <u>4</u>, and their estimated standard deviations

Atom	x	y	z	B(A^2)
I(1)	0.1182(2)	0.2803(2)	0.000	6.9(2)
I(2)	0.0473(2)	0.4376(3)	0.047(2)	8.1(3)
Co(1)	0.1374(3)	0.2768(3)	0.277(2)	4.1(3)
Co(2)	0.0639(2)	0.3365(3)	0.223(2)	1.7(2)
Co(3)	-0.0022(3)	0.3975(4)	0.044(2)	5.5(4)
P(1)	0.1308(6)	0.3409(9)	0.304(4)	5.8(8)
P(2)	0.0956(5)	0.2611(8)	0.376(4)	3.7(6)
P(3)	0.0182(5)	0.3477(8)	-0.045(4)	4.4(6)
P(4)	0.0036(7)	0.3798(9)	0.283(5)	6.5(8)
O(1)	0.101(1)	0.360(2)	0.267(8)	4.2(7)
O(2)	0.154(2)	0.369(2)	0.21(1)	10(1)
O(3)	0.138(2)	0.353(3)	0.48(1)	10(1)
O(4)	0.067(1)	0.281(2)	0.327(7)	4.2(7)
O(5)	0.088(2)	0.252(3)	0.60(1)	10(1)
O(6)	0.085(2)	0.213(3)	0.34(1)	10(1)
O(7)	0.047(1)	0.333(1)	0.026(8)	4.2(7)
O(8)	-0.002(1)	0.312(1)	-0.026(7)	3.0(6)
O(9)	0.026(1)	0.353(1)	-0.211(7)	3.0(6)
O(10)	0.031(1)	0.364(2)	0.345(7)	4.2(7)
O(11)	-0.018(1)	0.338(1)	0.307(7)	3.0(6)
O(12)	-0.007(1)	0.410(1)	0.395(7)	3.0(6)
C(21)	0.169(2)	0.264(2)	0.471(7)	5(1)
C(22)	0.154(2)	0.229(2)	0.412(7)	5(1)
C(23)	0.159(2)	0.227(2)	0.250(7)	5(1)
C(24)	0.177(2)	0.261(2)	0.209(7)	5(1)
C(25)	0.183(2)	0.283(2)	0.345(7)	5(1)
C(31)	-0.027(2)	0.401(2)	-0.139(8)	6(1)

Table 8. Continued

Atom	x	y	z	B(A2)
C(32)	-0.018(2)	0.440(2)	-0.090(8)	6(1)
C(33)	-0.030(2)	0.447(2)	0.061(8)	6(1)
C(34)	-0.045(2)	0.412(2)	0.106(8)	6(1)
C(35)	-0.044(2)	0.384(2)	-0.018(8)	6(1)

Table 9. Table of positional parameters for $[Cp^*Co[P(O)(OMe)_2]_2I]_2Co$, 5, and their estimated standard deviations

Atom	x	y	z	B(A^2)[a]
I	-0.16842(3)	-0.17505(2)	0.08055(3)	3.359(6)
Co(1)	0.0000	0.0000	0.0000	2.72(1)
Co(2)	-0.21443(5)	-0.26184(3)	-0.21556(5)	2.341(9)
P(1)	-0.2854(1)	-0.13423(7)	-0.2940(1)	2.42(2)
P(2)	0.0402(1)	-0.20339(7)	-0.1763(1)	2.69(2)
O(1)	-0.1846(3)	-0.0343(2)	-0.2080(3)	3.07(6)
O(2)	-0.3070(3)	-0.1504(2)	-0.4829(3)	3.35(6)
O(3)	-0.4680(3)	-0.1281(2)	-0.3004(4)	3.66(6)
O(4)	0.1067(3)	-0.0959(2)	-0.1069(3)	3.19(6)
O(5)	0.0947(3)	-0.2344(2)	-0.3328(3)	4.06(7)
O(6)	0.1479(4)	-0.2618(2)	-0.0664(4)	4.41(7)
C(1)	-0.3533(7)	-0.0757(4)	-0.5688(6)	5.7(1)
C(2)	-0.5003(5)	-0.0758(4)	-0.1653(6)	4.6(1)
C(3)	0.0837(6)	-0.1742(4)	-0.4485(5)	5.2(1)
C(4)	0.2545(6)	-0.2179(5)	0.0958(6)	5.8(1)
C(5)	-0.1904(4)	-0.4047(3)	-0.2959(5)	3.17(8)
C(6)	-0.2627(5)	-0.4025(3)	-0.1747(5)	3.54(9)
C(7)	-0.4112(5)	-0.3698(3)	-0.2264(5)	3.64(9)
C(8)	-0.4285(5)	-0.3546(3)	-0.3825(6)	3.9(1)
C(9)	-0.2883(5)	-0.3723(3)	-0.4250(5)	3.30(8)

---

[a] Anisotropically refined atoms are given in the form of the isotropic equivalent displacement parameter defined as: (4/3) * [a^2*B(1,1) + b^2*B(2,2) + c^2*B(3,3) + ab(cos gamma)*B(1,2) + ac(cos beta)*B(1,3) + bc(cos alpha)*B(2,3)].

Table 9. Continued

Atom	x	y	z	B(A^2)[a]
C(10)	-0.0441(5)	-0.4490(3)	-0.3003(7)	4.9(1)
C(11)	-0.1978(8)	-0.4354(4)	-0.0197(6)	6.1(1)
C(12)	-0.5323(6)	-0.3625(4)	-0.1391(7)	6.5(1)
C(13)	-0.5772(6)	-0.3362(4)	-0.4970(8)	6.7(1)
C(14)	-0.2684(7)	-0.3730(4)	-0.5880(5)	5.4(1)

Table 10. Table of positional parameters for CpCo[P(OMe)$_3$]I$_2$, 9, and their estimated standard deviations

Atom	x	y	z	B(A_2)[a]
Co	0.27308(7)	0.40299(2)	0.17110(6)	2.85(1)
I(1)	0.11458(5)	0.45014(1)	0.38461(4)	4.184(9)
I(2)	-0.01378(5)	0.34294(1)	0.03345(5)	4.976(9)
P	0.4072(2)	0.34520(4)	0.3651(2)	3.58(2)
O(1)	0.461(2)	0.2955(6)	0.278(2)	4.6(2)
O(2)	0.3337(8)	0.3289(2)	0.5263(7)	4.1(1)
O(3)	0.6285(8)	0.3627(3)	0.4771(8)	4.4(1)
O(1')	0.520(3)	0.307(1)	0.274(4)	6.4(6)
O(2')	0.261(1)	0.3002(4)	0.416(1)	5.5(3)
O(3')	0.523(1)	0.3584(4)	0.550(1)	4.9(2)
C(1)	0.595(1)	0.2563(3)	0.369(1)	8.9(3)
C(2)	0.142(1)	0.3084(3)	0.515(1)	6.6(2)
C(3)	0.6533(9)	0.4050(3)	0.5943(8)	5.8(1)
C(51)	0.4621(9)	0.4624(2)	0.1689(8)	5.0(1)
C(52)	0.2904(8)	0.4748(2)	0.0466(8)	5.3(1)
C(53)	0.2479(9)	0.4359(3)	-0.0785(7)	5.5(1)
C(54)	0.400(1)	0.3984(3)	-0.0344(8)	6.3(2)
C(55)	0.5324(7)	0.4161(3)	0.1189(8)	5.3(1)

---

[a] Anisotropically refined atoms are given in the form of the isotropic equivalent displacement parameter defined as: (4/3) * [a^2*B(1,1) + b^2*B(2,2) + c^2*B(3,3) +ab(cos gamma)*B(1,2) + ac(cos beta)*B(1,3) +bc(cos alpha)*B(2,3)].

Table 11. Selected bond distances and angles in $[CpCo[P(O)(OMe)_2]_2I]_2Co$, 3

Bond distances (Å)[a]

Co(1)-I	2.5571(5)	Co(1)-P(1)	2.1801(9)
Co(2)-I	3.0232(2)	Co(1)-P(2)	2.1692(9)
Co(2)-O(1)	2.015(2)	P(1)-O(1)	1.501(3)
Co(2)-O(2)	2.037(2)	P(2)-O(2)	1.506(2)

Bond angles (°)[a]

I-Co(2)-I	180.(0)	I-Co(1)-P(1)	91.41(3)
Co(1)-I-Co(2)	84.41(1)	I-Co(1)-P(2)	89.70(3)
O(1)-Co(2)-O(1)	180.0(0)	P(1)-Co(1)-P(2)	91.82(3)
O(1)-Co(2)-O(2)	87.49(9)	Co(1)-P(1)-O(1)	119.2(1)
O(2)-Co(2)-O(2)	180.0(0)	Co(1)-P(2)-O(2)	118.7(1)
Co(2)-O(1)-P(1)	126.2(1)		

[a] Numbers in parentheses are estimated standard deviations in the least significant digits.

Table 12. Selected bond distances and angles in $[CpCo[P(O)(OMe)_2]_2I]_2Co$, 4

Bond distances (Å)[a]

I(1)-Co(1)	2.55(2)	Co(1)-P(1)	2.15(3)
I(1)-Co(2)	3.65(1)	Co(1)-P(2)	2.16(3)
I(2)-Co(2)	3.75(1)	Co(3)-P(3)	2.04(3)
I(2)-Co(3)	2.63(2)	Co(3)-P(4)	2.16(5)
Co(2)-O(1)	1.89(5)	P(1)-O(1)	1.56(6)
Co(2)-O(4)	2.06(6)	P(2)-O(4)	1.52(6)
Co(2)-O(7)	1.87(7)	P(3)-O(7)	1.55(6)
Co(2)-O(10)	2.04(3)	P(4)-O(10)	1.48(6)

Bond angles (°)[a]

I(1)-Co(1)-P(1)	90.(1)	O(1)-Co(2)-O(4)	103.(2)
I(1)-Co(1)-P(2)	94.(1)	O(1)-Co(2)-O(7)	124.(3)
P(1)-Co(1)-P(2)	94.(1)	O(1)-Co(2)-O(10)	111.(2)
I(2)-Co(3)-P(3)	90.7(8)	O(4)-Co(2)-O(7)	112.(2)
I(2)-Co(3)-P(4)	91.(1)	O(4)-Co(2)-O(10)	103.(2)
P(3)-Co(3)-P(4)	95.(1)	O(7)-Co(2)-O(10)	101.(2)
Co(2)-O(1)-P(1)	131.(3)	Co(1)-P(1)-O(1)	121.(3)
Co(2)-O(4)-P(2)	124.(3)	Co(1)-P(2)-O(4)	124.(3)
Co(2)-O(7)-P(3)	134.(4)	Co(3)-P(3)-O(7)	120.(3)
Co(2)-O(10)-P(4)	127.(4)	Co(3)-P(4)-O(10)	123.(3)

[a] Numbers in parentheses are estimated standard deviations in the least significant digits.

Table 13. Selected bond distances and angles in [Cp*Co[P(O)(OMe)$_2$]$_2$I]$_2$Co, 5

Bond distances (Å)[a]

I-Co(1)	3.0241(2)	Co(2)-P(1)	2.1815(8)
I-Co(2)	2.5769(4)	Co(2)-P(2)	2.1926(8)
Co(1)-O(1)	2.009(2)	P(1)-O(1)	1.510(2)
Co(1)-O(4)	2.023(2)	P(2)-O(4)	1.512(2)

Bond angles (°)[a]

Co(1)-I-Co(2)	85.694(9)	O(1)-Co(1)-O(4')	91.74(8)
I-Co(1)-I'	180.(0)	I-Co(2)-P(1)	89.42(2)
I-Co(1)-O(1)	85.78(6)	I-Co(2)-P(2)	87.61(2)
I-Co(1)-O(1')	94.22(6)	P(1)-Co(2)-P(2)	92.00(3)
I-Co(1)-O(4)	84.59(6)	Co(2)-P(1)-O(1)	120.27(8)
I-Co(1)-O(4')	95.41(6)	Co(2)-P(2)-O(4)	119.07(8)
O(1)-Co(1)-O(1')	180.(0)	Co(1)-O(1)-P(1)	126.4(1)
O(1)-Co(1)-O(4)	88.26(8)	Co(1)-O(4)-P(2)	126.8(1)

[a] Numbers in parentheses are estimated standard deviations in the least significant digits.

Table 14. Selected bond lengths and angles in $CpCo[P(OMe)_3]I_2$, 9

Bond distances (Å)[a]			
Co-I(1)	2.5704(6)	O(3)-P	1.663(6)
Co-I(2)	2.5717(6)	O(1')-P	1.663(6)
Co-P	2.160(1)	O(2')-P	1.68(1)
O(1)-P	1.54(2)	O(3')-P	1.504(8)
O(2)-P	1.555(6)		

Bond angles (°)[a]			
I(1)-Co-I(2)	96.26(2)	O(2)-P-O(3)	97.4(3)
I(1)-Co-P	93.18(4)	Co-P-O(1')	107.(7)
I(2)-Co-P	92.43(4)	Co-P-O(2')	116.7(3)
Co-P-O(1)	111.9(6)	Co-P-O(3')	123.6(4)
Co-P-O(2)	125.0(2)	O(1')-P-O(2')	96.(1)
Co-P-O(3)	111.8(2)	O(1')-P-O(3')	111.1(9)
O(1)-P-O(2)	108.5(7)	O(2')-P-O(3')	98.2(5)
O(2)-P-O(3)	97.4(3)		

[a] Numbers in parentheses are estimated standard deviations in the least significant digits.

REFERENCES

1. Klaui, W.; Lenders, B.; Hessner, B.; Evertz, K. Organometallics 1988, 7, 1357.
2. Klaui, W. Z. Naturforschung. B. 1979, 34, 1403.
3. Klaui, W.; Buchholz, E. Angew. Chem. 1988, 100, 603.
4. Klaui, W.; Buchholz, E. Inorg. Chem. 1988, 27, 3500.
5. a) Klaui, W.; Otto, H.; Eberspach, W.; Buchholz, E. Chem. Ber. 1982, 115(5), 1922.
   b) Holt, E. M.; Klaui, W.; Zuckermann, J. J. J. Organomet. Chem. 1987, 335, 29.
   c) Klaui, W.; Muller, A.; Eberspach, W.; Boese, R.; Goldberg, I. J. Am. Chem. Soc. 1987, 109, 164.
6. a) Harder, V.; Dubler, E.; Werner, H. J. Organomet. Chem. 1974, 71, 427.
   b) Dubler, E.; Linowsky, L.; Klaui, W. Trans. Met. Chem. 1979, 4, 191.
   c) Klaui, W.; Muller, A.; Eberspach, W.; Boese, R.; Goldberg, I. J. Am. Chem. Soc. 1987, 109, 164.
   d) Nettle, A.; Valderrama, M.; Contreras, R.; Scotti, M.; Peters, K.; von Schering, H.; Werner, H. Polyhedron 1988, 7, 2095.
   e) Roman, E.; Tapia, F.; Berrera, M.; Garland, M.; Maroville, J.; Gianotti, C. J. Organomet. Chem. 1985, 297, C8.

7. a) Klaui, W.; Muller, A.; Scotti, M. J. Organomet. Chem. 1983, 253, 45.
   b) Klaui, W.; Okuda, J.; Scotti, M.; Valderrama, M.; J. Organomet. Chem. 1985, 280, C26.
8. Klaui, W.; Scotti, M.; Valderrama, M.; Rojas, S.; Sheldrick, G. M.; Jones, P. G.; Schroeder, T. Angew. Chem. 1985, 97, 697.
9. Klaui, W.; Muller, A.; Herbst, R.; Egert, E. Organometallics 1987, 6, 1824.
10. a) Kletzin, H.; Werner, H.; Serhadi, O.; Ziegler, M. L. Angew. Chem. 1983, 95, 49.
    b) Werner, H.; Kletzin, H.; Holn, A.; Paul, W.; Knaup, W.; Ziegler, M. L.; Serhadi, O. J. Organomet. Chem. 1986, 306, 227.
    c) Roder, K.; Werner, H. Angew. Chem. 1987, 99, 719.
11. Davis, R. V.; Verkade, J. G., submitted for publication in Organometallics.
12. a) Reilly, C. A.; McConnell, H. M.; Meisenheimer, R. G. Phys. Rev. 1955, 98, 264.
    b) Klein, M. P.; Holder, B. E. Phys. Rev. 1955, 98, 265.
    c) Evans, D. F. J. Chem. Soc. 1959, 2003.
    d) Bartle, K. D.; Jones, D. W.; Maricic, S. Croat. Chem. Acta 1968, 40, 227.
13. King, R. Inorg. Chem. 1966, 5, 82.

14. Frith, S. A.; Spencer, J. L. Inorg. Syn. 1985, 23, 15.

15. Towle, D. K.; Landon, S. J.; Brill, T. B.; Tulip, T. H. Organometallics 1982, 1, 295.

16. Sheldrick, G. M. In "Computing in Crystallography"; Schenk, H.; Olthof-Hazekamp, R.; Van Koningsveld, H.; Bassi, G. C., Eds.; Delft University: Delft, 1978.

17. Cromer, D. T.; Waber, J. T. "International Tables for X-ray Crystallography;" Kynoch: Birmingham, England, 1974; Vol. IV.

18. Schleman, E. V.; Brill, T. B. J. Organomet. Chem. 1987, 323(1), 103.

19. Klaui, W.; Neukomm, H. Org. Mag. Reson. 1977, 10, 126.

20. Harder, V.; Muller, J.; Werner, H. Helv. Chim. Acta 1971, 54, 1.

21. Macomber, R. S.; Kennedy, E. R. J. Org. Chem. 1976, 41, 3191.

22. Pignolet, L. H., ed. "Homogeneous Catalysis with Metal Phosphine Complexes"; Plenum: New York, 1983.

23. Parshall, G. W. "Homogeneous Catalysis"; John Wiley & Sons: New York, 1980.

24. Roe, D. M.; Maitlis, P. M. J. Chem. Soc., A. 1971, 3173.

25. Musher, J. I.; Corey, E. J. Tetrahedron 1962, 18, 791.

26. Thomas, L. C. "Interpretation of the Infrared Spectra of Organophosphorus Compounds"; Heyden: London, 1974.

27. Banci, L.; Bencini, A.; Benelli, C.; Gatteschi, D.; Zanchini, C. Structure and Bonding 1982, 52, 37.

28. Bart, J. C. J.; Favini, G.; Todeschini, R. Phosphorus and Sulfur 1983, 17, 205-220.

29. Bao, Q. B.; Landon, S. J.; Rheingold, A. L.; Haller, T. M.; Brill, T. B. Inorg. Chem. 1985, 24, 900.

30. Bondi, A. J. Phys. Chem. 1964, 68, 441.

31. Werner, H. Institut fur Anorgnische Chemie der Universitat Wurzburg, personal communication, 1988.

32. Beagley, B.; Parrott, C. T.; Ulbrecht, V.; Young, G. G. J. Mol. Struct. 1979, 52, 47.

33. Byers, L. R.; Dahl, L. F. Inorg. Chem. 1980, 19, 277.

SECTION II. SYNTHESIS AND REACTIVITY OF BI- AND TRICYCLIC PHOSPHORUS ESTERS CONTAINING PENDANT ALCOHOL GROUPS

INTRODUCTION

Pentacoordinated phosphorus is important to the reaction chemistry of phosphorus compounds. Five-coordinate phosphorus species are often invoked as reaction intermediates of both tri- and tetra-coordinate phosphorus compounds and are believed to be involved in their reactions with nucleophiles,[1] free radical reactions[2] and hydrolysis.[3] One of the factors which determines the products that are obtained in these reactions is the geometry of the intermediate. Two of the most energetically important geometries a pentacoordinate phosphorus adopts are the trigonal bipyramid (TBP) and the square pyramid (SP).[4] We make no destinction here between a square pyramidal and a rectangular pyramidal geometry.

The TBP geometry is by far the most common found in pentacoordinate phosphorus species, appearing both in reactive intermediates and in isolable phosphorus compounds. As a result of the study of these compounds, much insight into the nature of TBP intermediate species has been obtained. An interesting aspect of TBP compounds is the ability of their axial and equatorial ligands to undergo rapid exchange. Though several theories have been proposed to account for this exchange, the Berry pseudorotation mechanism[5] is the most widely accepted and is supported by correlations between the properties of pentacoordinate species in solution and their solid state data.[6] The Berry mechanism passes through a square planar intermediate in order to exchange the axial and equatorial ligands as shown below. Repeating this pseudorotation allows all of the

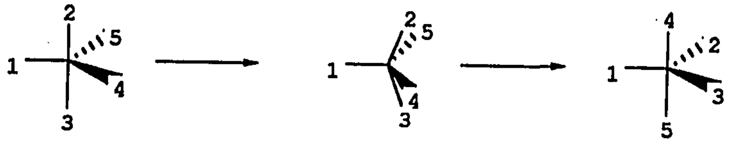

ligands to exchange. This exchange is not observed in all TBP compounds, however, and it can be inhibited by bulky substituents which disfavor the formation of the SP intermediate.[7]

The function of TBP species as reaction intermediates has been thoroughly investigated and the effects of different functional groups in these species determined.[8] As in the TBP compounds mentioned above, TBP intermediates are believed to undergo Berry pseudorotation to exchange axial and equatorial ligands and this exchange plays an important role in the reactions of these species. Several reaction studies and theoretical calculations indicate that the apical position of the TBP is preferred for both an incoming nucleophile and for a leaving group.[9] In many instances this preference requires a pseudorotation which places different leaving groups in an axial position and it can effect the products of such reactions.[3] This effect is also found in TBP species of silicon and a number of other elements.[10]

Since the SP geometry occurs as an intermediate in Berry pseudorotation, its potential stabilization in appropriate phosphorus compounds is worthy of consideration. In comparison with the TBP geometry, SP compounds are very rare. Only a few examples of compounds which contain greater than 70% SP structural characteristics are known[11] and all of these contain multiple four- and/or five-membered rings. In compounds containing multiple unsaturated five-membered rings the SP geometry is favored. Conformational energy calculations indicate that the SP geometry is normally slightly higher in energy than the TBP, but that factors such as ring strain can cause the TBP to rise in energy making the SP preferred.[12] Holmes has prepared a series of pentacoordinate phosphorus compounds containing two five-membered rings to determine what factors influence their geometry.[13] In these systems it is possible to obtain TBP, SP, or a mixture of both geometries, depending on the degree of saturation of the ring, the size and substitution of the ring, the size and electron donating ability of the exocyclic phosphorus substituent, the nature of the ring atoms which are bound to phosphorus and, the degree of hydrogen bonding in the solid state.[11b,c,e,f] The same factors also determine the geometry of the analogous pentacoordinate compounds of As,[14] Sb,[15] Si,[16] Ge[17] and Sn.[18] In systems containing a six-membered ring or in which the exocyclic substituent is a hydrogen, the geometry is always TBP.[19] This demonstrates the importance of the ring strain energy and the nature of the exocyclic phosphorus substituent on the geometry in these systems.

The tautomeric equilibrium between the tri- and pentacoordinated forms of tetraoxaphosphoranes containing two five-membered rings and a P-H bond was first observed in 1973.[20] The equilibrium between these two forms, shown in reaction 1, is believed to be present in all spiro(hydro)phosphoranes. ^{31}P NMR spectroscopy is the technique most

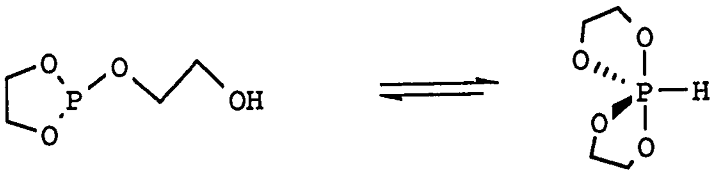

(1)

often used to study this equilibrium since phosphorus chemical shifts are highly indicative of the coordination geometry around phosphorus. Examples appear in the literature in which either the tricoordinate tautomer, or the pentacoordinate tautomer are present in solution.[21] In some systems both forms can be detected in the same solution by ^{31}P NMR spectroscopy.[21] Temperature and the basicity of the solvent have been found among the factors which influence the position of this equilibrium.[22] Studies have recently been broadened to include spiro(hydro)phosphoranes which contain a six-membered ring.[23] The stability of the pentacoordinate tautomer is not as great in these compounds and only one case is known in which this form is favored.[24] In all other instances, the tricoordinate tautomer is the only detectable isomer and the pentacoordinate tautomer is present only as an intermediate in the isomerization between the five- and six-membered ring containing phosphites shown in reaction 2. One factor which

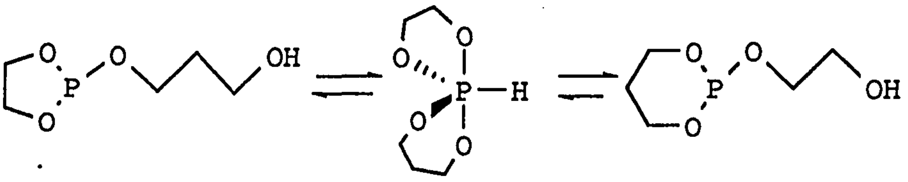

(2)

complicates the investigation of these compounds is their ability to undergo transesterification reactions with the alcohol functions of other phosphite molecules. These reactions yield phosphites which do not form pentacoordinate phosphorus species.

The reaction chemistry of a number of bicyclic phosphorus compounds has been investigated by this group[25] and the ability of these compounds to form pentacoordinate compounds has been documented.[26] In light of the ease with which the phosphites in reaction 1 form pentacoordinate species, a pendant alcohol function placed in the vicinity of the phosphorus in bicyclic compounds could also lead to the formation of five-coordinate phosphorus compounds. This bicyclic system would have the advantage of greater resistance towards intermolecular transesterification.

A heretofore untried approach for the preparation of SP pentacoordinate phosphorus compounds involves the use of a rigid tetradentate system to inhibit the formation of a TBP species. In such a system, any pentacoordinate compound formed would have to be SP. Compounds 1 and 2a-e were chosen for the investigation of such SP compounds since

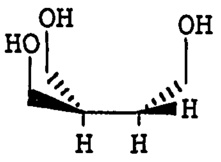

1

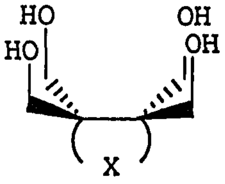

2a-e

	X
2a	H_2
2b	CH_2
2c	$(CH_2)_2$
2d	$(CH_2)_3$
2e	$(CH_2)_4$

phosphorus triester derivatives of 2a-e might be in equilibrium with the pentacoordinate form as shown in reaction 3. Reaction of the trivalent compounds with

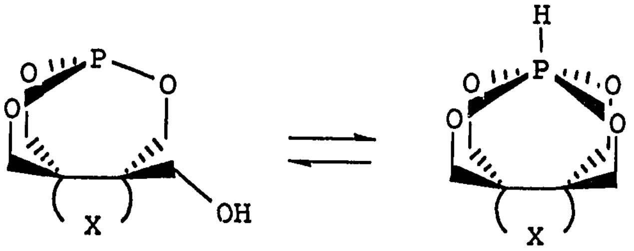

4a-e

(3)

positively charged electrophiles could yield neutral pentacoordinate SP phosphorus derivatives as shown in reaction 4. Such new SP compounds would be the first containing six- and seven-membered rings as well as the first with a proton as the exocyclic substituent. Analogous phosphorus esters of 1 would serve as model compounds for the tri- and tetracoordinate phosphorus species in reactions 3 and 4. The effect of the distance between pairs of alkoxy arms of the tetradentate system on the stability of the SP species could also be investigated by comparing compounds containing larger distances prepared from 2b, for example, with smaller distances stemming from 2d and 2e.

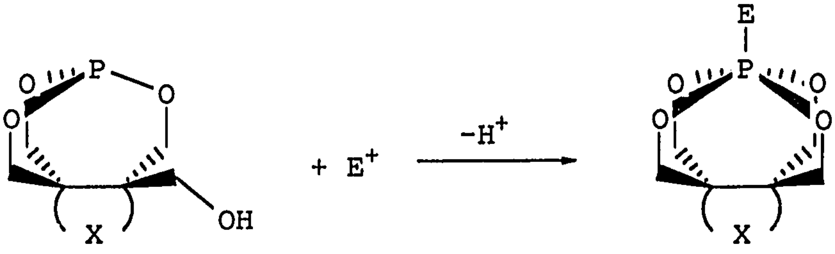

4a-e

(4)

We report here our preparation of several bicyclic tri- and tetracoordinate phosphorus compounds with pendant alcohol groups and our attempts to prepare SP pentacoordinate phosphorus compounds. The reaction of these compounds with the anhydrous acids CF_3COOH and CF_3SO_3H, as well as $Me_3O^+BF_4^-$ and $Ph_3C^+BF_4^-$, will be discussed in terms of the possible equilibrium between tri- or tetracoordinate phosphorus with pentacoordinate phosphorus species. The unusual rearrangement of the phosphite derivatives of 2a-e to new phosphonates will also be described and a mechanism for this reaction proposed.

EXPERIMENTAL SECTION

Physical Measurements

NMR spectra were obtained on Nicolet NT-300 (^1H), Bruker WM-200 (^{13}C) and Bruker WM-300 (^{31}P) instruments at room temperature. The COSY experiment was run on the Nicolet NT-300 spectrometer. All other two-dimensional experiments were performed on the Bruker WM-300 instrument. Variable temperature NMR measurements were recorded on the Bruker WM-300 instrument. Chemical shifts are given in ppm (positive downfield) relative to internal Me_4Si (^1H, ^{13}C) and external 85% H_3PO_4 (^{31}P) standards. The ^1H, ^{13}C and ^{31}P NMR signals of the compounds described in this paper are presented in Tables 1, 2 and 3, respectively.

Preparation of Compounds

Compounds 1[27] and 2a-e[28] were prepared as previously described. All reactions were performed with strict exclusion of moisture. Solvents were dried by standard methods and distilled before use. All other chemicals were used as received.

1-Phospha-2,7,8-trioxatricyclo[3.2.2]nonane, (3)

A solution containing 1 (0.6722 g, 5.595 mmole) and $P(NMe_2)_3$ (0.9549 g, 5.851 mmole) in 40 mL of tetrahydrofuran (THF) was heated to 65°C under nitrogen for three hours. The solution was allowed to cool to room temperature and the solvent removed under vacuum. The remaining solid residue was then extracted with 20 mL of chloroform and the chloroform extract placed on a silica gel chromatography column and eluted with ethyl acetate. Upon removal of solvent from the product-containing fractions, white solid 3 was obtained (yield 0.7679 g, 5.185 mmole, 92.7%).

4-hydroxymethyl-1-phospha-2,7,8-trioxatricyclo[3.2.2]nonane, (4a)

The preparation of this phosphite was accomplished by two different methods: 1) A suspension containing 2a (0.7301 g, 4.862 mmole) and $P(NMe_2)_3$ (0.8238 g, 5.048 mmole) in 35 mL of THF was heated to 65°C for four hours under nitrogen, producing a clear colorless solution. The solvent was removed under vacuum and the remaining material extracted with 15 mL of chloroform. The resulting solution was subjected to silica gel chromatography using ethyl acetate as the eluent and the fractions monitored by TLC to collect the product. Solvent removal from the product-containing fractions gave a thick oil which proved to be the phosphite (yield 0.2852 g, 1.601 mmole, 32.9%). 2) A mixture of 2a (0.1235 g, 0.8224 mmole) and $P(OMe)_3$ (0.1045 g, 0.8422 mmole) in 20 mL pyridine was heated to reflux for five hours after which the solvent was removed under vacuum. The remaining solid residue was subjected to sublimation

(120°C, 0.01 torr) to give white solid 4a (yield 0.0060 g, 0.034 mmole, 4.1%).

4-Hydroxymethyl-1-phospha-2,8,9-trioxatricyclo[4.2.2.$0^{4,6}$]-decane, (4b)

A suspension of 2b (0.6051 g, 3.731 mmole) and $P(NMe_2)_3$ (0.6297 g, 3.858 mmole) in 40 mL of THF was heated to 65°C for three hours under nitrogen. Solvent removal under vacuum followed by extraction of the solid residue with 20 mL of chloroform gave a clear colorless solution. This solution was then passed down a silica gel column with ethyl acetate and the fractions monitored by TLC to collect the product. Solvent removal under vacuum gave white solid 4b (yield 0.0879 g, 0.462 mmole, 12.4%).

4-Hydroxymethyl-1-phospha-2,9,10-trioxatricyclo[5.2.2.$0^{4,7}$]-undecane, (4c)

This phosphite was prepared by two different routes: 1) A suspension of 2c (0.8777 g, 4.981 mmole) and $P(NMe_2)_3$ (0.8420 g, 5.159 mmole) in 40 mL of THF was heated to 65°C for three hours. The solvent was then removed under vacuum and the resulting solid extracted with chloroform to isolate the chloroform-soluble material. The chloroform solution was then subjected to silica gel chromatography using ethyl acetate as the eluent. Monitoring the fractions by TLC allowed the isolation of white solid 4c upon solvent evaporation (yield 0.5251 g, 2.572 mmole, 51.6%). 2) To a solution of 2c (0.4760 g, 2.701 mmole) and NEt_3 (0.8713 g, 8.610 mmole) in 50 mL of THF was added dropwise under nitrogen a solution containing PCl_3 (0.3711 g, 2.702 mmole) in 20 mL THF. Filtration of the reaction mixture followed by silica gel chromatography of the filtrate with ethyl acetate gave white solid 4c (yield 0.1247 g, 0.6108 mmole, 22.6%).

4-Hydroxymethyl-1-phospha-2,10,11-trioxatricyclo-[6.2.2.$0^{4,8}$]dodecane, (4d)

Two methods were used to synthesize this phosphite: 1) A suspension containing 2d (0.9541 g, 5.015 mmole) and $P(NMe_2)_3$ (0.8531 g, 5.227 mmole) in 50 mL of THF was heated to 65°C under nitrogen for three hours. The clear colorless solution was allowed to cool to room temperature and the solvent was removed under vacuum. The solid residue was extracted with chloroform and the chloroform solution passed down a silica gel column using ethyl acetate as the eluent. TLC was used to monitor the fractions for product. The product fractions were combined and solvent removal under vacuum gave white solid 4d (yield 0.7362 g, 3.374 mmole, 67.3%). 2) A mixture containing 2d (0.8842 g, 4.648 mmole) and $P(OMe)_3$ (0.5864 g, 4.726 mmole) in 45 mL of pyridine was heated to reflux for five hours. The solvent was then removed under vacuum and the solid residue sublimed (120°C, 0.01 torr) to give white solid 4d (yield 0.0417 g, 0.191 mmole, 4.11%).

4-Hydroxymethyl-1-phospha-2,11,12-trioxatricyclo-[7.2.2.0^{4,9}]tridecane, (4e)

A suspension of 2e (0.6217 g, 3.043 mmole) and $P(NMe_2)_3$ (0.5182 g, 3.175 mmole) in 40 mL of THF was heated to 65°C for five hours under nitrogen. The solvent was then removed from the reaction mixture and the residue extracted with chloroform. The chloroform-soluble material was subjected to silica gel chromatography with ethyl acetate to give white solid 4e (yield 0.3061 g, 1.318 mmole, 43.3%).

4-Hydro-4-oxo-3,5,4-dioxophosphabicyclo[5,3,0]decane, (5a), and 3,7-dioxabicyclo[3.3.0]octane (6a)

A mixture of 2a (1.5001 g, 9.989 mmole) and HMPT (1.6348 g, 10.02 mmole) was heated to 65°C for three hours under nitrogen. The resulting oily solid was subjected to sublimation at 0.1 torr and 180°C for two days. The sublimate was then collected and passed down a silica gel column using ethyl acetate as the eluent. Fractions containing 6a followed by those containing 5a were collected and the solvent removed under vacuum. Recrystallization of 5a from ethanol gave pure product (yield of 5a 0.1938 g, 1.088 mmole, 10.9%; yield of 6a 0.4504 g, 3.946 mmole, 39.5%).

4-Hydro-4-oxo-4-phospha-3,5,9-trioxatricyclo[5.3.1.0]-undecane, (5b)

A mixture of 2b (1.6229 g, 10.01 mmole) and HMPT (1.6395 g, 10.04 mmole) was heated to 65°C for three hours under nitrogen. The resulting semi-solid material was sublimed for two days at 0.1 torr and 180°C. The sublimate was then purified with silica gel using ethyl acetate as the eluent to give 5b (yield 0.5804 g, 3.052 mmole, 30.5%).

4-Hydro-4-oxo-4-phospha-3,5,9-trioxatricyclo[5.3.2.0]-dodecane, (5c), and 3,7-dioxatricyclo[3.3.2.0]decane (6b)

A mixture of 2c (1.7609 g, 9.993 mmole) and HMPT (1.6354 g, 10.02 mmole) was heated to 65°C for three hours under nitrogen. The reaction mixture was sublimed and the sublimate chromatographed on silica gel with ethyl acetate. Removal of the solvent from the first fraction gave 6b and from the second fraction gave pure 5c which could be recrystallized from ethanol (yield of 5c 0.1878 g, 0.9199 mmole, 9.20%; yield of 6b 0.2217 g, 1.582 mmole, 15.8%).

4-Hydro-4-oxo-4-phospha-3,5,9-trioxatricyclo[5.3.3.0]-tridecane, (5d), and 3,7-dioxatricyclo[3.3.3.0]undecane (6c)

A mixture containing 2d (1.9003 g, 9.989 mmole) and HMPT (1.6399 g, 10.05 mmole) was heated to 65°C for three hours under nitrogen. The resulting oily product was sublimed for two days at 0.1 torr and 180°C. The sublimate was then subjected to silica gel chromatography using ethyl acetate to give first 6c and then 5d (yield of 5d 0.2018 g, 0.9249 mmole, 9.26%; yield of 6c 0.5698 g, 3.695 mmole, 37.0%).

4-Hydro-4-oxo-4-phospha-3,5,9-trioxatricyclo[5.4.3.0]-tetradecane, (5e), and 3,7-dioxatricyclo[4.3.3.0]dodecane (6d)

A mixture of 2e (2.0400 g, 9.987 mmole) and HMPT (1.6317 g, 9.998 mmole) was kept at 65°C under nitrogen for three hours. The product was then sublimed and the sublimate passed down a silica gel chromatography column with ethyl acetate to give first 6d and then 5e (yield of 5e 0.4855 g, 2.091 mmole, 20.9%; yield of 6d 0.2801 g, 1.665 mmole, 16.7%).

1-Triphenylmethyl-4-hydroxymethyl-1-phospha-2,7,8-trioxatricyclo[3.2.2]nonane tetrafluoroborate, (7a)

To a solution of 4a (0.2599 g, 1.459 mmole) in 20 mL of THF was added triphenylcarbenium tetrafluoroborate (0.5278 g, 1.599 mmole). The solution was stirred for three hours and 10 mL of benzene added to precipitate the phosphonium salt. After filtration and washing with benzene, white solid 7a was obtained (yield 0.5882 g, 1.157 mmole, 79.3%).

1-Triphenylmethyl-4-hydroxymethyl-1-phospha-2,8,9-trioxatricyclo[4.2.2.$0^{4,6}$]decane tetrafluoroborate, (7b)

Triphenylcarbenium tetrafluoroborate (0.3866 g, 1.171 mmole) was added to a solution containing 4b (0.2010 g, 1.052 mmole) in 10 mL of THF. The solution was stirred for three hours and 5 mL benzene added and the solution filtered. The resulting white solid 7b was washed with benzene and dried under vacuum (yield 0.4064 g, 0.7811 mmole, 74.2%).

1-Triphenylmethyl-4-hydroxymethyl-1-phospha-2,9,10-trioxatricyclo[5.2.2.$0^{4,7}$]undecane tetrafluoroborate, (7c)

To a room temperature solution containing 4c (0.3139 g, 1.537 mmole) in 10 mL of THF was added triphenylcarbenium tetrafluoroborate (0.5698 g, 1.726 mmole). The solution was stirred for three hours and 5 mL of benzene added to precipitate the product. The solution was filtered, the solid 7c washed with benzene and the product dried under vacuum (yield 0.7109 g, 1.330 mmole, 85.6%).

1-Triphenylmethyl-4-hydroxymethyl-1-phospha-2,10,11-trioxatricyclo[6.2.2.$0^{4,8}$]dodecane tetrafluoroborate, (7d)

A solution of 4d (0.6530 g, 2.993 mmole) in 10 mL of THF was treated with triphenylcarbenium tetrafluoroborate (1.0873 g, 3.2935 mmole) at room temperature. After three hours 5 mL of benzene was added and the resulting solid filtered, washed with benzene and dried in vacuo to give 7d as a white powder (yield 1.3948 g, 2.5438 mmole, 85.0%).

1-Methyl-4-hydroxymethyl-1-phospha-2,10,11-trioxatricyclo-[6.2.2.$0^{4,8}$]dodecane tetrafluoroborate, (8)

To a solution of 5d in THF was added solid $Me_3O^+BF_4^-$ in an NMR tube. Solid 8 formed upon removal of the solvent.

1,7-di(Hydroxymethyl)-4-oxo-4-triphenylmethyl-3,5,4-dioxaphosphabicyclo[5.3.0]decane, (9)

A mixture of 4d (0.2182 g, 1.001 mmole) and triphenylcarbenium tetrafluoroborate (0.3584 g, 1.086 mmole) was stirred in 6 mL of THF for 30 minutes and then cooled to -50°C. DBU (1,8-diazabicyclo[5.4.0]undec-7-ene, 0.164 mL, 1.10 mmole) was then added portion-wise, the suspension was stirred at -50°C for 15 minutes and allowed to warm to room temperature over three hours. Water (0.036 mL, 2.0 mmole) was then injected to the mixture and the solution stirred for 10 hours. The reaction mixture was poured into chloroform and the solution extracted with water (3 x 20 mL). The residue after concentration was chromatographed on silica gel to give 9 as a colorless oil. Recrystallization from chloroform-hexane (1:1) gave a white solid (yield 0.2127 g, 0.4445 mmole, 44.4%).

4-Methylbenzoate-1-phospha-2,7,8-trioxatricyclo[3.2.2]-nonane, (10a)

To a solution containing 4a (0.2555 g, 1.434 mmole), triethylamine (0.20 mL, 1.45 mmole) and DMAP (4-dimethylaminopyridine) (0.0176 g, 0.144 mmole) in 10 mL of chloroform was added benzoyl chloride (0.17 mL, 1.45 mmole). The solution was stirred for 20 hours, diluted with 10 mL of toluene and the chloroform removed under vacuum. The solution was then filtered and the solvent removed under vacuum. The resulting impure 10a was subjected to silica gel chromatography using chloroform as the eluent to give pure 10a (yield 0.2130 g, 0.7548 mmole, 52.6%).

4-Methylbenzoate-1-phospha-2,8,9-trioxatricyclo[4.2.2.$0^{4,6}$]-decane, (10b)

Benzoyl chloride (0.046 mL, 0.54 mmole) was added to a solution of 4b (0.1027 g, 0.5401 mmole), triethylamine (0.075 mL, 0.54 mmole) and DMAP (0.0061 g, 0.0499 mmole) in 5 mL chloroform and stirred for 12 hours. The solution was then diluted with 5 mL of toluene and the chloroform evaporated. After filtration and removal of the solvent under vacuum a white solid was obtained. Silica gel chromatography with chloroform gave pure 10b (yield 0.0592 g, 0.2012 mmole, 37.2%).

4-Methylbenzoate-1-phospha-2,9,10-trioxatricyclo-[5.2.2.$0^{4,7}$]undecane, (10c)

To a solution containing 4c (0.3874 g, 1.897 mmole), triethylamine (0.28 mL, 2.0 mmole) and DMAP (0.0246 g, 0.0201 mmole) in 10 mL chloroform was added benzoyl chloride (0.24 mL, 2.0 mmole). The solution was stirred for 24 hours and then diluted with 10 mL of toluene. Upon evaporation of the chloroform, the solution was filtered and the toluene removed under vacuum. The resulting solid was purified on silica gel with chloroform to give 10c (yield 0.2596 g, 0.8421 mmole, 44.4%).

4-Methylbenzoate-1-phospha-2,10,11-trioxatricyclo-[6.2.2.$0^{4,8}$]dodecane, (10d)

To a solution of 4d (0.1091 g, 0.5000 mmole) in 5 mL of chloroform containing triethylamine (0.070 mL, 0.50 mmole) and DMAP (0.0062 g, 0.051 mmole) was added benzoyl chloride (0.060 mL, 0.52 mmole). After 12 hours at room temperature, the reaction mixture was diluted with 5 mL of toluene and the chloroform evaporated. The solution was then filtered and the solvent removed under vacuum. The resulting solid residue was purified by silica gel chromatography with chloroform as the eluent to give 10d (yield 0.0752 g, 0.233 mmole, 46.7%).

1-Oxo-4-hydroxymethyl-1-phospha-2,7,8-trioxatricyclo-[3.2.2]nonane, (11a)

This phosphate was prepared by two different methods: 1) A 1.2 M solution of tBuOOH in toluene (2.4 mL, 2.9 mmole) was added dropwise to a solution of 4a (0.3518 g, 1.975 mmole) in 50 mL of toluene in an ice bath. Filtration gave white solid 11a which was washed with toluene and air dried (yield 0.3618 g, 1.864 mmole, 94.4%). 2) To a cooled solution of 1,2,4-triazole (2.070 g, 30.0 mmole) in 30 mL of dioxane was added dropwise $POCl_3$ (1.536 g, 10.0 mmole). Triethylamine (3.030 g, 29.9 mmole) was then added dropwise and the mixture stirred for one hour. The reaction mixture was then filtered and the filtrate slowly added dropwise to a solution of 2a (1.160 g, 7.72 mmole) in 25 mL of pyridine. The solution was stirred an additional three hours and the solvent removed under vacuum at 60°C. The solid residue was extracted with chloroform and placed in a freezer for two days to precipitate the remaining unreacted triazole. Solvent was removed from the resulting solution and the solid recrystallized from isopropanol (yield 0.491 g, 2.53 mmole, 32.8%).

1-Oxo-4-hydroxymethyl-1-phospha-2,8,9-trioxatricyclo-[4.2.2.$0^{4,6}$]decane, (11b)

To a solution of 4b (0.3307 g, 1.739 mmole) in 50 mL of toluene cooled in an ice bath was added dropwise a 1.2 M solution of tBuOOH in toluene (2.1 mL, 2.5 mmole). Filtration of the solid precipitate formed, followed by washing with toluene gave 11b (yield 0.3374 g, 1.637 mmole, 94.1%).

1-Oxo-4-hydroxymethyl-1-phospha-2,9,10-trioxatricyclo-[5.2.2.0^{4,7}]undecane, (11c)

Two methods proved useful in the preparation of 11c: 1) A 1.2 M solution of tBuOOH in toluene (2.2 mL, 1.9 mmole) was added dropwise to a solution of 4c (0.3763 g, 1.843 mmole) in 50 mL of toluene cooled in an ice bath. The precipitate which formed was filtered, washed with toluene and dried in air to give white solid 11c (yield 0.3603 g, 1.636 mmole, 88.8%). 2) Phosphorus oxychloride (0.768 g, 5.01 mmole) was added dropwise to a cooled solution containing 1,2,4-triazole (1.035 g, 15.0 mmole) in 30 mL dioxane. Triethylamine (1.515 g, 15.0 mmoles) was then added and the mixture stirred for one hour. The reaction mixture was then added to a solution of 2c (0.880 g, 4.99 mmole) in 25 mL of pyridine. The mixture was stirred for three hours and the solvent removed under vacuum at 60°C. The solid residue was extracted into chloroform and placed in a freezer to precipitate unreacted triazole. The solvent was then removed from the resulting solution and the solid recrystallized from ethanol (yield 0.0020 g, 0.0908 mmole, 1.8%).

1-Oxo-4-hydroxymethyl-1-phospha-2,10,11-trioxatricyclo-[6.2.2.0^{4,8}]dodecane, (11d)

This phosphate was prepared by two different routes: 1) A 1.2 M solution of tBuOOH in toluene (1.8 mL, 1.5 mmole) was added dropwise to a solution of 4d (0.3088 g, 1.415 mmole) in 50 mL of toluene cooled in an ice bath. Filtration of the resulting precipitate followed by washing with toluene and drying in the air gave white solid 11d (yield 0.3078 g, 1.314 mmole, 92.9%). 2) To a cooled solution containing 1,2,4-triazole (1.035 g, 15.0 mmole) in 30 mL of dioxane was added dropwise $POCl_3$ (0.768 g, 5.01 mmole). Triethylamine (1.515 g, 15.0 mmole) was added and the mixture stirred for an additional one hour. The reaction mixture was then added to a solution containing 2d (0.901 g, 4.74 mmole) in 25 mL pyridine. The solution was stirred for three hours and the solvent removed under vacuum at 60°C. The solid was extracted into chloroform and placed in a freezer to crystallize the unreacted triazole impurity. Removal of the solvent under vacuum from the resulting solution gave a white solid which could be recrystallized from ethanol (yield 0.490 g, 2.24 mmole, 47.2%).

1-Oxo-4-hydroxymethyl-1-phospha-2,11,12-trioxatricyclo-[7.2.2.0^{4,9}]tridecane, (11e)

To a solution of 4e (0.4128 g, 1.778 mmole) in 50 mL of toluene cooled in an ice bath was added a 1.2 M solution of tBuOOH in toluene (2.2 mL, 1.8 mmole). Filtration of the precipitate, washing with toluene and air drying gave a white solid which recrystallizated from ethanol to give 11e (yield 0.3922 g, 1.580 mmole, 88.9%).

1-Thio-4-hydroxymethyl-1-phospha-2,7,8-trioxatricyclo-[3.2.2]nonane, (12a)

A suspension of 4a (0.1976 g, 0.9401 mmole) and sulfur (0.0482 g, 1.50 mmole) in 25 mL of a 50:50 mixture of carbon disulfide and benzene was heated to 50°C for one week. After solvent evaporation the solid residue was purified on silica gel with ethyl acetate to give 12a (yield 0.0655 g, 0.312 mmole, 33.2%).

1-Thio-4-hydroxymethyl-1-phospha-2,9,10-trioxatricyclo-[5.2.2.$0^{4,7}$]undecane, (12b)

A suspension containing 4c (0.5424 g, 2.296 mmole) and sulfur (0.1005 g, 3.135 mmole) in 50 mL of a 50:50 mixture of carbon disulfide and benzene was kept at 50°C for one week. The solvent was then removed under vacuum, the solid residue dissolved in ethyl acetate and the resulting solution subjected to silica gel chromatography using ethyl acetate as the eluent. Evaporation of the solvent from the product containing fraction gave pure 12c (yield 0.2214 g, 0.9372 mmole, 40.8%).

1-Thio-4-hydroxymethyl-1-phospha-2,10,11-trioxatricyclo-[6.2.2.0^{4,8}]dodecane, (12c)

A suspension of 4d (0.850 g, 3.90 mmole) and sulfur (0.187 g, 5.83 mmole) in a 50:50 mixture of carbon disulfide and benzene was heated to 50°C for one week. After solvent evaporation, the residue was purified on silica gel with a chloroform-methanol mixture (50:1) to give 12d which could be crystallized from acetonitrile-benzene (yield 0.437 g, 1.74 mmole, 44.8%).

1-Seleno-4-hydroxymethyl-1-phospha-2,7,8-trioxatricyclo-[3.2.2]nonane, (13a)

A suspension of 4a (0.6565 g, 3.686 mmole) and finely divided red selenium (0.4183 g, 5.297 mmole) in 40 mL of toluene was heated to 80°C for four days. The hot solution was filtered and the solvent removed under vacuum to give 13a (yield 0.2143 g, 0.8336 mmole, 22.6%).

1-Seleno-4-hydroxymethyl-1-phospha-2,8,9-trioxatricyclo-[4.2.2.0^{4,6}]decane, (13b)

A suspension containing 4b (0.8831 g, 4.644 mmole) and finely divided red selenium (0.6391 g, 8.094 mmole) in 40 mL of toluene was heated to 80°C for four days. The hot solution was filtered and the solvent removed under vacuum to give white solid 13b (yield 0.1481 g, 0.5503 mmole, 11.8%).

1-Seleno-4-hydroxymethyl-1-phospha-2,9,10-trioxatricyclo-[5.2.2.$0^{4,7}$]undecane, (13c)

A suspension of 4c (0.9227 g, 4.519 mmole) and finely divided red selenium (0.6021 g, 7.625 mmole) in 40 mL of toluene was kept at 80°C for four days. The hot solution was filtered and allowed to cool to room temperature to give crystals of 13c (yield 0.3088g, 1.091 mmole, 24.1%).

1-Seleno-4-hydroxymethyl-1-phospha-2,10,11-trioxatricyclo-[6.2.2.$0^{4,8}$]dodecane, (13d)

A suspension of 4d (1.0013 g, 4.589 mmole) and finely divided red selenium (0.5612 g, 7.107 mmole) in 40 mL of toluene was heated to 80°C for 4 days. The hot solution was filtered and allowed to cool to room temperature to give crystals of 13d (yield 0.3312 g., 1.1114 mmole, 24.3%).

1-Seleno-4-hydroxymethyl-1-phospha-2,11,12-trioxatricyclo-[7.2.2.$0^{4,9}$]tridecane, (13e)

A suspension containing 4e (1.2838 g, 5.528 mmole) and finely divided red selenium (0.7241 g, 9.170 mmole) in 50 mL of toluene was heated to 80°C for four days. The hot solution was filtered and the solvent removed under vacuum giving white solid 13e (yield 0.3188 g, 1.024 mmole, 18.5%).

1-Borino-4-hydroxymethyl-1-phospha-2,7,8-trioxatricyclo-[3.2.2]nonane, (14a)

To a solution of 4a (0.5330 g, 2.992 mmole) in 40 mL of THF was slowly added dropwise a 1.00 M solution of THF•BH_3 in THF (3.2 mL, 3.2 mmole). After the solution was stirred an additional two hours, the solvent was removed under vacuum to give white solid 14a (yield 0.0895 g, 0.466 mmole, 15.6%).

1-Borino-4-hydroxymethyl-1-phospha-2,8,9-trioxatricyclo-[4.2.2.$0^{4,6}$]decane, (14b)

To a solution containing 4b (0.2577 g, 1.355 mmole) in 40 mL of THF was slowly added dropwise a 1.0 M solution of THF•BH_3 in THF (1.5 mL, 1.5 mmole). The solution was stirred an additional two hours and then the solvent was removed under vacuum. The resulting white solid was the borane adduct 14b (yield 0.0312 g., 0.1531 mmole, 11.3%).

1-Borino-4-hydroxymethyl-1-phospha-2,9,10-trioxatricyclo-[5.2.2.$0^{4,7}$]undecane, (14c)

A 1.0 M solution of THF•BH_3 in THF (1.4 mL, 1.4 mmole) was slowly added dropwise to a solution of 4c (0.02535 g, 1.242 mmole) in 40 mL of THF. The solvent was removed after an additional two hours, giving white solid 14c (yield 0.0916 g, 0.4203 mmole, 33.8%).

1-Borino-4-hydroxymethyl-1-phospha-2,10,11-trioxatricyclo-[6.2.2.0^{4,8}]dodecane, (14d)

To a solution of 4d (0.4297 g, 1.969 mmole) in 40 mL of THF was slowly added dropwise a 1.0 M solution of THF•BH_3 in THF (2.2 mL, 2.2 mmole). After an additional two hours of stirring the solvent was removed under vacuum to give the white solid borane adduct (yield 0.1424 g, 0.6135 mmole, 31.2%).

1-Borino-4-hydroxymethyl-1-phospha-2,11,12-trioxatricyclo-[7.2.2.0^{4,9}]tridecane, (14e)

To a solution containing 4e (0.1718 g, 0.7398 mmole) in 40 mL of THF was slowly added dropwise a 1.0 M solution of THF•BH_3 in THF (1.0 mL, 1.0 mmole). After an additional two hours, the solvent was removed under vacuum giving white solid 14e (yield 0.0492 g, 0.2001 mmole, 27.0%).

4-Methylbenzoate-1-oxo-1-phospha-2,10,11-trioxatricyclo-[6.2.2.0^{4,8}]dodecane, (15)

A pyridine (2.0 mL) solution of 11d (0.0617 g, 0.263 mmole) was treated with benzoyl chloride (0.043 mL, 0.37 mmole) followed by addition of DMAP (0.0032 g, 0.026 mmole). After two days the solution was diluted with 3 mL of toluene and evaporated to dryness. The residue was chromatographed on silica gel with ethyl acetate and recrystallized from 1:1 chloroform-hexanes (yield 0.0669 g, 0.1978 mmole, 75.3%).

1-Oxo-4-methoxymethyl-1-phospha-2,10,11-trioxatricyclo-[6.2.2.0^{4,8}]dodecane, (16)

A suspension of sodium hydride (0.0233 g, 0.929 mmole; oil free) in 6.0 mL of dry dioxane was mixed with 11d (0.1437 g, 0.6136 mmole) at room temperature and stirred until the evolution of hydrogen ceased (ca. one hour). Dimethyl sulfate (0.064 mL, 0.0676 mmole) was then added and the mixture stirred for 10 hours. After solvent removal under vacuum, the solid residue was extracted with chloroform and the chloroform-soluble material chromatographed on silica gel with ethyl acetate. Recrystallization from chloroform-hexane (1:1) gave 16 (yield 0.0420 g., 0.1692 mmole, 27.6%).

1-Oxo-4-(butyldimethyl)silyloxymethyl-1-phospha-2,10,11-trioxatricyclo[6.2.2.0^{4,8}]dodecane, (17)

To a solution of 11d (0.1099 g, 0.4693 mmole) in 2.0 mL of dimethylformamide containing triethylamine (0.079 mL, 0.57 mmole) and DMAP (0.0030 g, 0.024 mmole) was added *tert*-butyldimethylsilyl chloride (0.0850 g, 0.564 mmole). The solvent was removed under vacuum and the residue purified on silica gel to give 17 after recrystallization from 1:1 chloroform-hexane (yield 0.0630 g, 0.181 mmole, 38.5%).

1-Oxo-1-phospha-2,7,8-trioxatricyclo[3.2.2]nonane, (18)

A solution containing 3 (0.2118 g, 1.430 mmole) in 50 mL of toluene was cooled in an ice bath and to it was added dropwise a 1.2 M solution of tBuOOH in toluene (1.8 mL, 2.2 mmole). The white precipitate which formed, was filtered off and then washed with toluene and dried in the air to give 18 (yield 0.2066 g, 1.259 mmole, 88.0%).

1-Borino-1-phospha-2,7,8-trioxatricyclo[3.2.2]nonane, (19)

To a solution of 3 (0.6703 g, 4.526 mmole) in 40 mL of THF was slowly added dropwise a 1.0 M solution of THF•BH_3 in THF (4.8 mL, 4.8 mmole). After the solution was stirred an additional two hours, the solvent was removed under vacuum to give white solid 19 (yield 0.6232 g, 3.848 mmole,85.0%).

1-Seleno-1-phospha-2,7,8-trioxatricyclo[3.2.2]nonane, (20)

A suspension of 3 (0.6710 g, 4.531 mmole) and finely divided red selenium (0.5301 g, 6.714 mmole) in 35 mL of toluene was kept at 80°C for 12 hours. The hot solution was filtered and allowed to cool to room temperature forming white crystals of 20 (yield 0.6644 g, 2.926 mmole, 64.6%).

Reactions of 4a-e with anhydrous protic acids

The reactions of the title phosphites were carried out with CF_3O_2H and CF_3SO_3H in essentially the same manner. To a solution of the appropriate phosphite in THF was added 0.01 equivalents of acid in THF. The solution was stirred for 12 hours and monitored by ^{1}H NMR and ^{31}P NMR spectroscopies. In the case of H_3PO_3, 0.1 equivalent of the acid was added to a solid sample of 4c and the resulting mixture sublimed at 1.0 torr and 120°C. The sublimate was analyzed by ^{31}P NMR spectroscopy.

Reactions of 4a-e with amines

Phosphites 4a-e were reacted with pyridine, Et_3N and DBU using the same general procedure. To a solution of the appropriate phosphite in THF was added 0.01 equivalents of base in THF. The solution was stirred for 12 hours and monitored by ^{1}H and ^{31}P NMR spectroscopies.

Reaction of 4a-e with water

To solutions containing 4a-e in THF was added 0.01 equivalent of H_2O in THF. The solution was stirred for 12 hours and monitored by ^{1}H NMR and ^{31}P NMR spectroscopies.

X-ray diffraction data

The same general procedure was used for all five structure determinations. A crystal of 2d, 5c, 9, 11c, or 11d, grown by slow evaporation from saturated CH_2Cl_2, was mounted on a glass fiber and centered on an Enraf-Nonius CAD4 diffractometer. Cell dimensions and the orientation matrix were obtained from least-squares refinement using setting angles of 25 reflections in the range $25 < \text{two-theta} < 34°$. During data collection, three representative reflections were checked every 60 min. as orientation and intensity standards. Since the change in intensity was less than the error in the measurements, no decay correction was applied. Lorentz and polarization corrections were applied to the data, and empirical absorbtion corrections, based on a series of psi-scans, were initially applied to the data. Refinement of the structure was carried out using the SHELX76 package.[29] Scattering factors were obtained from the usual sources.[30]

In all five structures, 25 reflections chosen from a rotation photograph were indexed to give the approximate unit cell which subsequent solution of the structure showed to be of a specific symmetry. The structure was solved with the use of over 3000 unique reflections in each case with $I > 2\sigma(I)$.

Structure Solution and Refinement

All the structures were solved by direct methods. All non-hydrogen atoms were located from a direct methods E-map. Following full-matrix least-squares refinement of these atoms, any remaining non-hydrogen atoms were located from difference Fourier syntheses. After convergence of the least-squares calculations, including anisotropic thermal parameters for all of the non-hydrogen atoms, a difference map revealed all the expected hydrogen atoms. In the case of structures 5c and 11c the positional coordinates of the hydrogen atoms were refined, while the respective isotropic temperature factors were held constant. In structures 2d, 9 and 11d, hydrogen atoms were included in calculated positions "riding" on the adjacent carbon or phosphorus atoms. A single isotropic thermal parameter was refined for all of the phenyl hydrogen atoms, and likewise for all of the alkyl hydrogen atoms. The parameters thus defined were refined in full-matrix least-squares calculations. The crystal data for all five structures are summarized in Table 4. The final positional parameters are given in Tables 5, 6, 7, 8 and 9 for 2d, 5c, 9, 11c and 11d, respectively. Selected bond lengths and angles for these respective compounds are given in Tables 10-14. The ORTEP diagrams of 2d, 5c, 9, 11c and 11d are presented in Figures 1-5, respectively.

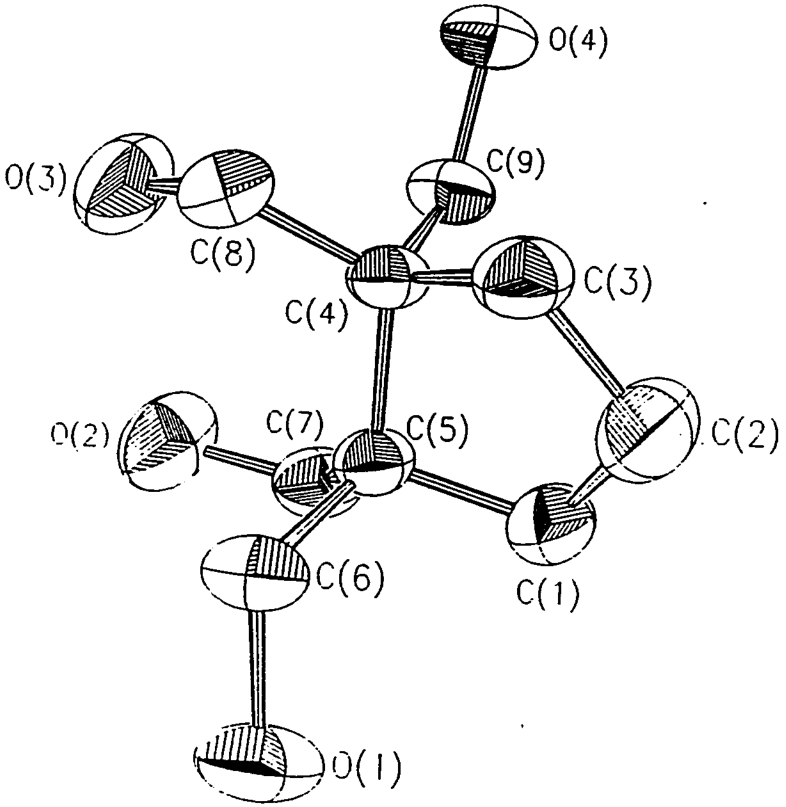

Figure 1. ORTEP drawing of 2d, with ellipsoids at the 50% probability level

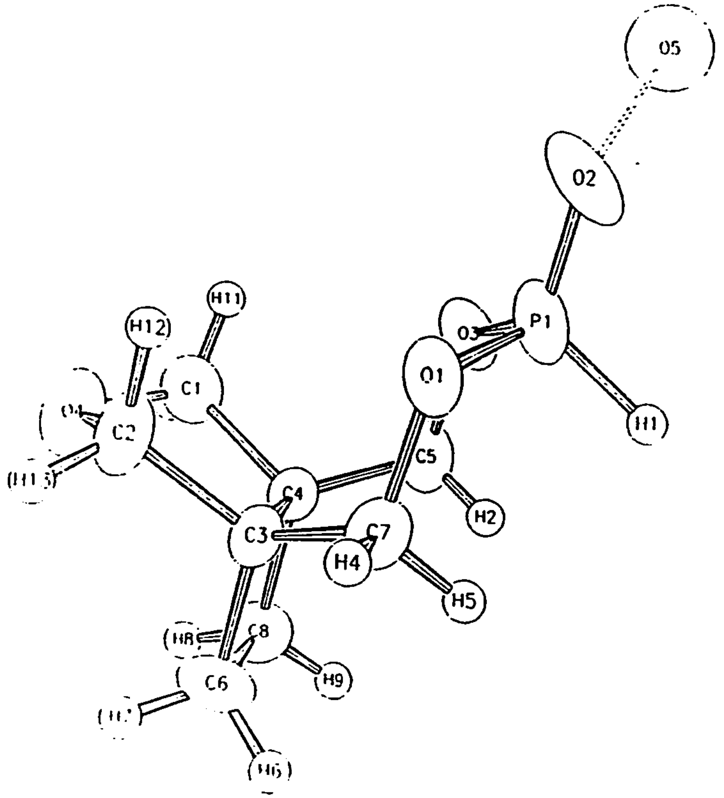

Figure 2. ORTEP drawing of <u>5c</u>, with ellipsoids at the 50% probability level

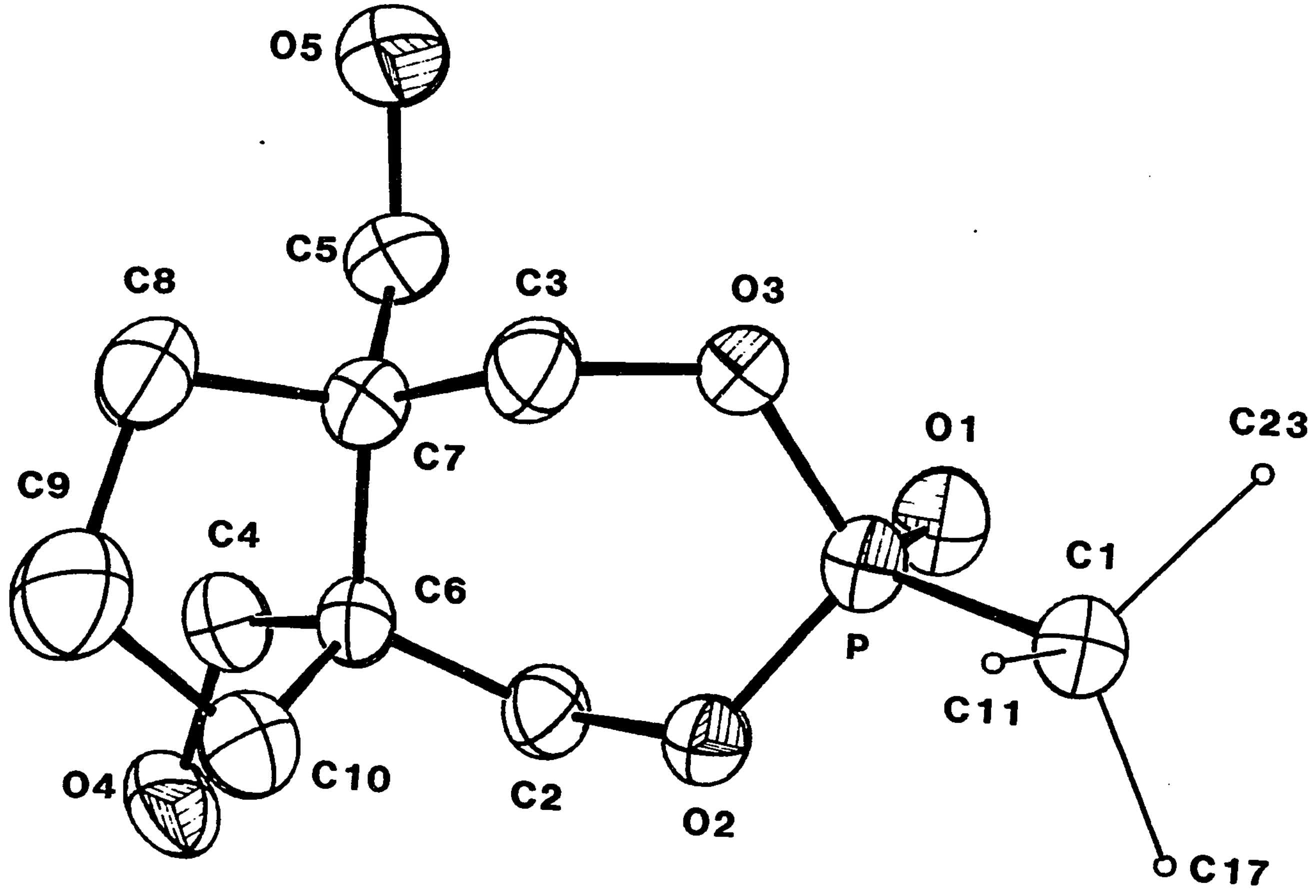

Figure 3. ORTEP drawing of 9, with ellipsoids at the 50% probability level

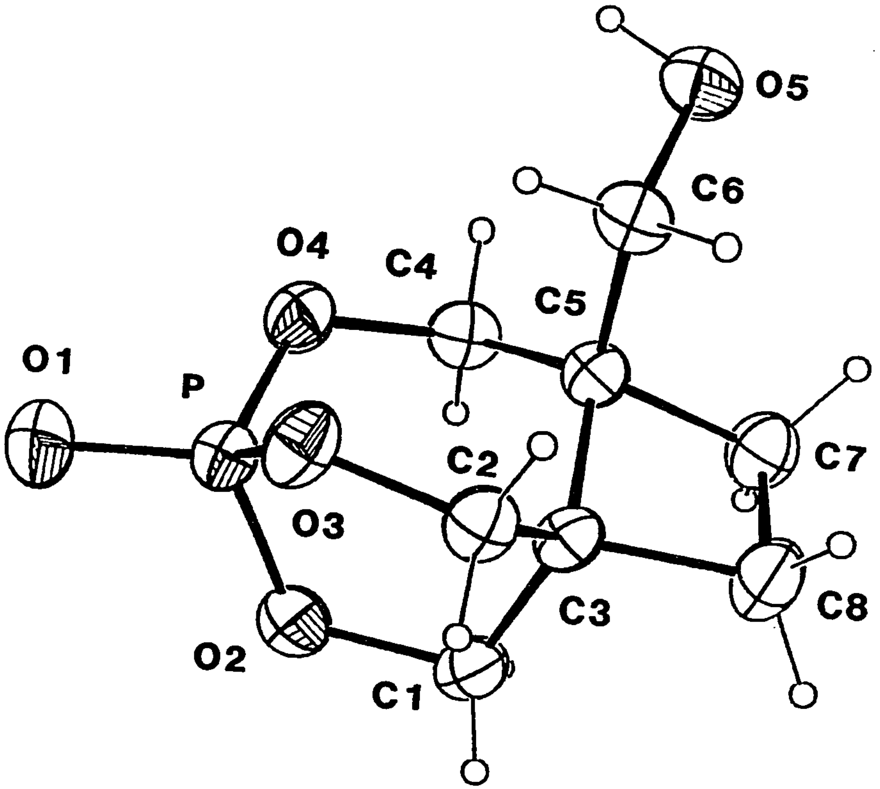

Figure 4. ORTEP drawing of 11c, with ellipsoids at the 50% probability level

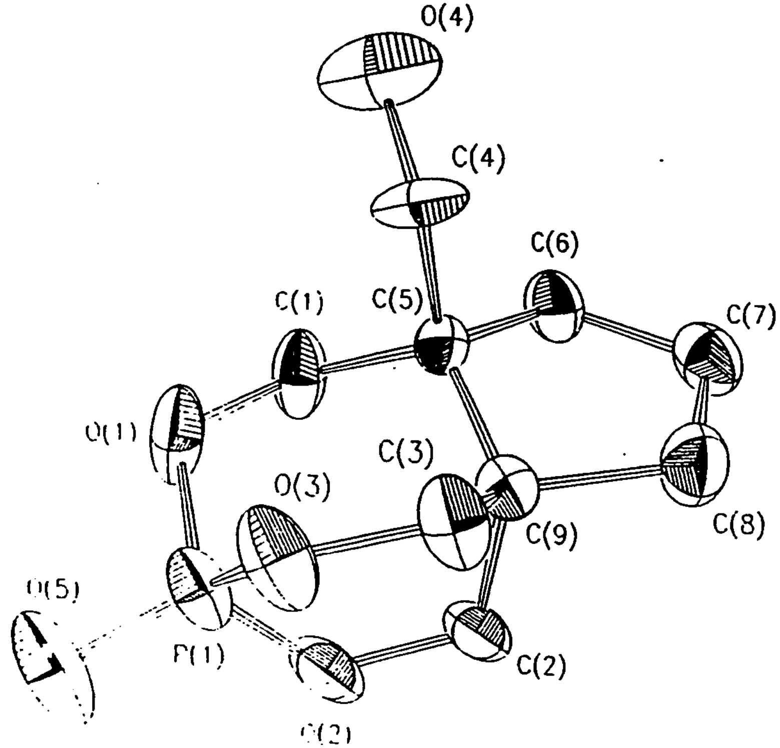

Figure 5. ORTEP drawing of 11d, with ellipsoids at the 50% probability level

RESULTS AND DISCUSSION

Synthetic Pathways

Phosphites 3 and 4a-e could be prepared by the reaction of the appropriate alcohol with P(NMe$_2$)$_3$ in THF (reaction 5). Reaction 5 could be performed both with and without solvent. Initially the purification of the phosphites proved to be much more difficult than anticipated. Although ^{31}P NMR and ^{1}H NMR spectroscopy of the crude product prior to sublimation showed the phosphite to be the major phosphorus-containing product of the reaction, attempts to purify the phosphite by sublimation (0.1 torr, 180°C) gave the new compounds 5a-e and the known tricyclic ethers 6a-d shown in reaction 6. Due to stereochemistry about the phosphorus atom, compounds 5a-e appear as pairs of

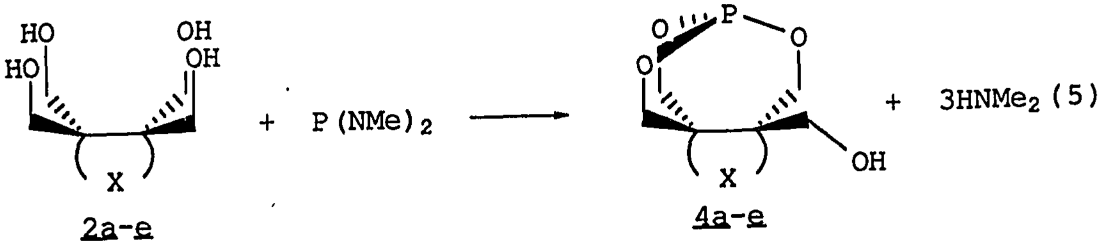

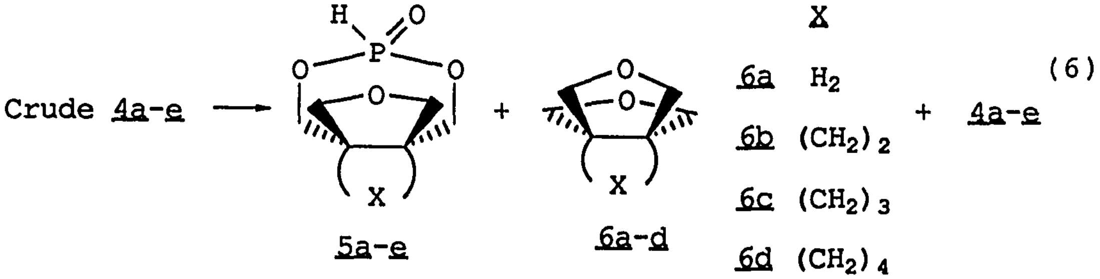

diastereomers. Compounds 6a-d were previously prepared by reaction of the tetraalcohols 2a, 2c-e with catalytic amounts of acid as shown in reaction 7.[28] Only ca. 1% of

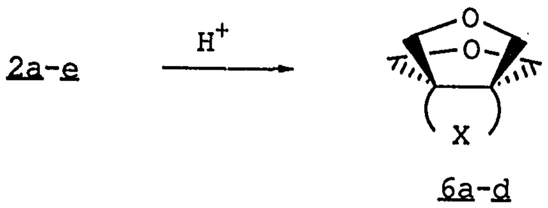

(7)

the sublimate was found to be in the form of the phosphite ester, and the polymeric sublimation residue contained no detectable phosphite. The phosphonates 5a-e could also be prepared by reaction of the chromatographically purified phosphites with trace amounts of anhydrous acids as shown in reaction 8. Monitoring the acidic solutions by ^{31}P NMR and

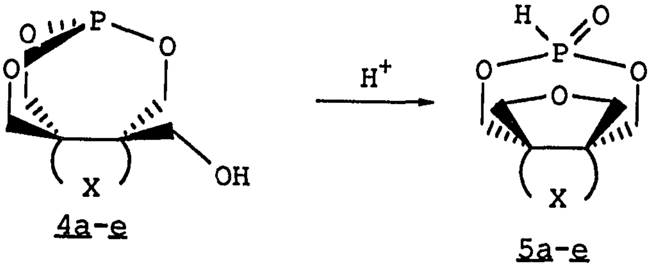

(8)

^{1}H NMR spectroscopy showed that the rearrangement of the phosphite to phosphonate began almost immediately. Solutions containing small amounts of water were also found to promote the formation of the phosphonate species while solutions containing dry solvent showed no signs of rearrangement. In samples treated with the bases pyridine, Et_3N and DBU, no phosphonate or cyclic ether products could be detected. In order to determine if acid might be playing a role in the rearrangement in solid samples subjected to sublimation, a mixture containing purified 4c and a small amount of freshly prepared phosphorous acid was heated under vacuum (1.0 torr, 120°C). The resulting sublimate was a mixture containing 4c (32%), 5c (45%) and 6b (23%) as shown in reaction 9. Purified samples of 4a-e could be easily

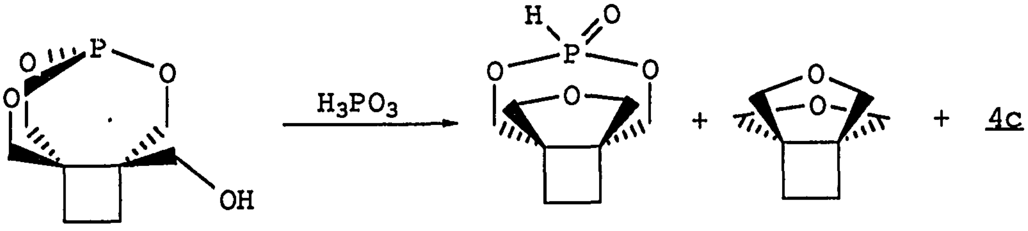

4c 5c 6b (9)

sublimed at 0.01 torr and 85°C while at 5.0 torr, 85°C a roughly 80/20 mixture of phosphite and phosphonate, as shown by ^{1}H NMR and ^{3}P NMR spectroscopies, was obtained. These data suggest a competitive acid-catalyzed rearrangement for the formation of 5a-e, and acid-assisted pyrolysis of the phosphonate to give 6a-d and presumably HPO_2 polymer.

A possible mechanism for the acid catalyzed rearrangement is shown in Scheme 1. In the upper pathway, the oxygen is protonated. Such a protonated intermediate is similar to one proposed in the acid-catalyzed hydrolysis of

Scheme 1

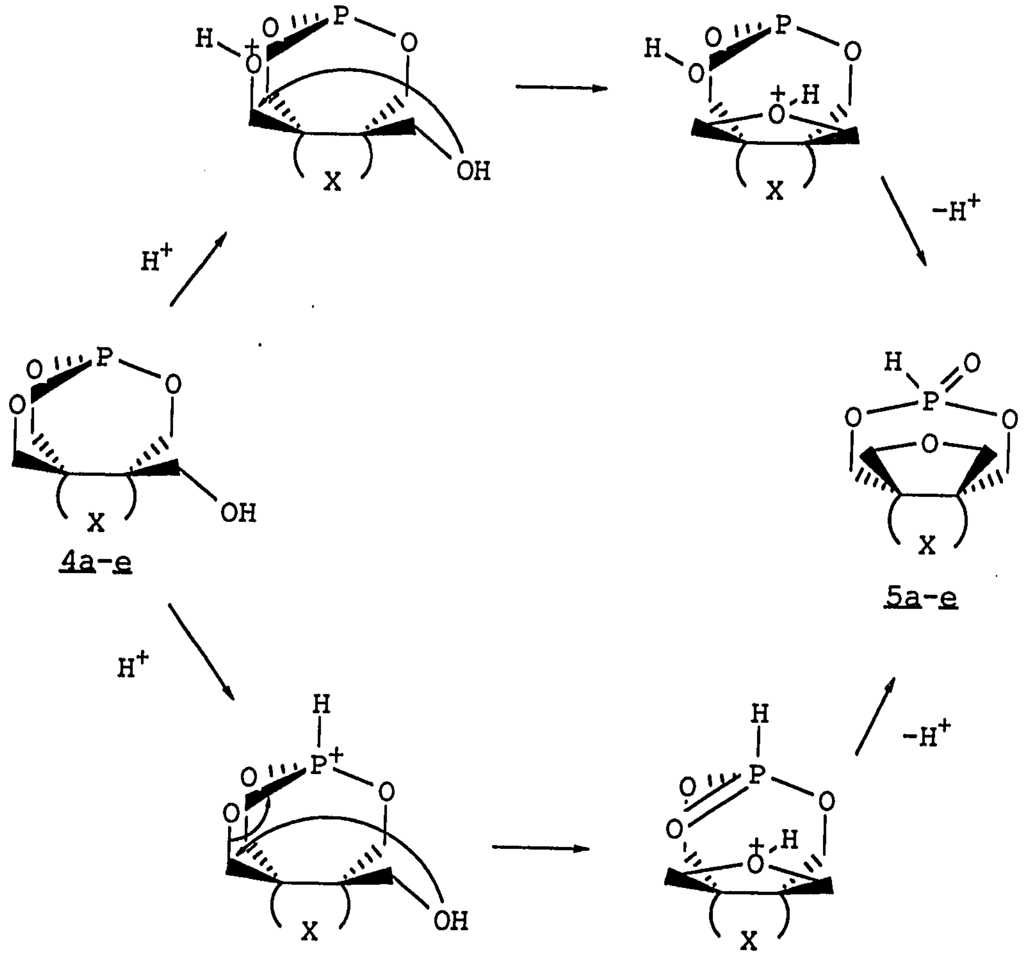

phosphite and phosphate esters.[31] As in the reactions of the tetraalcohols with acid to form diethers 6a-d,[28] the protonation of this oxygen forms a good leaving group making the adjacent carbon atom more susceptible to nucleophilic attack in the second step. The POH function rearranges in the next step and the cyclic ether group loses the remaining proton. The lower pathway involves an initial intermediate protonated at phosphorus, the more active of the two pathways in the acid catalyzed hydrolysis of phosphite esters.[31] Nucleophilic attack of the carbon, as in the first pathway, by the adjacent alcohol function gives the cyclic ether and forms a P==O bond. We consider this pathway to be probably of lesser importance, based on the results of reactions of 4a-e with electrophiles. In reactions of the phosphites with $Ph_3C^+BF_4^-$ and with $Me_3O^+BF_4^-$, alkylation takes place exclusively at phosphorus to give 7a-e and 8 as shown in reaction 10. These species, similar to the

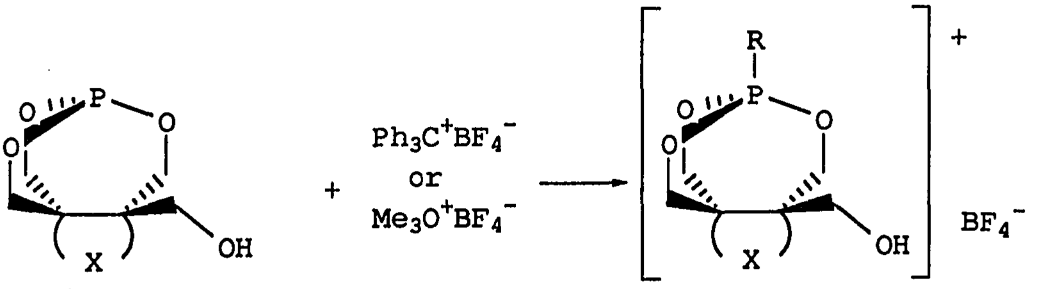

(10)

7a-e R = Ph_3C

8 R = Me

phosphorus-protonated intermediate in Scheme 1, do not undergo spontaneous rearrangement to form the corresponding phosphonates indicating that the C-O bond is not sufficiently activated (at least for carbenium ions) for nucleophilic attack by the adjacent alcohol group. Treatment of 7d with water, however, results in the very slow formation of 9 (reaction 11) showing that nucleophilic attack on the C-O-P carbon is possible but that it is relatively slow. Nucleophilic reactions of analogous species protonated at phosphorus are probably also slow, supporting the oxygen-protonated pathway in Scheme 1 as the dominant one.

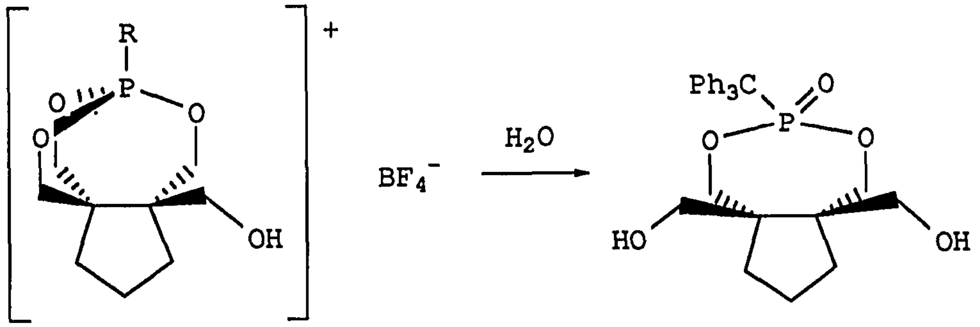

7d 9 (11)

In an attempt to trap any pentacoordinate species formed in the equilibrium envisioned in reaction 4, compounds 4a-e were reacted with PhC(O)Cl in the presence of Et_3N and catalytic amounts of DMAP (reaction 12). In this reaction, the pentacoordinate tautomer would be deprotonated and the

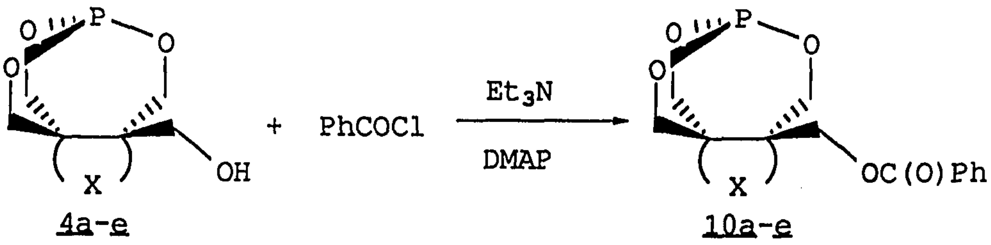

(12)

resultant anion would be expected to react with the PhC(O)Cl to yield a pentacoordinate compound. However, the benzoate derivatives, 10a-e, were isolated.

The phosphate (11a-e), thiophosphate (12a-c), selenophosphate (13a-e) and BH_3 (14a-e) derivatives of 4a-e have also been synthesized. The phosphates 11a-e could be prepared either by reaction of tris-triazolephosphine oxide with the appropriate tetraalcohol (2a-d) or by oxidation of

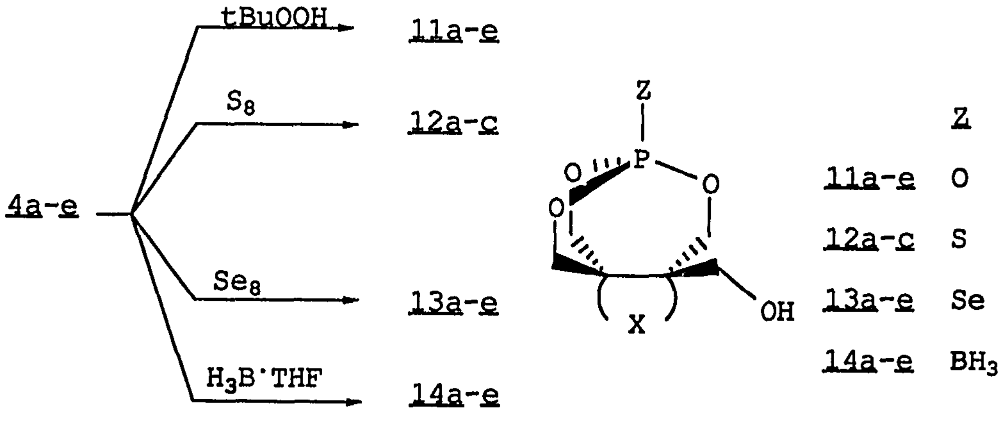

(13)

(14)

(15)

(16)

4a-e (reaction 13). Reaction of 4a-e with elemental sulfur (reaction 14), with elemental selenium (reaction 15) and with $BH_3{\cdot}THF$ (reaction 16) yielded 12-14, respectively. Attempts to trap a pentacoordinate species by derivatization of the phosphate oxygen of 11d with electrophiles (with concomitant deprotonation and coordination of the alkoxy arm) resulted in the isolation of tetracoordinate phosphorus compounds 15, 16 and 17 as shown in reaction 17.

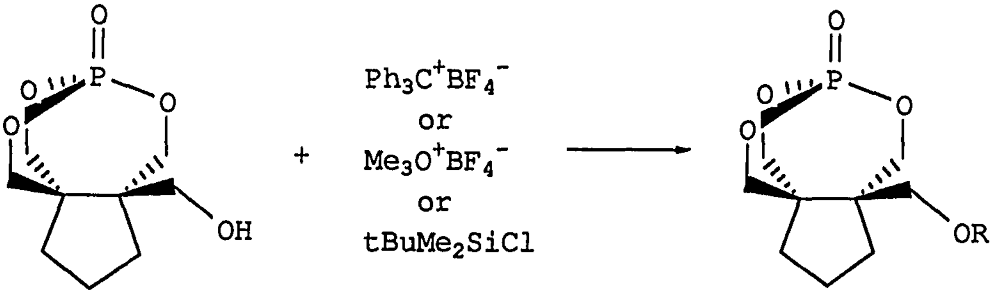

(17)

11d

	R
15	Ph_3C
16	Me
17	$tBuMe_2Si$

Results

The ^{1}H, ^{13}C and ^{31}P NMR data for compounds 3-20 are summarized in Tables 1, 2 and 3, respectively. All of the protons of the tricoordinate form and the pentacoordinate forms of 4c are labeled below. The higher symmetry of the pentacoordinate form requires the ^{1}H NMR spectrum of this compound to exhibit a simple ABX pattern. The proton spectra of 4a-e and their derivatives are in reality very complex. This is due to their tricoordinate nature which insert scheme

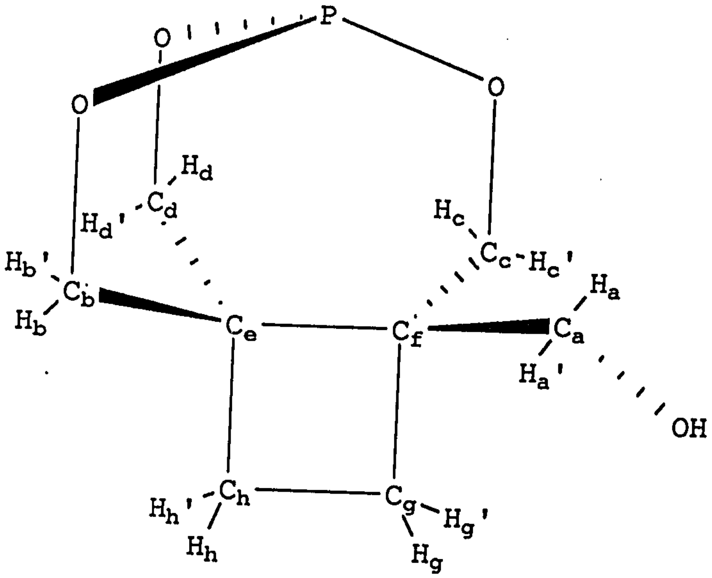

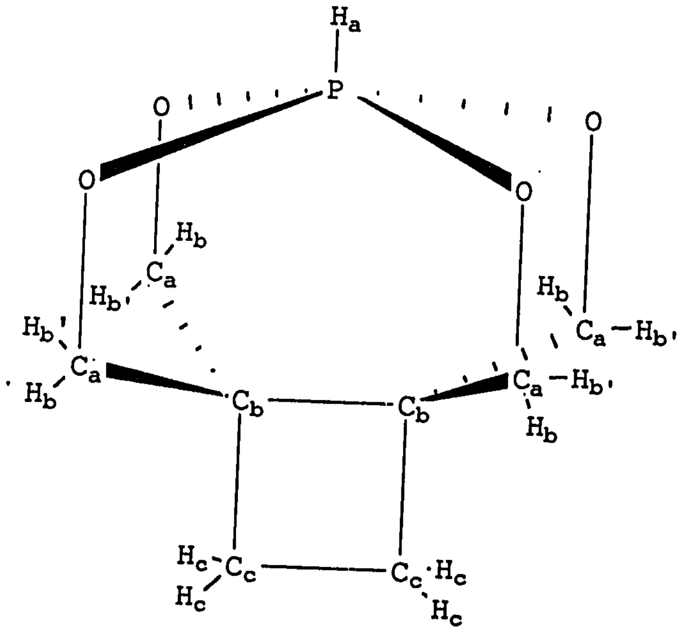

renders all of the protons in these compounds inequivalent. The complexity of the spectra of these compounds rules out the pentacoordinate structure as the dominant form in solution. In order to determine whether detectable amounts of the pentacoordinate tautomer was present, it was necessary to assign the ^1H NMR shifts and couplings in these compounds.

A useful model for the interpretation of these ^1H NMR spectra was phosphite 3. In this compound and its derivatives the lack of the alcoholic arm increases the symmetry of the molecule making the proton NMR simpler and, therefore, easier to assign. Comparison of the coupling constants and proton chemical shifts in 3 with those of previously investigated bicyclic phosphorus compound 21,

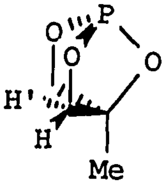

21

which is of similar symmetry, confirmed the ^1H NMR assignments. A common feature of 21 and 3 is the smaller value of $^3J(POCH)$ in comparison with $^3J(POCH')$.[32] This effect has also been found in derivatives of 4a-e.

To make the interpretation of the ^1H NMR spectra of <u>4a</u>-<u>e</u> and their derivatives easier, the complete assignment of the spectrum of <u>4c</u> using a number of NMR techniques was accomplished. The region of the ^1H NMR spectrum of <u>4c</u> containing methylene protons a-d is shown in Figure 6. It is seen from the figure that several of the proton resonances overlap. The chemical shift of proton a was identified by its $^3J(HOCH_a)$ value using d_6-DMSO as the solvent. This solvent allows the observation of the alcohol resonances and couplings which are normally not detected due to rapid proton exchange. In addition, the chemical shift of the alcoholic proton could be observed in this solution. To determine which signals in the one-dimensional ^1H NMR spectrum were coupled, a COSY[33] experiment was performed (Figure 7). Using these data the positions of protons a, b, b', d and d' could be tentatively assigned as shown in the figure. The resonances of protons a', c and c' were found to overlap. This experiment was also useful in detecting the four-bond "W" coupling between protons b and d, observed in rigid bicyclic systems containing protons in a "W" orientation to one another.[34] To unambiguously establish the chemical shifts of protons a-d, a ^1H-^{13}C correlated two-dimensional NMR spectrum using bilinear pulses[35] was obtained. For each carbon atom of the molecule, this technique (which allows suppression of coupling in the

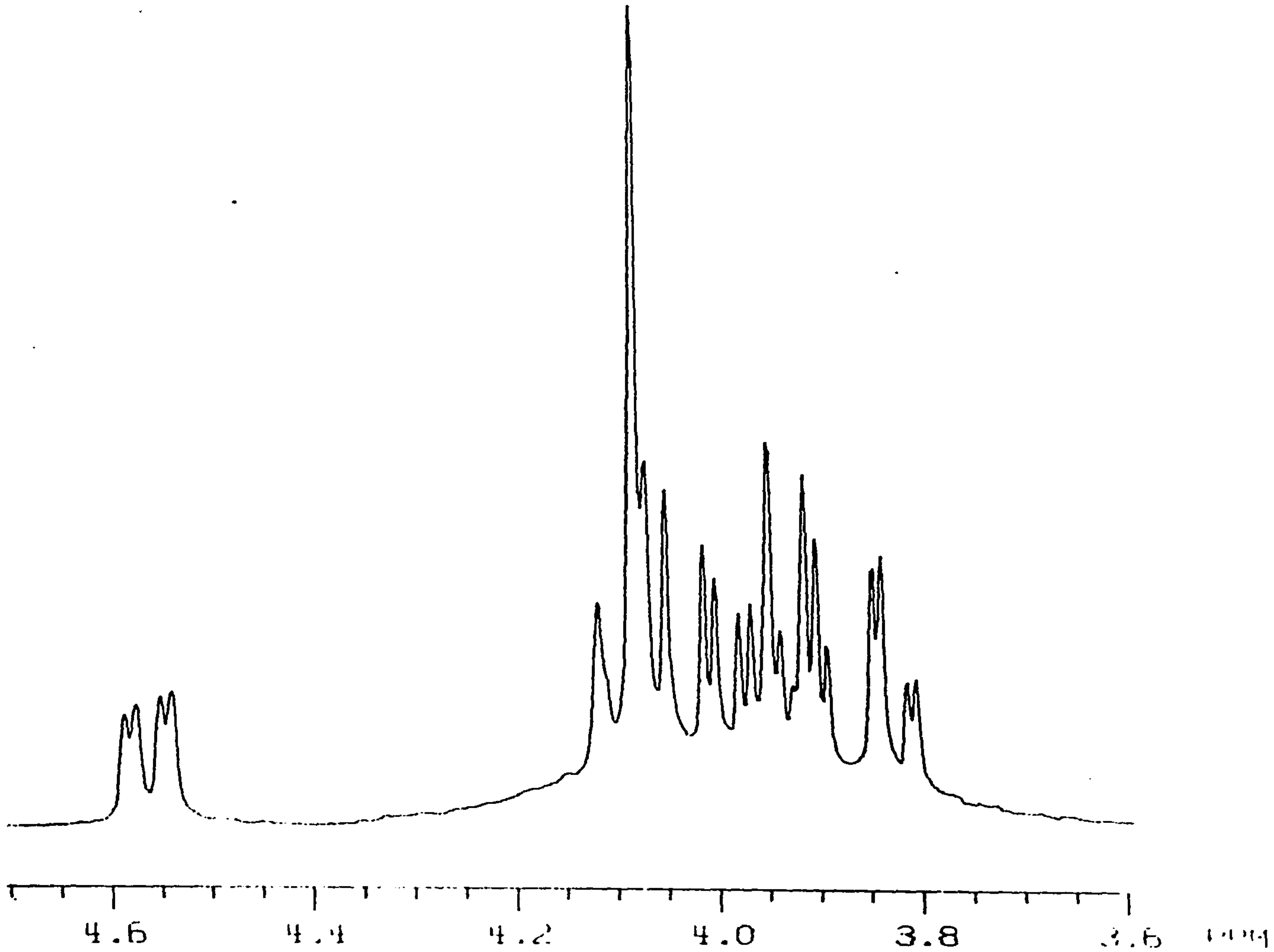

Figure 6. ^1H NMR spectrum of <u>4c</u> showing the region of protons H_a through H_d

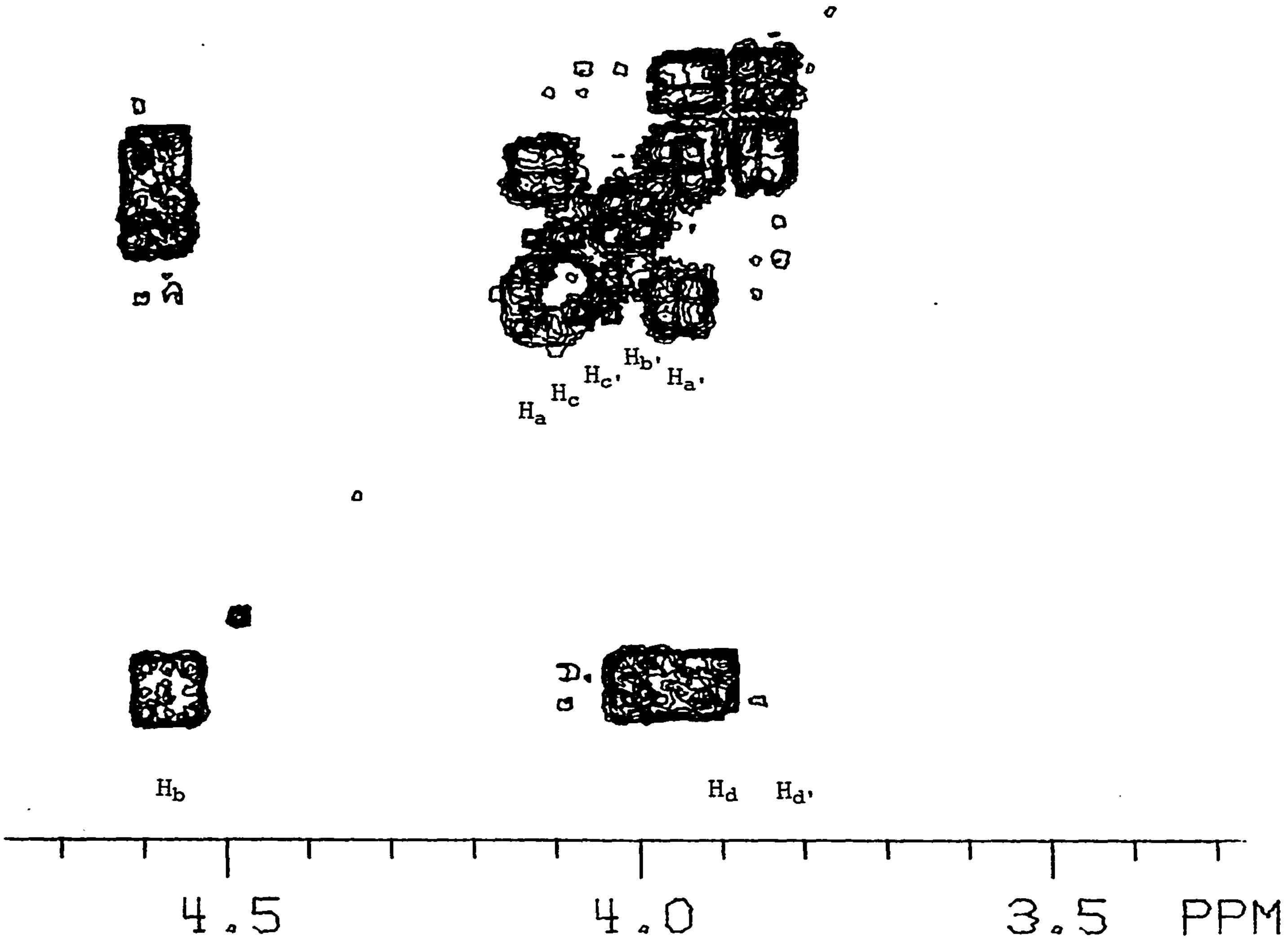

Figure 7. COSY spectrum of 4c showing the region of protons H_a through H_d

^{1}H-^{13}C-chemical-shift-correlation maps) gave a one-dimensional decoupled ^{1}H NMR spectrum of the protons bound to that carbon atom. From these data the chemical shifts of protons a', c and c' were obtained and the assignment of protons a, b, b', d and d' were confirmed. Two-dimensional indirect J spectroscopy with a selective spin flip,[36] an NMR experiment which allows the direct measurement of geminal couplings without resolution of the complete coupling pattern, was used to determine the geminal ($^{2}J(HCH)$) couplings of the eight methylene protons of interest, as well as the four methylene protons of the cyclobutane ring. These values of $^{2}J(HCH)$ were then used with data from a normal ^{1}H-^{13}C correlated two-dimensional NMR experiment[37] to determine all of the remaining proton-proton and proton-phosphorus couplings. With the assignment of <u>4c</u> complete, the interpretation of the ^{1}H NMR spectra of tri- and tetracoordinate compounds in Table 1 was straightforward. No signals assignable to a pentacoordinate compound appeared in the ^{1}H NMR spectra of any of these compounds.

Several trends in coupling constants and chemical shifts are found in the data presented in Table 1. As in other phosphorus compounds, the values of $^{3}J(POCH)$ depend on the derivatization at phosphorus and show little variation among compounds with identical phosphorus functionality. Similarities can also be found in the proton-proton couplings of phosphorus derivatives of the same tetraalcohol. The functionality on phosphorus, or on the oxygen of the free arm, has little effect on the position and the line shape of the methyne protons of the derivatives of 4a or of the protons of the monocyclic rings in derivatives of 4b-e. In 4a and its derivatives, the methyne protons appear in the range 2.6 to 1.6 ppm, similar to derivatives of 3, while the ring protons of 4b, 4c, 4d and 4e and their derivatives appear at ca. 2.3-2.0 ppm, 2.4-1.9 ppm, 2.1-1.5 ppm and, 2.2-1.6 ppm, respectively. This indicates that little change occurs in the geometry of the carbon backbone of these compounds upon derivatization of the phosphorus atom. The "W" coupling, $^4J(H_bCCCH_d)$, observed in 4c is present in the ^{1}H NMR spectra of all of the derivatives of 4a-e and is a further indication of the rigid nature of these compounds. Examination of Table 1 also shows that in compounds containing a carbocyclic ring the chemical shift of proton b appears significantly downfield with respect to the other seven methylene protons in this region of the spectrum. Derivatives of 2a do not exhibit this effect and the chemical shift of proton b appears within the range of the other methylene protons. The major difference between derivatives of 4a and derivatives of 4b-e can be seen in Figure 8. As shown in this figure, two cage conformations are available to 4a

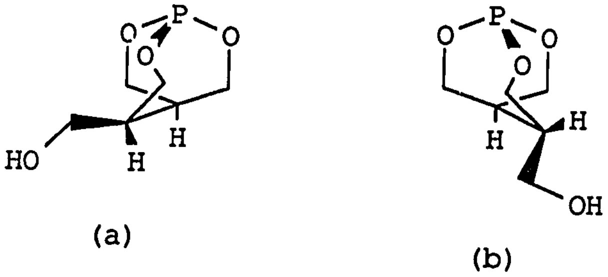

(a)

(b)

Figure 8. Conformations possible for <u>4a</u> (a and b)

while only one is possible in derivatives of 2b-e. Steric arguments suggest conformation b should be the preferred conformation in 4a with the alcoholic arm nearly eclipsing the methyne proton. In compounds 4b-e and their derivatives, the formation of conformation b is inhibited by the steric restrictions imposed by the carbocyclic ring. This restriction places the alcoholic arm in closer proximity to proton b and interaction between the oxygen of the alcohol group and this proton could cause the low field shift observed for it.

Compounds 5c and 9, shown below, yield ^{1}H NMR spectra indicative of conformational equilibria present in 1,3,2-dioxaphosphepanes and 1,3,2-dioxaphosphepenes in solution.[38] In the case of 5c, the presence of a pair of diastereomers is readily apparent from the pairs of similar, yet inequivalent, proton signals. The similarity of $^3J(POCH_a)$ and $^3J(POCH_{a'})$ values in the pair of 5c

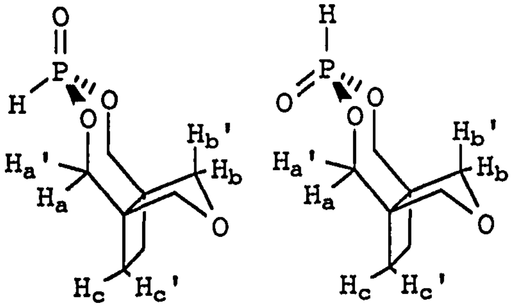

5c

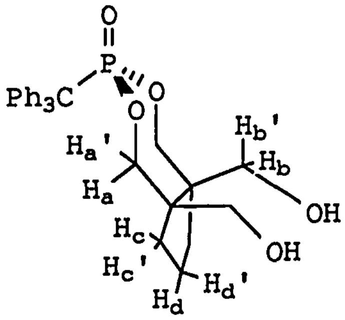

9

diastereomers and in compound 9 shows that these protons are experiencing both axial and equatorial environments in solution. Dioxaphosphepanes not undergoing any kind of conformational change exhibit differences in the $^{3}J(POCH)$ values of 10 Hz or greater.[38] In the case of 9 this conformational exchange is probably a twist-twist equilibrium since the five-membered ring is flexible and would resist the formation of an eclipsed conformation around the carbons of the fused rings which is necessary for the formation of chair or boat forms of the seven-membered ring. For compound 5c the equilibrium is probably not simple. The energy difference between the planar and puckered forms of cyclobutane is small and could allow both the chair and the twist conformations of the 1,3,2-dioxaphosphepane ring to be present. In dioxaphosphepanes believed to exhibit a chair-chair equilibrium, however, protons H_a and $H_{a'}$ do not appear to be coupled, unlike 5c in which $^{2}J(H_aCH_{a'})$ is ca. 12.9 Hz. These values are comparable to $^{2}J(H_aCH_{a'})$ in twist-twist equilibrating dioxaphosphepanes whose coupling constants are ca. 11.8 Hz.[38] Based on these comparisons, both isomers of 5c appear to be undergoing a twist-twist conformational equilibrium in solution.

The ^{13}C NMR data also demonstrate the lack of symmetry in 4a-e. All of the carbon atoms of 4c are inequivalent in the tricoordinate form while in the pentacoordinate form only three types of carbons would be present. Using the straightforward ^{13}C NMR assignment of 3 and information gained from the series of two-dimensional experiments obtained for 4c, the ^{13}C NMR spectrum of this compound was assigned. An INADEQUATE NMR experiment[39] performed on this compound, which allows the observation of carbon-carbon couplings and indicates the connectivity in the carbon backbone of the molecule, confirmed these assignments. Based on the interpretation of the spectrum of 4c, the ^{13}C NMR spectra of the remaining compounds in Table 2 were assigned.

In the derivatives of 4a-e a much smaller $^{2}J(POC)$ was observed for carbon b than for either carbons c or d, the latter two couplings always being very similar to one another. This phenomenon, and the fact that this carbon appears farther downfield than the other carbon resonances, is probably the result of the interaction of the alcoholic arm with proton b and hence indirectly with carbon b. Similarly, the value of $^{3}J(POCC)$ was always much greater for bridgehead carbon e than that of bridgehead carbon f. It has been shown that the number of bond pathways through which two atoms can couple may influence the coupling constants, with the result that larger J values are found in systems with more coupling pathways.[40] This may explain the

^2J(POC) values of carbons e and f found in derivatives of 4a-e. For carbon e there are two three-bond paths through which coupling can occur, but for carbon f there is only one such pathway. Based on the number of coupling pathways, $^2J(POC_f)$ should be smaller (as is observed) than $^2J(POC_e)$. As with the ^{1}H NMR P-H couplings of these compounds, though large differences are observed in the coupling constants of the different phosphorus derivatives, derivatives of 4a-e containing identical functionality at phosphorus tend to have similar values of ^2J(POC) and ^3J(POCC). This emphasizes the structural similarity in all of the derivatives of 4a-e. In none of the ^{13}C NMR spectra is there any detectable presence of pentacoordinate species. Variable temperature ^{13}C NMR spectroscopy of 4c showed no evidence of exchange of the alcohol group or the formation of pentacoordinate species up to 100°C. The latter experiment yielded data consistent only with the presence of the tricoordinate form of these compounds.

The ^{13}C NMR spectrum of 9 is consistent with the structure proposed for this compound. As in 4a-e and their derivatives, the methylene carbon containing the alcohol group appears at lower field than the methylene carbons of the seven-membered ring. Also, ^3J(POCC) is not observed and is contained in one three-bond pathway similar to 4a-e and their derivatives discussed above, which also do not contain detectable $^{3}J(POCC_{f})$ coupling.

In the past, ^{31}P NMR spectroscopy has been used to investigate the tautomeric equilibrium of tricoordinate phosphorus compounds with pentacoordinate species. The chemical shifts of tricoordinate species appear in the range 140-130 ppm and their pentacoordinate tautomers give signals which are much farther upfield at -30 to -45 ppm.[20-24] With this in mind, the ^{31}P NMR spectra of 4a-e and their derivatives, presented in Table 3, were collected. Derivatives of 3 have shifts similar to their 4a-e counterparts showing that the presence of the pendant alcoholic group has little effect on the phosphorus atom. Each group of phosphorus compounds gives chemical shifts typical for their particular functionality[41] and none of these compounds have signals lying in the range expected for pentacoordinate species. Thus, in no instance was any signal detected in the -10 to -60 ppm region. This result strongly supports the absence of a five-coordinate phosphorus tautomer in these systems. In the case of compounds 13a-e, and 20 the correlation of their P-Se coupling constants[42] allowed the determination of the relative Lewis basicity of the corresponding phosphites 4a-e and 3. Based on the values of $^{1}J(PSe)$ presented in Table 3, all of the phosphites have similar basicities, indicating that the presence of carbocyclic rings in the system has little effect on the phosphorus-containing portion of the molecule. Comparison of the P-Se coupling constants with those of known compounds[43] shows 3 and 4a-e to be only slightly less basic than the bicyclic compound 22. The fact that similar derivatives have similar chemical shifts suggests little change in the geometry around phosphorus in going from derivatives of 1 to 2a to 2e. Compounds 5a-e and 9 also have ^{31}P NMR chemical shifts typical of compounds with similar derivitization at phosphorus and in the case of 5a-e, consistant with pairs of diastereomers in solution.[41]

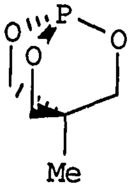

22

Description of the Structures

The structure of tetraalcohol 2d is shown in Figure 1. This compound shows a high degree of intermolecular hydrogen bonding between alcohol groups and all of the bond distances presented in Table 6 are well within the normal range.[44] The conformation of the five-membered ring is the half chair form causing the pairs of arms on carbons 4 and 5 to be staggered. All of the C-O bond distances (average 1.427 Å) and the O-C-C bond angles (average 112.3°) are the same within experimental error as are the hydrogen bond lengths (average 2.660 Å). All of the C-C bond lengths (average 1.537 Å) are likewise the same within experimental error with the exception of the C(4)-C(5) bond distance (1.576(4) Å), which is slightly elongated (0.04 Å) in relation to the other C-C bonds. This bond length is similar to, although slightly longer than, distances determined from molecular mechanics calculations and conformational analysis of 2,2-dimethylbutane (1.5478 Å),[45] 2,3-dimethylbutane (1.552 Å)[46] and tricyclo[3,3,2,0]decane (1.556 Å).[47] Because of the lengthening of the C(4)-C(5) bond, the C(1)-C(5)-C(4) and C(3)-C(4)-C(5) bond angles (102.4(2)°) are smaller than the other three angles of the five-membered ring (average 106.7°). This elongation may also in part be due to steric effects resulting from having four groups on adjacent carbon atoms of the ring. The remaining bond angles around C(4) and C(5) are all similar (average 109.3°) with the exception of C(4)-C(5)-C(7) (116.1(2)°) and C(5)-C(4)-C(8) (116.2(2)°) which are significantly (6.9°) larger. In light of the fact that O(2) and O(3) are hydrogen bonded to one another, the 116° bond angles may be the result of the optimization of hydrogen bonding between O(2) and O(3).

Phosphate 11c, shown in Figure 4, is a tricyclic derivative of 2c containing a phosphorus atom bound to three of the oxygens of the 2c backbone and to a lone oxygen atom. The carbon-oxygen backbone of the molecule contains only slight deviations from the C-C distances found in 2d, including the C-C distances in the four-membered ring. In this slightly puckered ring, the elongation of the C(4)-C(5) bond is of the same magnitude as that in 2d and probably results from steric effects due to the substitution of the four-membered ring. The phosphorus atom in 11c is in a roughly tetrahedral environment of oxygens with a slight twist of the OPO_3 group, with respect to the axis defined by P and the midpoint of C_3 and C_f, similar to the twist of this group found in 23[48] and 24.[49] The O-P-O bond angles

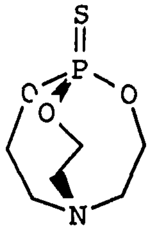

23

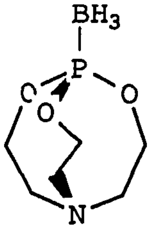

24

containing the phosphoryl oxygen yield slightly larger values (average 111.66°) than those containing only cage oxygen atoms (average 107.19°) and this deviation from tetrahedrality is a common occurrence in the structures of acyclic, monocyclic and bicyclic phosphate esters.[50]

Selected structural data for the two related bicyclic compounds (25[51] and 26[52]) and one tricyclic compound (27)[53]

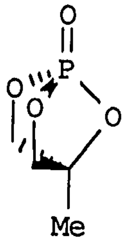

25

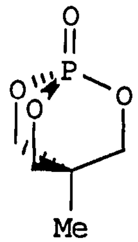

26

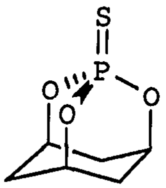

27

shown below are presented in Table 15 for comparison with 11c. The decrease in strain in going from highly strained 25 to the less strained 26 and 27 is evident from the P-O-C bond angles which in unstrained acyclic systems are ca. 120°.[25] For 25 these values are much lower (average 102.3°) than for 26 (average 115.3°) and 27 (average 113°). Comparison of these values with the analogous angles in 11c (average 119.7°) places this compound at the end of this list of phosphates in terms of ring strain. In fact this value indicates that there is little, if any, strain present in this region of the molecule. In combination with the NMR evidence showing that 11c and 22 have nearly the same basicity, this lack of strain gives support to the postulate that the relatively lower basicity of bicyclic phosphites compared to their acyclic analogs is predominantly the result of the constrained orientation of the lone electron pairs of the three oxygen atoms relative to the phosphorus lone pair, rather than the strain present in the molecule.[54]

Examination of the P-O bond distances in Tables 13 and 15 shows a longer P-O(2) distance in 25 than that in 11c. This is a function of the higher ring strain present in the region containing O(2) in 25. The P-O(3) and P-O(4) distances, contained in the less strained six-membered ring, are similar to those found in the structure of 11c. The P==O bond distance in 11c is typical of all phosphates including acyclic, monocyclic and bicyclic phosphates.[50] Although this P==O bond length is in the typical range, the phosphoryl oxygen also hydrogen bonds to the alcohol group of an adjacent molecule. Because of this hydrogen bonding the interaction between the alcohol group and proton b, detected in the NMR spectra of 11c, is not present in the solid state.

The structure of the tricyclic phosphate derivative 11d is presented in Figure 5. It is similar in structure to 11c and also to the analogous methylsilyl derivative of 2d, 28.[55] Although the relatively high standard deviations

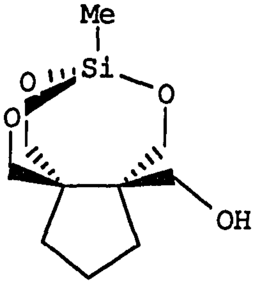

28

found in the bond distances and angles of 28 precludes comparison of these values with their counterparts in 11d, the structural data of 11c can be compared with that of 11d. With the exception of a slight reduction of the P-O(3) and P-O(4) distances, the distances found in the structure of 11d are equivalent to those of 11c within experimental error. Examination of the bond angles found in Table 14 shows that there are many small differences between the structure of 11c and that of 11d. The O(2)-P-O(3) angle is somewhat smaller in 11d (106.36(15)°) than the comparable distance in 11c (108.44(8)°). The P-O(2)-C(3) angle in 11d (119.46(21)°) is also smaller than that of 11c (120.5(1)°) while the P-O(4)-C(2), O(2)-C(3)-C(6) and O(3)-C(1)-C(5) angles of 11d (121.09(23)°, 112.48(29)° and 113.32(30)°, respectively) are somewhat larger than their counterparts in 11c (118.3(1)°, 107.4(2)° and 110.7(1)°, respectively). The remaining angles containing the carbon atoms of the cyclic ring in 11d are all distorted in comparison with those of 11c, as is expected in going from a cyclobutane to a cyclopentane derivative. The twist chair conformation of the five-membered ring, in which the four substituents on the ring are staggered rather than eclipsed, is present in 11d. This phosphate also contains a hydrogen bond between the phosphoryl oxygen and the alcohol group of an adjacent phosphate molecule as was found for 11c.

The X-ray structure of one of the diastereoisomers of 5c, displayed in Figure 2, contains a 1,3,2-dioxaphosphepane ring which is in a chair conformation similar to that found in 29 and 30.[56] As in the latter two compounds, in which

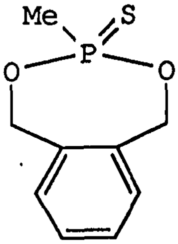

29

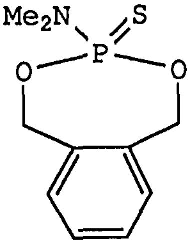

30

the unsaturation in the ring restricts its flexibility, the presence of the chair form of the seven-membered ring of 5c is probably due to the rigidity placed upon the system by the planar cyclobutane ring. The presence of this form in the crystal structure demonstrates the low energy difference between the planar and puckered conformations of the cyclobutane ring as well as the small difference in energy between the chair and twist forms of the seven-membered ring, the latter conformation being preferred by 5c in solution as demonstrated by its ^{1}H NMR spectrum. The more

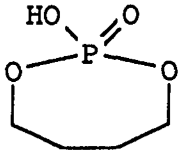

31

flexible 31[57] exhibits a twist-boat conformation of the seven-membered ring in the crystal. Unlike 11c, the cyclobutane ring in 5c is planar and the C-C-C bond angles in this ring are all ca. 90°. The high estimated standard deviations in the C-C bond distances do not allow a comparison of these distances but the expected elongation of the C-C bridgehead bond observed in 2d and 11c probably occurs. The cyclic ether ring is, for the same reason as the seven-membered ring, in the envelope rather than the half-chair form with C-C-C, C-C-O and C-O-C bond angles of ca. 103°. The P==O, P-O, O-C and C-C bond distances in 5c compare well with those of 29, 30 and 31, as well as with those of other cyclic phosphonate compounds.[50] As a result of the use of non-anhydrous solvent in the recrystallization of 5c, a hydrogen bonded water molecule appears in the unit cell as shown in Figure 9. This water molecule is hydrogen bonded through its two hydrogen atoms to two nearby phosphoryl oxygens and to two nearby phosphonate hydrogen atoms in a roughly tetrahedral geometry.

The structure of 9 is shown in Figure 3 and the 1,3,2-dioxaphosphepane ring in this compound is in the twist chair conformation. Although calculations and NMR data suggest this form to be the most stable of the possible conformations of cycloheptane,[58] 9 represents the first structurally characterized 1,3,2-dioxaphosphepane to exhibit

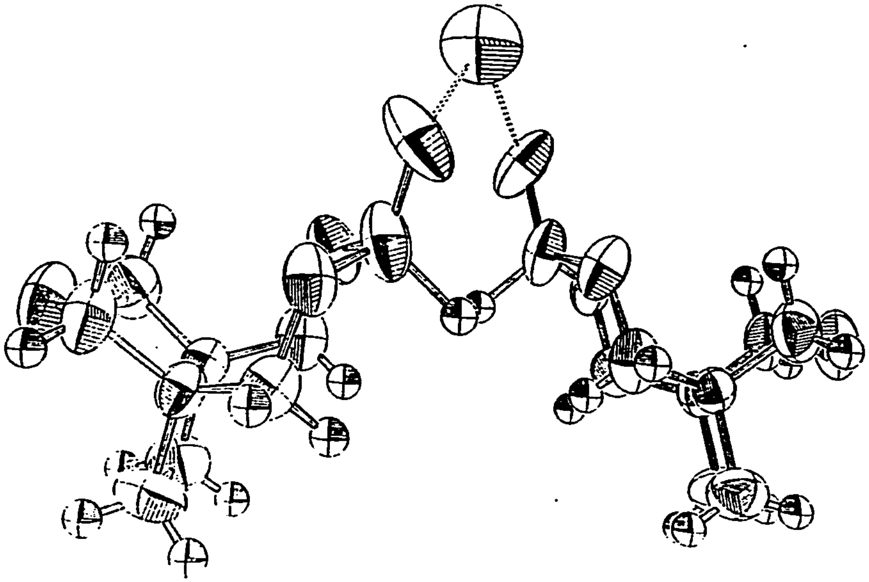

Figure 9. ORTEP drawing of 5c showing the hydrogen bonded water molecule in the unit cell

this conformation. The presence of this orientation is probably the result of the higher degree of flexability of the cyclopentane ring (which can easily adopt a staggered configuration around the bridgehead carbon atoms) in comparison with the cyclobutane ring in 5c which forces eclipsing around the bridgehead carbons in this tricyclic structure. The relatively high estimated standard deviations in the P-O, O-C and C-C distances of the seven-membered ring make comparisons of these bond lengths with those of the compounds 29-31 unreliable. Comparisons can be made, though, with the bond angles of these structures. Unlike 5c, 29, 30 and 31, compound 9 shows a great deal of variation within the pairs of P-O-C, and C-C-C angles of the seven-membered ring. While the P-O-C angles in 5c are the same within experimental error (121.2(5)° and 120.3(5)°) the analogous bond angles in 9 (115.7(2)° and 125.5(2)°) differ by nearly 10°. The same effect is also found in the C-C-C angles in 9 (117.0(3) and 113.8(3)°) although the difference (3°) is much smaller. Since the pairs of P-O-C, O-C-C and C-C-C bond angles in the twist boat conformation of 31 bare the same relationship as in 5c, the differences in the C-C-C and P-O-C angles in 9 are probably not due to distortion inherent in the twist chair form of the 1,3,2-dioxaphosphepane system. Though steric effects caused by the presence of the bulky triphenylmethyl substituent on phosphorus could lead to the distortion of the seven-membered ring, the hydrogen bonding found in this system is probably also a factor in this distortion. The triphenylmethyl group itself shows no sign of distortion and the three C(1)-C distances and C-C(1)-C bond angles are the same within experimental error. The triphenylmethyl group, however, is so large that only one of the alcohol groups of an adjacent molecule can hydrogen bond to the phosphoryl oxygen. Since the remaining alcohol function cannot approach the phosphoryl oxygen, it is hydrogen bonded to the phosphoryl-bound alcohol group of another molecule. This dissymmetry, the result of both the bulky substituent on phosphorus and the hydrogen bonding in the solid, probably also plays a role in the distortion found in the 1,3,2-dioxaphosphepane ring.

Because of the conformation of the dioxaphosphepane ring in 9, the conformation of the cyclopentane ring is a puckered one rather than the envelope as was found for the cyclic ether group of 5c. As in the structure of 5c, the C-C bond distances and bond angles of the five-membered ring in 9 are all the same within experimental error. The P==O bond distance and O(1)-P-O bond angles are similar to those present in 5c.

CONCLUSIONS

It has been shown that it is possible to prepare bi- and tricyclic phosphorus compounds 4-20 containing pendant alcohol groups. The structural and spectroscopic properties of these compounds, as well as their reactivity, indicate they are (with one notable exception) similar to known bicyclic phosphorus species. NMR spectroscopic examination of 4-20 indicates they are tri- or tetracoordinate displaying no evidence for the tautomeric equilibrium between these forms and pentacoordinate species. A very unusual feature of phosphites 4a-e is that they undergo an unusual acid catalyzed rearrangement to form phosphonates 5a-e. This reaction is tentatively proposed to proceed by two different pathways in which the intermediates are either protonated at phosphorus or protonated at one of the oxygens. However, the pathway involving protonation at phosphorus is believed to be a minor pathway based on the hydrolysis of 7d which is very slow and yields 9. The structure of the latter compound, determined by X-ray means represents the first 1,3,2-dioxaphosphepane containing a twist chair conformation.

Table 1. ^{1}H NMR spectral data (chemical shifts (ppm) and coupling constants (Hz)) for compounds 3-5, 7-20

Compounds	3[a]	4a[b]	4b[b]	4c[b]	4d[a]	4e[a]
Ha	3.46	3.45	3.42	3.51	3.49	
[$^2J(H_aCH_{a'})$]		10.65	10.43	10.38	10.30	10.12
[$^4J(H_aCCCH_c)$]					0.60	
[$^3J(H_aCOH)$]		5.25	5.19	5.30		
[$^3J(H_aCCH_f)$]		6.38				
$H_{a'}$		3.38	4.11	4.06	3.86	3.80
[$^2J(H_{a'}CH_a)$]		10.65	10.43	10.38	10.30	10.12
[$^4J(H_{a'}CCCH_c)$]					0.60	
[$^3J(H_{a'}COH)$]		5.25	5.19	5.30		
[$^3J(H_{a'}CCH_f)$]		6.79				
H_b		4.21	4.61	4.53	4.20	4.27
[$^2J(H_bCH_{b'})$]		10.99	10.66	10.78	10.70	10.53
[$^3J(H_bCOP)$]		1.20	1.12	1.20	2.00	1.99
[$^4J(H_bCCCH_d)$]		3.60	3.61	3.60	3.20	3.59
[$^3J(H_bCCH_e)$]		2.62				

---

[a] $CDCl_3$.

[b] DMSO.

Table 1. Continued

Compounds	3[a]	4a[b]	4b[b]	4c[b]	4d[a]	4e[a]
$H_{b'}$		4.14	3.85	3.99	3.69	3.68
$[^2J(H_{b'},CH_b)]$		10.99	10.66	10.78	10.70	10.53
$[^3J(H_{b'},COP)]$		3.35	3.60	3.60	3.20	3.45
$[^3J(H_{b'},CCH_e)]$		3.35				
H_c	4.07	4.00	3.99	4.05	3.84	3.84
$[^2J(H_cCH_{c'})]$		11.34	11.93	4.40	11.80	11.68
$[^3J(H_cCOP)]$	7.62	10.86	10.61		3.30	11.13
$[^4J(H_cCCCH_a)]$					0.60	
$[^3J(H_cCCH_f)]$	6.08	5.86				
$H_{c'}$		3.86	4.05	4.08	3.95	3.99
$[^2J(H_{c'},CH_c)]$		11.34	11.93	4.40	11.80	11.68
$[^3J(H_{c'},COP)]$		4.73	3.46		12.00	3.24
$[^3J(H_{c'},CCH_f)]$		9.85				
$[^4J(H_{c'},CCCH_{a'})]$					0.60	
H_d	4.27	3.87	3.77	3.93	3.74	3.77
$[^2J(H_dCH_{d'})]$	9.88	10.53	10.30	10.28	11.20	11.50
$[^3J(H_dCOP)]$	2.98	3.20	3.33	3.40	3.20	3.19
$[^4J(H_dCCCH_b)]$		3.60	3.61	3.60	3.20	3.59
$[^3J(H_dCCH_e)]$	2.18	2.78				

Table 1. Continued

Compounds	$\underline{3}^a$	$\underline{4a}^b$	$\underline{4b}^b$	$\underline{4c}^b$	$\underline{4d}^a$	$\underline{4e}^a$
$H_{d'}$	3.94	4.29	3.90	3.82	3.76	3.82
$[^2J(H_{d'}CH_d)]$	9.88	10.53	10.30	10.28	11.20	11.50
$[^3J(H_{d'}COP)]$	3.21	3.81	3.89	2.68	3.20	3.24
$[^3J(H_{d'}CCH_e)]$	1.54	3.81				
H_e	2.27	1.89				
$[^3J(H_eCCH_f)]$	4.08					
$[^3J(H_eCCH_b)]$		2.62				
$[^3J(H_eCCH_{b'})]$		3.35				
$[^3J(H_eCCH_d)]$	2.18	2.78				
$[^3J(H_eCCH_{d'})]$	1.54	3.81				
H_f	2.13	1.61				
$[^3J(H_fCH_e)]$	4.08					
$[^3J(H_fCCH_a)]$		6.38				
$[^3J(H_fCCH_{a'})]$		6.79				
$[^3J(H_fCCH_c)]$	6.08	5.86				
$[^3J(H_fCCH_{c'})]$		9.85				
H		5.11	5.03	4.91		
$[^3J(HOCH_a)]$		5.25	5.19	5.30		
$[^3J(HOCH_{a'})]$		5.25	5.19	5.30		
ring			1.98m	2.10m	1.89m	1.76m

Table 1. Continued

Compounds	5a[a]	5b[a]	5c[a]	5d[a]	5e[a]	9[a]
H_a	3.89m[c]	3.66m[c]	3.71 3.66	3.75m[c]	3.90m[c]	3.61
$[^2J(H_aCH_{a'})]$			9.13 9.31			11.80
$[^3J(H_aCOH)]$						
$[^3J(H_aCCH_f)]$						
$H_{a'}$			3.84 3.83			3.65
$[^2J(H_{a'}CH_a)]$			9.13 9.31			11.80
$[^3J(H_{a'}COH)]$						
$[^3J(H_{a'}CCH_f)]$						

---

[c] Detailed NMR analyses were not carried out for this compound. The values given include the resonances for H_a, $H_{a'}$, H_b and $H_{b'}$.

Table 1. Continued

Compounds	5a^a	5b^a	5c^a	5d^a	5e^a	9^a
H_b			4.66			4.13
			4.34			
$[^2J(H_bCH_{b'})]$			12.93			12.83
			12.98			
$[^3J(H_bCOP)]$			14.10			18.50
			19.16			
$[^4J(H_bCCCH_d)]$						
$[^3J(H_bCCH_e)]$						
$H_{b'}$			3.95			3.24
			4.04			
$[^2J(H_{b'}CH_b)]$			12.93			12.83
			12.98			
$[^3J(H_{b'}COP)]$			19.07			13.05
			17.16			
$[^3J(H_{b'}CCH_e)]$						
H_c	6.84	6.80	6.83	6.84	6.92	
	6.96	6.98	6.95	6.95	7.03	
$[^2J(H_cCH_{c'})]$						
$[^3J(H_cCOP)]$	7.15	7.22	7.17	7.20	7.22	
	6.95	6.99	6.98	7.01	7.00	
$[^3J(H_cCCH_f)]$						

Table 1. Continued

Compounds	5a^a	5b^a	5c^a	5d^a	5e^a	9^a
$H_{c'}$						
$[^2J(H_{c'}CH_c)]$						
$[^3J(H_{c'}COP)]$						
$[^3J(H_{c'}CCH_f)]$						
H_d						
$[^2J(H_dCH_{d'})]$						
$[^3J(H_dCOP)]$						
$[^4J(H_dCCCH_b)]$						
$[^3J(H_dCCH_e)]$						
$H_{d'}$						
$[^2J(H_{d'}CH_d)]$						
$[^3J(H_{d'}COP)]$						
$[^3J(H_{d'}CCH_e)]$						
H_e	2.09					
$[^3J(H_eCCH_f)]$						
$[^3J(H_eCCH_b)]$						
$[^3J(H_eCCH_{b'})]$						
$[^3J(H_eCCH_d)]$						
$[^3J(H_eCCH_{d'})]$						

Table 1. Continued

Compounds	$\underline{5a}^a$	$\underline{5b}^a$	$\underline{5c}^a$	$\underline{5d}^a$	$\underline{5e}^a$	$\underline{9}^a$
H_f						
$[^3J(H_fCH_e)]$						
$[^3J(H_fCCH_a)]$						
$[^3J(H_fCCH_{a'})]$						
$[^3J(H_fCCH_c)]$						
$[^3J(H_fCCH_{c'})]$						
H						
$[^3J(HOCH_a)]$						
$[^3J(HOCH_{a'})]$						
ring		2.08m	1.98m	2.48m	1.85m	1.5m
			1.95m			
Ph						7.35m

Table 1. Continued

Compounds	7a[d]	7b[d]	7c[d]	7d[d]	8e[d]
H_a	3.50m[e]	3.67m[e]	3.73m[e]	3.80m[e]	3.94m[e]
$[^2J(H_aCH_{a'})]$					
$[^3J(H_aCOH)]$					
$[^3J(H_aCCH_f)]$					
$H_{a'}$					
$[^2J(H_{a'}CH_a)]$					
$[^3J(H_{a'}COH)]$					
$[^3J(H_{a'}CCH_f)]$					
H_b					
$[^2J(H_bCH_{b'})]$					
$[^3J(H_bCOP)]$					
$[^4J(H_bCCCH_d)]$					
$[^3J(H_bCCH_e)]$					
$H_{b'}$					
$[^2J(H_{b'}CH_b)]$					
$[^3J(H_{b'}COP)]$					
$[^3J(H_{b'}CCH_e)]$					

---

[d] Acetonitrile.

[e] Detailed NMR analyses were not carried out for this compound. The value given includes the resonances for H_a, $H_{a'}$, H_b, $H_{b'}$, H_c, $H_{c'}$, H_d and $H_{d'}$.

Table 1. Continued

Compounds	7a[d]	7b[d]	7c[d]	7d[d]	8e[d]
H_c					
$[^2J(H_cCH_{c'})]$					
$[^3J(H_cCOP)]$					
$[^3J(H_cCCH_f)]$					
$H_{c'}$					
$[^2J(H_{c'}CH_c)]$					
$[^3J(H_{c'}COP)]$					
$[^3J(H_{c'}CCH_f)]$					
H_d					
$[^2J(H_dCH_{d'})]$					
$[^3J(H_dCOP)]$					
$[^4J(H_dCCCH_b)]$					
$[^3J(H_dCCH_e)]$					
$H_{d'}$					
$[^2J(H_{d'}CH_d)]$					
$[^3J(H_{d'}COP)]$					
$[^3J(H_{d'}CCH_e)]$					

Table 1. Continued

Compounds	7a[d]	7b[d]	7c[d]	7d[d]	8e[d]
H_e	2.16m[f]				
$[^3J(H_eCCH_f)]$					
$[^3J(H_eCCH_b)]$					
$[^3J(H_eCCH_{b'})]$					
$[^3J(H_eCCH_d)]$					
$[^3J(H_eCCH_{d'})]$					
H_f					
$[^3J(H_fCH_e)]$					
$[^3J(H_fCCH_a)]$					
$[^3J(H_fCCH_{a'})]$					
$[^3J(H_fCCH_c)]$					
$[^3J(H_fCCH_{c'})]$					
H					
$[^3J(HOCH_a)]$					
$[^3J(HOCH_{a'})]$					
ring		2.37m	2.34m	1.7m	2.27m
Ph_3C	7.5m	7.5m	7.5m	7.5m	
Me					2.61

---

[f] Detailed NMR analyses were not carried out for this compound. The value given includes the resonances for H_e and H_f.

Table 1. Continued

Compounds	10a^a	10b^a	10c^a	10d^a	15^a
H_a	3.94m^e	3.86m^e	4.02m^e	4.50	4.48
[$^2J(H_aCH_{a'})$]				11.10	11.21
[$^3J(H_aCOH)$]					
[$^3J(H_aCCH_f)$]					
$H_{a'}$				4.53	4.52
[$^2J(H_a{'}CH_a)$]				11.10	11.21
[$^3J(H_a{'}COH)$]					
[$^3J(H_a{'}CCH_f)$]					
H_b				4.35	4.51
[$^2J(H_bCH_{b'})$]				10.80	10.90
[$^3J(H_bCOP)$]				1.71	3.72
[$^4J(H_bCCCH_d)$]					3.72
[$^3J(H_bCCH_e)$]					
$H_{b'}$				3.84	4.22
				10.80	10.90
[$^2J(H_{b'}CH_b)$]				3.20	6.74
[$^3J(H_{b'}COP)$]					
[$^3J(H_{b'}CCH_e)$]					

Table 1. Continued

Compounds	<u>10a</u>^{a}	<u>10b</u>^{a}	<u>10c</u>^{a}	<u>10d</u>^{a}	<u>15</u>^{a}
H_c				4.04	4.05
$[^2J(H_cCH_{c'})]$				12.03	12.20
$[^3J(H_cCOP)]$				3.10	3.20
$[^3J(H_cCCH_f)]$					
$H_{c'}$				4.14	4.36
$[^2J(H_{c'}CH_c)]$				12.03	12.00
$[^3J(H_{c'}COP)]$				12.03	33.20
$[^3J(H_{c'}CCH_f)]$					
H_d				3.91	4.14
$[^2J(H_dCH_{d'})]$					11.20
$[^3J(H_dCOP)]$					11.40
$[^4J(H_dCCCH_b)]$					3.72
$[^3J(H_dCCH_e)]$					
$H_{d'}$				3.91	4.34
$[^2J(H_{d'}CH_d)]$					11.20
$[^3J(H_{d'}COP)]$					7.18
$[^3J(H_{d'}CCH_e)]$					

Table 1. Continued

Compounds	10a^a	10b^a	10c^a	10d^a	15^a
H_e	1.68m^f				
$[^3J(H_eCCH_f)]$					
$[^3J(H_eCCH_b)]$					
$[^3J(H_eCCH_{b'})]$					
$[^3J(H_eCCH_d)]$					
$[^3J(H_eCCH_{d'})]$					
H_f					
$[^3J(H_fCH_e)]$					
$[^3J(H_fCCH_a)]$					
$[^3J(H_fCCH_{a'})]$					
$[^3J(H_fCCH_c)]$					
$[^3J(H_fCCH_{c'})]$					
H					
$[^3J(HOCH_a)]$					
$[^3J(HOCH_{a'})]$					
ring		2.18m	2.24m	1.80m	1.83m
Ph	7.23	7.20	7.23	7.21	7.30

Table 1. Continued

Compounds	11a[a]	11b[a]	11c[a]	11d[a]	11e[a]	18[a]
H_a	3.56	3.89m[e]	4.21	3.52	3.75m[e]	
$[^2J(H_aCH_{a'})]$	11.13		10.73	10.70		
$[^3J(H_aCCH_c)]$				1.00		
$[^3J(H_aCOH_f)]$						
$H_{a'}$	3.50		4.31	3.70		
$[^2J(H_{a'}CH_a)]$	11.13		10.73	10.70		
$[^4J(H_{a'}CCCH_c)]$				0.90		
$[^3J(H_{a'}COH)]$						
$[^3J(H_{a'}CCH_f)]$	6.71					
H_b	4.52		5.20	4.51		
$[^2J(H_bCH_{b'})]$	10.15		10.72	10.70		
$[^3J(H_bCOP)]$	10.15		5.99	8.00		
$[^4J(H_bCCCH_d)]$	1.54		3.56	3.70		
$[^3J(H_bCCH_e)]$	2.19[illegible]					
$H_{b'}$	4.62		4.74	4.19		
$[^2J(H_{b'}CH_b)]$	10.15		10.72	10.70		
$[^3J(H_{b'}COP)]$	10.15					
$[^3J(H_{b'}CCH_e)]$	3.26					

Table 1. Continued

Compounds	11a^{a}	11b^{a}	11c^{a}	11d^{a}	11e^{a}	18^{a}
H_c	3.79		4.43	3.88		4.18
$[{}^2J(H_cCH_{c'})]$	12.00		11.42	11.90		
$[{}^3J(H_cCOP)]$	8.84		3.13	3.10		18.33
$[{}^4J(H_cCCCH_a)]$				1.00		
$[{}^3J(H_cCCH_f)]$	9.98					6.15
$H_{c'}$	4.16		4.54	4.19		
$[{}^2J(H_{c'}CH_c)]$	12.00		11.42	11.90		
$[{}^3J(H_c'COP)]$	27.28			33.10		
$[{}^3J(H_c'CCH_f)]$	5.48					
$[{}^3J(H_{c'}CCCH_{a'})]$				0.90		
H_d	4.18		4.46	4.01		4.27
$[{}^2J(H_dCH_{d'})]$	8.34		10.72	10.70		9.37
$[{}^3J(H_dCOP)]$	8.34		10.72	10.70		7.06
$[{}^4J(H_dCCCH_b)]$	1.54		3.56	3.70		
$[{}^3J(H_dCCH_e)]$	3.34					1.36
$H_{d'}$	4.52		4.57	4.20		4.57
$[{}^2J(H_{d'}CH_d)]$	8.34		10.72	10.70		9.37
$[{}^3J(H_{d'}COP)]$	1.85		5.41	6.80		
$[{}^3J(H_{d'}CCH_e)]$	1.85					2.13

Table 1. Continued

Compounds	$\underline{11a}^a$	$\underline{11b}^a$	$\underline{11c}^a$	$\underline{11d}^a$	$\underline{11e}^a$	$\underline{18}^a$
H_e	2.58					2.43
$[^3J(H_eCCH_f)]$						4.42
$[^3J(H_eCCH_b)]$	2.19					
$[^3J(H_eCCH_{b'})]$	3.26					
$[^3J(H_eCCH_d)]$	3.34					1.36
$[^3J(H_eCCH_{d'})]$	1.85					2.13
H_f	2.35					2.35
$[^3J(H_fCH_e)]$						4.42
$[^3J(H_fCCH_a)]$	6.46					
$[^3J(H_fCCH_{a'})]$	6.71					
$[^3J(H_fCCH_c)]$	5.48					6.15
$[^3J(H_fCCH_{c'})]$	9.98					
H						
$[^3J(HOCH_a)]$						
$[^3J(HOCH_{a'})]$						
ring		2.25m	2.43m	2.01m	2.22m	

Table 1. Continued

Compounds	$\underline{12a}^{a}$	$\underline{12b}^{a}$	$\underline{12c}^{a}$	$\underline{16}^{a}$	$\underline{17}^{a}$
H_a	3.73m^{e}	3.64m	3.51	3.45	3.65
$[^2J(H_aCH_{a'})]$			10.70	9.0	9.70
$[^4J(H_aCCCH_c)]$			1.20		
$[^3J(H_aCOH)]$					
$[^3J(H_aCCH_f)]$					
$H_{a'}$		3.64m	3.70	3.49	3.75
$[^2J(H_{a'}CH_a)]$			10.70	9.0	9.70
$[^3J(H_{a'}COH)]$					
$[^3J(H_{a'}CCH_f)]$					
H_b		4.30m	4.54	4.43	4.44
$[^2J(H_bCH_{b'})]$			10.70	10.70	10.70
$[^3J(H_bCOP)]$			8.20	8.00	8.20
$[^4J(H_bCCCH_d)]$			3.70	3.60	3.60
$[^3J(H_bCCH_e)]$					
$H_{b'}$		4.30m	4.21	4.14	4.14
$[^2J(H_{b'}CH_b)]$			10.70	10.70	10.70
$[^3J(H_{b'}COP)]$			7.20	7.00	6.80
$[^3J(H_{b'}CCH_e)]$					

Table 1. Continued

Compounds	12a[a]	12b[a]	12c[a]	16[a]	17[a]
H_c		3.98m	3.96	3.89	3.87
[$^2J(H_cCH_{c'})$]			11.90	11.90	12.00
[$^3J(H_cCOP)$]			4.10	3.20	2.80
[$^4J(H_cCCCH_a)$]			1.20		
[$^3J(H_cCCH_f)$]					
$H_{c'}$		4.30m	4.21	4.18	4.16
[$^2J(H_{c'}CH_c)$]			11.90	11.90	12.00
[$^3J(H_{c'}COP)$]			33.50	33.10	33.60
[$^3J(H_{c'}CCH_f)$]					
H_d		3.98m	4.02	4.02	4.05
[$^2J(H_dCH_{d'})$]			10.90	10.70	10.70
[$^3J(H_dCOP)$]			10.60	10.70	10.70
[$^4J(H_dCCCH_b)$]			3.70	3.60	3.60
[$^3J(H_dCCH_e)$]					
$H_{d'}$		4.30m	4.26	4.24	4.23
[$^2J(H_{d'}CH_d)$]			10.90	10.70	10.70
[$^3J(H_{d'}COP)$]			7.70	7.00	7.50
[$^3J(H_{d'}CCH_e)$]					

Table 1. Continued

Compounds	12a^a	12b^a	12c^a	16^a	17^a
H_e	1.81m^f				
[$^3J(H_eCCH_f)$]					
[$^3J(H_eCCH_b)$]					
[$^3J(H_eCCH_{b'})$]					
[$^3J(H_eCCH_d)$]					
[$^3J(H_eCCH_{d'})$]					
H_f					
[$^3J(H_fCH_e)$]					
[$^3J(H_fCCH_a)$]					
[$^3J(H_{fC}CH_{a'})$]					
[$^3J(H_fCCH_c)$]					
[$^3J(H_fCCH_{c'})$]					
H					
[$^3J(HOCH_a)$]					
[$^3J(HOCH_{a'})$]					
ring		2.48m	2.36m	2.19m	2.32m
Me				3.38	0.075
					0.079
tBu					0.90

Table 1. Continued

Compounds	13a^g	13b^g	13c^g	13d^g	13e^g	20^g
H_a	3.67m^e	3.86m^e	3.62m^e	3.40	3.67m^e	
$[^2J(H_aCH_{a'})]$				10.40		
$[^4J(H_aCCCH_c)]$				1.01		
$[^3J(H_aCOH_f)]$				5.17		
$[^3J(H_aCCH_f)]$						
$H_{a'}$				3.54		
$[^2J(H_{a'}CH_a)]$				10.40		
$[^3J(H_{a'}COH)]$				5.17		
$[^3J(H_{a'}CCH_f)]$						
H_b				4.64		
$[^2J(H_bCH_{b'})]$				10.45		
$[^3J(H_bCOP)]$				7.76		
$[^4J(H_bCCCH_d)]$				3.59		
$[^3J(H_bCCH_e)]$						
$H_{b'}$				4.30		
$[^2J(H_{b'}CH_b)]$				1.45		
$[^3J(H_{b'}COP)]$				7.78		
$[^3J(H_{b'}CCH_e)]$						

---

^{g}Xylene/d_6-benzene.

Table 1. Continued

Compounds	13a[g]	13b[g]	13c[g]	13d[g]	13e[g]	20[g]
H_c				4.01		4.10
$[^2J(H_cCH_{c'})]$				11.61		
$[^3J(H_cCOP)]$				5.34		
$[^4J(H_cCCCH_a)]$				1.01		
$[^3J(H_cCCH_f)]$						
$H_{c'}$				4.17		
$[^2J(H_{c'}CH_c)]$				11.61		
$[^3J(H_{c'}COP)]$				33.09		
$[^3J(H_{c'}CCH_f)]$						
H_d				4.01		
$[^2J(H_dCH_{d'})]$				10.58		
$[^3J(H_dCOP)]$				10.58		
$[^4J(H_dCCCH_b)]$				3.59		
$[^3J(H_dCCH_e)]$						
$H_{d'}$				4.32		
$[^2J(H_{d'}CH_d)]$				10.58		
$[^3J(H_{d'}COP)]$				8.22		
$[^3J(H_{d'}CCH_e)]$						

Table 1. Continued

Compounds	13a^g	13b^g	13c^g	13d^g	13e^g	20^g
H_e	1.77m^f					2.18m
$[^3J(H_eCCH_f)]$						
$[^3J(H_eCCH_b)]$						
$[^3J(H_eCCH_{b'})]$						
$[^3J(H_eCCH_d)]$						
$[^3J(H_eCCH_{d'})]$						
H_f						
$[^3J(H_fCH_e)]$						
$[^3J(H_fCCH_a)]$						
$[^3J(H_fCCH_{a'})]$						
$[^3J(H_fCCH_c)]$						
$[^3J(H_fCCH_{c'})]$						
H				5.03		
$[^3J(HOCH_a)]$				5.17		
$[^3J(HOCH_{a'})]$				5.17		
ring		2.27m	2.37m	10.65m	1.94m	

Table 1. Continued

Compounds	14a[d]	14b[d]	14c[d]	14d[d]	14e[d]	19[d]
H_a	3.45m	3.62m[e]	3.64m	3.55m	3.71m[e]	
$[^2J(H_aCH_{a'})]$						
$[^3J(H_aCOH)]$						
$[^3J(H_aCCH_f)]$						
$H_{a'}$	3.45m		3.69m	3.55m		
$[^2J(H_{a'}CH_a)]$						
$[^3J(H_{a'}COH)]$						
$[^3J(H_{a'}CCH_f)]$						
H_b	4.19m		4.82m	4.65m		
$[^2J(H_bCH_{b'})]$						
$[^3J(H_bCOP)]$						
$[^4J(H_bCCCH_d)]$						
$[^3J(H_bCCH_e)]$						
$H_{b'}$	4.50m		4.30m	4.05m		
$[^2J(H_{b'}CH_b)]$						
$[^3J(H_{b'}COP)]$						
$[^3J(H_{b'}CCH_e)]$						

Table 1. Continued

Compounds	14a^{d}	14b^{d}	14c^{d}	14d^{d}	14e^{d}	19^{d}
H_c	4.10m		3.84m	3.93m		4.17
$[^2J(H_cCH_{c'})]$						
$[^3J(H_cCOP)]$						13.63
$[^3J(H_cCCH_f)]$						6.08
$H_{c'}$	3.92m		4.11m	4.20		
$[^2J(H_{c'}CH_c)]$						
$[^3J(H_{c'}COP)]$						
$[^3J(H_{c'}CCH_f)]$						
H_d	4.50m		3.76m	4.05		4.46
$[^2J(H_dCH_{d'})]$						9.31
$[^3J(H_dCOP)]$						6.92
$[^4J(H_dCCCH_b)]$						
$[^3J(H_dCCH_e)]$						1.25
$H_{d'}$	4.58m		4.17m	4.20		4.18
$[^2J(H_{d'}CH_d)]$						9.31
$[^3J(H_{d'}COP)]$						7.04
$[^3J(H_{d'}CCH_e)]$						1.61

Table 1. Continued

Compounds	$\underline{14a}^d$	$\underline{14b}^d$	$\underline{14c}^d$	$\underline{14d}^d$	$\underline{14e}^d$	$\underline{19}^d$
H_e						
$[^3J(H_eCCH_f)]$						4.63
$[^3J(H_eCCH_b)]$						
$[^3J(H_eCCH_{b'})]$						
$[^3J(H_eCCH_d)]$						1.25
$[^3J(H_eCCH_{d'})]$						1.61
H_f						
$[^3J(H_fCH_e)]$						4.63
$[^3J(H_fCCH_a)]$						
$[^3J(H_{fC}CH_{a'})]$						
$[^3J(H_fCCH_c)]$						
$[^3J(H_fCCH_{c'})]$						6.08
H						
$[^3J(HOCH_a)]$						
$[^3J(HOCH_{a'})]$						
ring		2.04m	2.27m	2.31m	1.97m	

Table 2. ^{13}C NMR data (chemical shift, (ppm) and coupling constants (Hz)) for compounds 3-4, 7d, 9, 11, 12, 13a, 13c, 13d, 14, 18, and 19

Compound	3[a]	4a[a]	4b[a]	4b[a]	4d[a]	4e[a]
Carbon						
a	62.18s	62.25s	62.46s	61.37s	61.60s	
b	63.98s	72.19s	72.30s	72.25d	72.72s	
$J(C_b\text{-}P)$				<2.4	2.24	
c	67.91s	68.78d	68.54d	68.97d	66.57d	66.70d
$J(C_c\text{-}P)$		4.29	5.05	5.26	3.66	3.19
d	61.35d	63.21d	67.80d	68.52d	66.37d	65.18d
$J(C_d\text{-}P)$	6.85	4.9	5.73	5.02	5.93	5.89
e	34.29d	36.08d	32.17d	44.80d	49.08d	48.66d
$J(C_e\text{-}P)$	14.35	12.81	14.43	14.71	12.23	12.50
f	47.57s	47.34s	37.59s	49.16d	54.77s	51.61s
$J(C_f\text{-}P)$				5.01		
g			20.37	22.25s	32.91s	30.43s

---

[a] $CDCl_3$.

Table 2. Continued

Compound	3[a]	4a[a]	4b[a]	4b[a]	4d[a]	4e[a]
Carbon						
h				21.64s	29.93s	28.17s
i					21.21s	20.75s
j						19.82s

Table 2. Continued

Compound	7d[b]	9[c]	18[a]	11a[a]	11b[a]	11c[a]
Carbon						
a	61.30s	63.98		61.79s	61.37s	61.29s
b	80.87	70.61d		74.56d	74.52d	77.38d
$J(C_b\text{-}P)$	7.1	7.4		7.17	7.82	7.9
c	75.97d		71.83d	70.59d	70.21d	71.84d
$J(C_c\text{-}P)$	7.9		5.66	5.07	5.30	7.2
d	75.18d		62.93d	66.44d	68.17d	69.50d
$J(C_d\text{-}P)$	8.0		7.21	6.7	7.11	3.4
e	52.40d	51.87s	32.73d	36.07d	32.20d	50.37d
$J(C_e\text{-}P)$	13.8		13.24	13.66	15.74	13.15
f	56.88s		34.032s	46.72s	37.22s	55.72s
$J(C_f\text{-}P)$						

---

[b] Acetonitrile.

[c] Xylene/d_6-benzene.

Table 2. Continued

Compound	<u>7d</u>[b]	<u>9</u>[c]	<u>18</u>[a]	<u>11a</u>[a]	<u>11b</u>[a]	<u>11c</u>[a]
g	31.52s	28.92s			19.58s	31.34s
h	30.42s					30.34s
i	21.40s	17.99s				21.19s
P-<u>C</u>Ph$_3$	66.35d	62.28d				
[J(P-C)]	[300.4]	[32.0]				
	130.26s	127.99s				
	130.90d	130.96d				
	[5.1]	[6.1]				
	136.61d	140.46d				
	[6.9]	[6.4]				

Table 2. Continued

Compound	11d[a]	11e[a]	12a	12b	12c	13a[c]
a	61.58s	61.76s	60.89	61.01	60.32s	59.94
b	74.76d	75.44d	73.71	74.2	77.40d	73.11
$J(C_b-P)$	6.279	7.7	8.5	8.2	8.3	9.49
c	70.92d	66.17d	71.03	70.69	72.01d	71.82
$J(C_c-P)$	6.230	5.9	8.8	9.2	9.4	9.97
d	67.85d	65.45d	63.2	70.33	70.15	62.48
$J(C_d-P)$	7.136	7.00	9.0	10.0	9.2	10.24
e	44.73d	49.01d	36.0	45.52	49.81d	35.32
$J(C_e-P)$	14.84	13.27	13.7	14.7	14.6	18.99
f	49.12s	51.72s	46.8	49.47	55.30	46.37
$J(C_f-P)$						
g	23.13s	30.61s		25.51	31.41s	
h	21.78s	27.95s		21.39	29.97s	
i		20.83s			21.10s	
j						

Table 2. Continued

Compound	13c^{c}	13d^{c}	19^{b}	14a^{b}	14b^{b}
Carbon					
a	59.27	59.02		60.9	61.2
b	73.70	76.62		74.5	74.5
J(C_b-P)	9.15	9.64		7.36	7.36
c	70.59	71.18	70.84	71.0	70.3
J(C_c-P)	10.30	10.46	8.00	9.11	8.69
d	69.80	69.47	63.60	62.6	69.4
J(C_d-P)	10.39	10.87	10.18	11.57	12.46
e	44.61	48.85	33.68	36.0	31.8
J(C_e-P)	18.58	18.61	14.82	13.88	13.77
f	48.95	54.02	34.39	47.2	38.0
J(C_f-P)					
g	25.37	30.49			19.4
h	21.53	28.68			
i		20.28			
j					

Table 2. Continued

Compound	14c[b]	14d[b]	14e[b]
Carbon			
a	61.59	61.4	61.5
b	74.60	77.5	75.2
$J(C_b-P)$	7.51	8.6	8.2
c	71.17	71.3	66.7
$J(C_c-P)$	9.96	11.86	9.2
d	70.29	70.3	64.1
$J(C_d-P)$	12.05	10.1	12.2
e	45.43	49.8	48.8
$J(C_e-P)$	13.97	13.72	14.01
f	49.69	55.9	52.0
$J(C_f-P)$			
g	25.51	30.7	31.0
h	21.50	30.4	27.4
i		21.3	20.5
j			

Table 3. ^{31}P NMR spectral data (chemical shifts (ppm) and coupling constants (Hz)) for compounds 3-5, 7-20

Compounds		Chemical Shift				
		a	b	c	d	e
3[a]	115.59					
4a-e[a]		113.99	111.73	114.58	111.45	113.23
5a-e[a]		12.09	15.21	14.32	12.00	12.45
[J(P-H)]		[715]	[722]	[717]	[720]	[722]
		11.38	14.72	13.97	11.39	11.67
		[695]	[699]	[698]	[701]	[700]
7a-e[b]		47.99	49.42	50.61	50.90	49.01
8[b]	35.23					
9[a]	30.07					
10a-d[a]		113.57	112.18	115.08	111.03	
11a-e[a]		-5.71	-5.80	-4.65	-5.29	-5.88
12a-c[a]		55.60		56.53	62.31	

---

[a] $CDCl_3$.

[b] Acetonitrile.

Table 3. Continued

Compounds		Chemical Shift				
		a	b	c	d	e
13a-e[c]		61.22	61.77	62.84	61.78	61.20
[J(P-Se)]		[1054]	[1054]	[1054]	[1050]	[1052]
14a=e[c]		106.24	105.92	107.13	106.73	106.79
[J(P-B)]		[97.12]	[95.69]	[94.20]	[97.44]	[97.83]
15[a]	-6.78					
16[a]	-6.15					
17[a]	-6.46					
18[a]	-5.23					
19[c]	107.04					
[J(P-B)]	[100.34]					
20[c]	60.91					
[J(P-Se)]	[1054]					

[c] Xylene/d_6-benzene.

Table 4. Crystallographic data for 2d, 5c, 9, 11c and 11d

Compound	2d	5c	9	11c	11d
mol. wt.	190.24	213.17	597.91	220.16	234.19
Space group	pl	C2/c	$P2_1/c$	$P2_1/n$	$P2_1/c$
a, /	7.342(3)	11.452(8)	15.638(2)	7.022(1)	7.5446(28)
b, /	11.857(3)	6.451(3)	11.119(3)	10.5157(9)	11.1327(46)
c, /	6.333(2)	26.03(5)	17.404(3)	13.122(2)	12.0613(33)
alpha, deg	100.47(3)				
beta, deg	115.57(3)	93.03(14)	106.06(1)	103.340(8)	91.141(29)
gamma, deg	85.51(4)				
Vol, $/^3$	489.03(24)	1920(4)	2908.2	942.8(2)	1012.849(62)
d_{calcd}, g/cm^3	1.29	1.47	1.38	1.55	1.536
Z	2	8	4	4	4
lambda	MoK_a	MoK_a	MoK_a	MoK_a	MoK_a
mo, cm^{-1}	0.94	2.64	4.0	2.761	2.616
cryst. size, mm		0.25 x 0.25 x 0.40	0.40 x 0.40 x 0.20	0.35 x 0.38 x 0.28	0.20 x 0.18 x 0.35
refl. coll.	±h, ±k, ±l	±h, ±k, ±l	±h, ±k, ±l	±h, ±k, ±l	±h, ±k, ±l

---

[a] The goodness of fit is defined as $[w F_o - F_c)^2/(n_o-n_u)]^{1/2}$, where n_o and n_u denote the number of data and variables, respectively.

Table 4. Continued

Compound	2d	5c	9	11c	11d
no of refl. coll.	2158	1801	3801	1651	3872
unique data w/$F^2 > 2s(F^2)$	1117	763	2304	1140	1118
range, deg	0-50	0-50	0-45	4-50	0-50
final R, %	6.2	6.6	4.4	3.53	6.8
final R_w, %	7.7	6.0	5.6	4.37	8.4
GOF[a]	0.95		1.66	1.37	
no. of var.	118		408	167	136
temp., °C	25±1	25±1	20±1	-20±1	23±1
mode	omega-scans	omega-scans	omega-scans	theta-2 theta	omega-scans
max. trans factor			1.00		
min. trans factor			0.84		

Table 5. Positional parameters (x 10^4) for 2d and their estimated standard deviations[a]

Atom	x	y	z	U_{iso}[b]
O(1)	3136(4)	0296(2)	3626(5)	70(1)
O(2)	-0483(4)	1394(2)	-1114(5)	80(1)
O(3)	-0482(4)	3605(2)	0627(6)	80(2)
O(4)	3135(4)	4705(2)	-0490(5)	70(1)
C(1)	5224(5)	1504(3)	1646(7)	56(2)
C(2)	6619(6)	2500(3)	3312(9)	77(2)
C(3)	5222(5)	3496(3)	3576(7)	55(2)
C(4)	3089(5)	3173(2)	1656(6)	42(1)
C(5)	3089(5)	1828(2)	1433(6)	43(1)
C(6)	2811(5)	1491(3)	3510(6)	54(2)
C(7)	1527(6)	1181(3)	-0887(6)	55(2)
C(8)	1527(6)	3821(3)	2407(7)	55(2)
C(9)	2816(5)	3508(3)	-0699(6)	54(2)
H(11)	526	140	-4	76
H(12)	572	74	235	76
H(21)	754	274	258	76
H(22)	754	226	497	76
H(31)	572	426	337	76
H(32)	526	361	530	76
H(61)	380	197	513	76
H(62)	130	170	331	76
H(71)	166	145	-232	76
H(72)	183	30	-95	76
H(81)	166	356	399	76
H(82)	183	471	277	76
H(91)	380	303	-133	76
H(92)	130	330	-201	76

[a] The estimated standard deviations in the parentheses are for the least significant digits. Parameters for hydrogen atoms are multiplied by 10^3.

[b] for anisotropically refined atoms, $U_{iso} \equiv 10^3/3 \; \Sigma U_{ij} a_i^* a_j^* \vec{a}_i \cdot \vec{a}_j$; where the temperature factors are defined as $\exp(-2\pi^2 \Sigma h_i h_j a_i^* a_j^* U_{ij})$.

Table 6. Positional parameters for 5c and their estimated standard deviations

Atom	x	y	x
P	0.8403(2)[a]	0.2553(5)	0.2012(1)
O(1)	0.7364(4)	0.1723(9)	0.1653(2)
O(2)	0.8221(6)	0.4693(11)	0.2155(2)
O(3)	0.9556(4)	0.2296(9)	0.1727(2)
O(4)	0.8582(6)	0.0835(11)	0.0265(2)
O(5)	1.0000	0.7117(17)	0.2500
C(1)	0.9532(9)	0.1170(17)	0.0624(3)
C(2)	0.7600(8)	0.0700(16)	0.0570(3)
C(3)	0.7987(6)	-0.0711(12)	0.1013(2)
C(4)	0.9337(6)	-0.0361(11)	0.1053(2)
C(5)	0.9922(8)	0.0254(16)	0.1559(3)
C(6)	0.8160(9)	-0.2960(14)	0.0866(4)
C(7)	0.7325(7)	-0.0413(15)	0.1481(3)
C(8)	0.9534(8)	-0.2640(16)	0.0915(4)
H(1)	0.851(5)	0.111(9)	0.241(2)
H(2)	0.973(5)	-0.063(9)	0.181(2)
H(3)	1.079(5)	0.034(9)	0.153(2)
H(4)	0.641(5)	-0.059(9)	0.142(2)
H(5)	0.764(5)	-0.136(9)	0.177(2)
H(6)	0.791(5)	-0.405(9)	0.108(2)
H(7)	0.786(5)	-0.340(9)	0.055(2)
H(8)	0.966(5)	-0.289(9)	0.060(2)
H(9)	0.978(5)	-0.345(9)	0.121(2)
H(10)	1.032(5)	0.086(9)	0.046(2)
H(11)	0.964(5)	0.267(9)	0.074(2)
H(12)	0.736(5)	0.219(9)	0.067(2)
H(13)	0.694(5)	0.010(9)	0.034(2)

[a] The estimated standard deviations in the parentheses are for the least significant digits. Parameters for hydrogen atoms are multiplied by 10^3.

Table 7. Positional parameters for 9 and their estimated standard deviations[a]

Atom	x	y	z	B(Å^2)
P	0.28793(7)	0.11323(9)	0.45653(6)	3.21(3)
O(1)	0.3489(2)	0.1582(2)	0.5301(20	3.97(7)
O(2)	0.3198(2)	-0.0044(2)	0.4223(1)	3.25(7)
O(3)	0.2770(2)	0.2091(2)	0.3884(2)	3.88(7)
O(4)	0.5389(2)	-0.0911(3)	0.3293(2)	4.32(8)
O(5)	0.3917(2)	0.3787(3)	0.2983(2)	5.7)1)
C(1)	0.1766(2)	0.0739(3)	0.4677(2)	3.2(1)
C(2)	0.4089(2)	0.0010(4)	0.4099(2)	3.2(10
C(3)	0.2762(3)	0.1833(4)	0.3057(2)	3.6(1)
C(4)	0.5070(3)	0.0294(4)	0.3252(2)	3.9(1)
C(5)	0.4293(3)	0.2675(4)	0.3316(3)	4.3(1)
C(6)	0.4079(2)	0.0357(3)	0.3254(2)	2.80(9)
C(7)	0.3683(2)	0.1612(3)	0.2951(2)	3.1(1)
C(8)	0.3529(3)	0.1509(4)	0.2029(2)	4.3(1)
C(9)	0.3415(4)	0.0175(4)	0.1828(3)	5.6(1)
C(10)	0.3532(3)	-0.0501(4)	0.2614(2)	3.7(1)
C(11)	0.1106(3)	0.0480(4)	0.3847(2)	3.5(1)
C(12)	0.0292(3)	0.1076(4)	0.3598(3)	4.8(1)
C(13)	-0.0319(3)	0.0781(5)	0.2878(3)	6.2(2)
C(14)	-0.0138(4)	-0.0110(5)	0.2403(3)	6.1(2)
C(15)	0.0666(4)	-0.0707(5)	0.2644(3)	5.2(1)
C(16)	0.1279(3)	-0.0422(4)	0.3358(2)	4.1(1)

---

[a] Starred atoms were refined isotropically. Anisotropically refined atoms are given in the form of the isotropic equivalent displacement parameter defined as: (4/3) * [a^2*B(1,1) + b^2*B(2,2) + c^2*B(3,3) + ab(cos gamma)*B(1,2) + ac(cos beta)*B(1,3) + bc(cos alpha)*B(2,3)].

Table 7. Continued

Atom	x	y	z	B(Å^2)
C(17)	0.1869(3)	-0.0384(4)	0.5217(2)	3.7(1)
C(18)	0.2510(3)	-0.0404(5)	0.5950(3)	6.0(1)
C(19)	0.2591(3)	-0.1390(7)	0.6455(4)	8.2(2)
C(20)	0.2029(4)	-0.2363(6)	0.6234(4)	7.3(2)
C(21)	0.1391(4)	-0.2335(5)	0.5528(4)	6.3(2)
C(22)	0.1297(3)	-0.1344(4)	0.5018(3)	4.6(1)
C(23)	0.1456(2)	0.1839(4)	0.5084(2)	3.5(1)
C(24)	0.1502(3)	0.2997(4)	0.4797(3)	4.7)1)
C(25)	0.1223(3)	0.3976(5)	0.5153(3)	6.2(2)
C(26)	0.0884(3)	0.3817(6)	0.5796(3)	6.3(2)
C(27)	0.0830(3)	0.2671(6)	0.6084(3)	6.2(2)
C(28)	0.1121(3)	0.2671(6)	0.5740(2)	4.8(1)
H(1)	0.417(4)	0.11&(5)	0.611(4)	10.(2)*
H(2)	0.405(4)	0.394(5)	0.253(3)	9.(2)*
C(29)	0.6475(4)	0.4256(5)	0.5937(3)	7.4(2)
Cl(1)	0.5415(8)	0.3393(9)	0.5822(7)	8.5(3)
Cl(2)	0.633(1)	0.477(1)	0.5032(7)	14.3(5)
Cl(3)	0.734(1)	0.332(2)	0.602(1)	18.6(8)
Cl(4)	0.7548(7)	0.418(1)	0.6396(9)	15.8(4)
Cl(5)	0.6445(8)	0.356(1)	0.4942(5)	17.1(4)
Cl(6)	0.5751(6)	0.3343(7)	0.6249(4)	6.1(2)
Cl(7)	0.570(2)	0.344(2)	0.592(2)	31.(1)
Cl(8)	0.740(1)	0.335(2)	0.6362(9)	14.5(4)
Cl(9)	0.641(1)	0.5254(9)	0.5213(9)	11.4(4)

Table 8. Table of positional parameters for *11c* and their estimated standard deviations

Atom	x	y	z	$B(\text{Å}^2)$
P	0.10854(6)	0.12860(5)	0.64068(4)	2.68(1)
O(1)	0.2939(2)	0.0579(1)	0.6662(2)	4.04(4)
O(2)	-0.0748(2)	0.0419(1)	0.6300(1)	3.05(3)
O(3)	0.0843(2)	0.1998(1)	0.5337(1)	3.00(3)
O(4)	0.1019(2)	0.2293(1)	0.7281(1)	2.97(3)
O(5)	-0.1217(2)	0.5533(1)	0.6770(1)	3.15(3)
C(1)	-0.2670(2)	0.0951(2)	0.5801(2)	2.67(4)
C(2)	-0.1121(2)	0.2321(2)	0.4712(2)	2.47(3)
C(3)	-0.2505(2)	0.2317(2)	0.5450(2)	2.20(3)
C(4)	-0.0876(2)	0.2801(2)	0.7399(2)	2.60(4)
C(5)	-0.2044(2)	0.3303(2)	0.6375(2)	2.24(3)
C(6)	-0.1138(2)	0.4532(2)	0.6060(2)	2.55(4)
C(7)	-0.4290(2)	0.3476(2)	0.6225(2)	2.90(4)
C(8)	-0.4591(2)	0.2900(2)	0.5115(2)	3.04(4)
H(0)	-0.005(4)	0.552(3)	0.728(3)	3.9(7)[a]
H1	-0.334(3)	0.085(2)	0.640(2)	1.5[b]
H2	-0.316(3)	0.045(2)	0.525(2)	1.5[b]
H3	-0.139(3)	0.170(2)	0.421(2)	1.5[b]
H4	-0.099(3)	0.313(2)	0.440(2)	1.5[b]
H5	-0.150(3)	0.214(2)	0.766(2)	1.5[b]
H6	-0.051(3)	0.348(2)	0.794(2)	1.5[b]

---

[a] Atom refined isotropically.

[b] Thermal parameter fixed.

Anisotropically refined atoms are given in the form of the isotropic equivalent displacement parameter defined as: (4/3) * [a^2*B(1,1) + b^2*B(2,2) + c^2*B(3,3) + ab(cos gamma)*B(1,2) + ac(cos beta)*B(1,3) + bc)cos alpha)*B(2,3)].

Table 8. Continued

Atom	x	y	z	B(Å^2)
H7	-0.188(3)	0.482(2)	0.535(2)	1.5^b
H8	0.018(3)	0.437(2)	0.600(2)	1.5^b
H9	-0.482(3)	0.295(2)	0.668(2)	1.5^b
H10	-0.469(3)	0.440(2)	0.630(2)	1.5^b
H11	-0.468(3)	0.353(2)	0.458(2)	1.5^b
H12	-0.571(3)	0.233(2)	0.492(2)	1.5^b

Table 9. Positional parameters for 11d and their estimated standard deviations

Atom	x	y	z
P(1)	1.0011(1)	0.2080(1)	0.6041(1)
O(1)	0.8682(4)	0.2695(3)	0.5353(2)
O(2)	1.1249(3)	0.2960(2)	0.6695(2)
O(3)	1.1244(4)	0.1278(2)	0.5327(2)
O(4)	0.9179(3)	0.1256(2)	0.6921(2)
O(5)	1.3618(4)	-0.1545(2)	0.6133(2)
C(1)	1.3055(5)	0.1028(4)	0.5722(3)
C(2)	1.0200(5)	0.0863(3)	0.7898(3)
C(3)	1.2312(5)	0.2510(3)	0.7644(3)
C(4)	1.2468(5)	-0.0847(3)	0.6796(3)
C(5)	1.3138(4)	0.0457(3)	0.6859(3)
C(6)	1.2159(5)	0.1164(3)	0.7785(3)
C(7)	1.5076(5)	0.0470(4)	0.7292(3)
C(8)	1.4946(6)	0.0276(4)	0.8537(3)
C(9)	1.3171(6)	0.0794(4)	0.8870(3)

Table 10. Selected bond distances and angles in <u>2d</u>

Bond Distances (Å)

O(1) - C(6)	1.429(4)	C(1) - C(2)	1.536(5)
O(2) - C(7)	1.426(4)	C(1) - C(5)	1.538(4)
O(3) - C(8)	1.425(4)	C(2) - C(3)	1.536(5)
O(4) - C(9)	1.429(4)	C(3) - C(4)	1.536(4)
C(4) - C(8)	1.527(4)	C(4) - C(5)	1.576(4)
C(4) - C(9)	1.538(4)	C(5) - C(7)	1.528(4)
C(5) - C(6)	1.538(4)		
O(1) -)(1')	2.654(3)	O(3) - O(4')	2.669(S)
O(1) - O(1)	2.654(3)1	O(4) - O(4")	2.656(3)

Bond Angles (°)

C(2) - C(1) - C(5)	106.7(2)	C(6) - 0(1) - 0(1')	115.8(2)
C(1) - C(2) - C(3)	106.0(3)	C(6) - 0(1) - 0(2')	126.8(2)
C(2) - C(3) - C(4)	106.9(2)	C(7) - 0(2) - 0(3)	104.1(2)
C(3) - C(4) - C(5)	102.4(2)	C(7) - 0(2) - 0(1')	116.2(2)
C(3) - C(4) - C(8)	109.6(20	C(8) - C(3) - 0(2)	104.2(2)
C(3) - C(4) - C(9)	109.9(2)	C(8) - 0(3) - 0(4")	116.0(2)
C(5) - C(4) - C(8)	116.2(2)	C(9) - 0(4) - 0(4")	115.6(2)
C(5) - C(4) - C(9)	110.1(2)	C(9) - 0(4) - 0(4")	115.6(2)
C(8) - C(4) - C(9)	108.5(2)		
C(1) - C(5) - C(4)	102.4(2)		
C(1) - C(5) - C(6)	110.0(2)		

Table 10. Continued

Bond Angles (°)	
C(1) - C(5) - C(7)	109.5(2)
C(4) - C(5) - C(6)	110.1(2)
C(4) - C(5) - C(7)	116.1(2)
C(6) - C(5) - C(7)	108.5(2)
0(1) - C(6) - C(5)	112.6(2)
0(2) - C(7) - C(5)	112.0(2)
0(3) - C(8) - C(4)	112.1(2)
0(4) - C(9) - C(4)	112.5(2)

Table 11. Selected bond distances and angles in 5c

	Bond Distances (Å)		
P-O2	1.447(7)	P-O3	1.558(6)
P-O1	1.569(5)	O3-C5	1.456(10)
O1-C7	1.449(10)	C5-C4	1.500(11)
C7-C3	1.483(11)	C4-C8	1.533(12)
C3-C6	1.515(12)	C4-C1	1.517(12)
C34-C2	1.516(11)	C1-O4	1.412(12)
C2-O4	1.414(11)	C6-C8	1.585(14)
C3-C4	1.561(10)		
O2...O5	2.685(9)		
	Bond Angles (°)		
O3-P-O1	108.3(3)	C1-O4-C2	104.2(7)
O1-P-O2	111.3(4)	O3-P-O2	111.1(4)
P-O1-C7	121.2(5)	P-O3-C5	120.3(5)
O1-C7-CA3	111.6(6)	O3-C5-C4	112.3(7)
C7-C3-C2	113.9(6)	C5-C4-C1	113.5(7)
C3-C6-C8	89.9(7)	C4-C8-C6	89.2(7)
C3-C2-O4	104.8(7)	C4-C1-O4	104.5(7)
C7-C3-C6	114.2(7)	C5-C4-C8	113.3(7)
C6-C3-C2	114.9(7)	C8-C4-C1	115.0(7)
C4-C3-C7	118.3(6)	C3-C4-C5	119.5(6)
C4-C3-C2	102.3(6)	C3-C4-C1	103.2(6)

Table 12. Selected bond distances and angles in 9

Bond Distances (Å)

P	O(1)	1.457(2)	C(4)	C(6)	1.551(6)
P	O(2)	1.574(3)	C(5)	C(7)	1.541(5)
P	O(3)	1.568(3)	C(6)	C(7)	1.559(5)
P	C(1)	1.857(4)	C(6)	C(10)	1.536(5)
O(1)	H(1)	1.58(5)	C(7)	C(8)	1.558(5)
O(2)	C(2)	1.470(5)	C(8)	C(9)	1.524(6)
O(3)	C(3)	1.463(5)	C(9)	C(10)	1.527(6)
O(4)	C(4)	1.424(5)	C(1)	C(11)	1.552(5)
O(4)	H(1)	1.12(5)	C(1)	C(17)	1.544(6)
O(4)	H(2)	1.88(6)	C(1)	C(23)	1.557(6)
O(5)	C(5)	1.421(5)	C(2)	C(6)	1.515(5)
O(5)	H(2)	0.89(6)	C(3)	C(7)	1.522(6)

Bond Angles (°)

O(1)	P	O(2)	114.8(1)
O(1)	P	O(3)	109.8(2)
O(1)	P	C(1)	113.2(2)
O(2)	P	O(3)	104.9(1)
O(2)	P	C(1)	104.4(2)
O(3)	P	C(1)	109.3(2)
P	O(1)	H(1)	143.(2)
P	O(2)	C(2)	115.7(2)
P	O(3)	C(3)	125.5(2)

Table 12. Continued

Bond Angles (°)

C(4)	0(4)	H(1)	114.(3)
C(4)	0(4)	H(2)	106.(2)
H(1)	0(4)	H(2)	114.(4)
C(5)	0(5)	H(2)	111.(4)
P	C(1)	C(11)	110.3(3)
P	C(1)	C(17)	108.1(2)
P	C(1)	C(23)	106.3(2)
C(11)	C(1)	C(17)	110.3(3)
C(11)	C(1)	C(23)	111.0(3)
C(17)	C(1)	C(23)	110.7(3)
0(2)	C(2)	C(6)	113.4(3)
0(3)	C(3)	C(7)	113.6(3)
0(4)	C(4)	C(6)	112.2(3)
0(5)	C(5)	C(7)	111.1(3)
C(2)	C(6)	C(4)	104.4(2)
C(2)	C(6)	C(7)	117.0(3)
C(2)	C(6)	C(10)	113.6(3)
C(4)	C(6)	C(7)	110.1(3)
C(4)	C(6)	C(10)	109.1(3)
C(7)	C(6)	C(10)	102.7(3)
C(3)	C(7)	C(5)	108.9(4)
C(3)	C(7)	C(6)	113.8(3)
C(3)	C(7)	C(8)	104.8(3)

Table 12. Continued

Bond Angles (°)			
C(5)	C(7)	C(6)	113.8(3)
C(5)	C(7)	C(8)	112.5(3)
C(6)	C(7)	C(8)	102.6(3)
C(7)	C(8)	C(9)	106.4(3)
C(8)	C(9)	C(10)	107.2(3)
C(6)	C(10)	C(9)	104.4(3)
C(1)	C(11)	C(12)	121.1(4)
C(1)	C(11)	C(16)	120.8(3)
C(12)	C(11)	C(16)	117.9(3)
C(11)	C(12)	C(13)	120.6(4)
C(12)	C(13)	C(14)	120.7(5)
C(13)	C(14)	C(15)	119.2(4)
C(14)	C(15)	C(16)	120.7(5)
C(11)	C(16)	C(15)	120.9(4)
C(1)	C(17)	C(18)	120.0(4)
C(1)	C(17)	C(22)	121.6(3)
C(18)	C(17)	C(22)	118.3(4)
C(17)	C(18)	C(19)	120.7(5)
C(18)	C(19)	C(20)	120.1(5)
C(19)	C(20)	C(21)	119.3(6)
C(20)	C(21)	C(22)	121.1(5)
C(17)	C(22)	C(21)	120.4(3)
C(1)	C(23)	C(24)	120.8(3)

Table 12. Continued

Bond Angles (°)			
C(1)	C(23)	C(28)	121.0(4)
C(24)	C(23)	C(28)	118.2(4)
C(23)	C(24)	C(25)	121.0(5)
C(24)	C(25)	C(26)	120.3(5)
C(25)	C(26)	C(27)	119.3(5)
C(26)	C(27)	C(28)	120.8(5)
C(23)	C(28)	C(27)	120.4(5)
0(1)	H(1)	0(4)	174.(6)
0(4)	H(2)	0(5)	166.(5)

---

[a] Numbers in parentheses are estimated standard deviations in the least significant digits.

Table 13. Selected bond distances and angles in 11c

Bond Distances (Å)

P	0(1)	1.463(1)	0(5)	H(0)	0.93(4)
P	0(2)	1.563(1)	C(1)	C(3)	1.521(2)
P	0(3)	1.564(2)	C(2)	C(3)	1.522(2)
P	0(4)	1.572(1)	C(3)	C(5)	1.573(3)
0(1)	H(0)	1.78(4)	C(3)	C(8)	1.555(2)
0(2)	C(1)	1.468(2)	C(4)	C(5)	1.499(3)
0(3)	C(2)	1.472(2)	C(5)	C(6)	1.539(2)
0(4)	C(4)	1.475(2)	C(5)	C(7)	1.555(2)
0(5)	C(6)	1.415(2)	C(7)	C(8)	1.546(3)
0(5)	H(0)	0.93(4)	C(6)	H(7)	1.01(3)
C(1)	H(1)	1.01(2)	C(6)	H(8)	0.96(2)
C(1)	H(2)	0.90(3)	C(7)	H(9)	0.95(2)
C(2)	H(3)	0.92(3)	C(7)	H(10)	1.03(2)
C(2)	H(4)	0.96(2)	C(8)	H(11)	0.96(3)
C(4)	H(5)	0.96(2)	C(8)	H(12)	0.97(2)
C(4)	H(6)	1.00(3)			

Bond Angles (°)

0(1)	P	0(2)	113.25(8)	C(1)	C(3)	C(8)	109.0(1)
0(1)	P	0(3)	111.08(8)	C(2)	C(3)	C(5)	116.2(1)
0(1)	P	0(4)	110.66(8)	C(2)	C(3)	C(8)	121.2(2)
0(2)	P	0(3)	106.18(8)	C(5)	C(3)	C(8)	88.3(1)
0(2)	P	0(4)	106.97(7)	0(4)	C(4)	C(5)	110.7(1)

Table 13. Continued

Bond Angles (°)

O(3)	P	O(4)	108.44(8)	C(3)	C(5)	C(4)	115.6(1)
P	O(1)	H(0)	137(1)	C(3)	C(5)	C(6)	111.8(1)
P	O(2)	C(1)	118.3(1)	C(3)	C(5)	C(7)	87.6(1)
P	O(3)	C(2)	120.5(1)	C(4)	C(5)	C(6)	111.2(2)
P	O(4)	C(4)	120.3(1)	C(4)	C(5)	C(7)	118.9(1)
C(6)	O(5)	H(0)	108.(2)	C(6)	C(5)	C(7)	109.7(1)

Table 14. Selected distances and angles in 11d

Bond Distances (Å)			
P-O(1)	1.5448(29)	C(2)-C(5)	1.5130(5)
P-O(2)	1.5571(26)	C93)-C(6)	1.5123(56)
P-O(3)	1.5605(27)	C(4)-C(6)	1.5390(49)
P-O(5)	1.4599(30)	C(5)-C(6)	1.5630(47)
O(1)-C(1)	1.4626(46)	C(5)-C(9)	1.5580(52)
O(2)-C(2)	1.4719(45)	C(6)-C(7)	1.5422(52)
O(3)-C(3)	1.4652(49)	C(7)-C(8)	1.5220(59)
O(4)-C(4)	1.4220(48)	C(8)-C(9)	1.5196(66)
C(1)-C(5)	1.5242(53)		

Bond Angles (°)			
O(1)-P-O(2)	105.87(14)	C(6)-C(5)-C(9)	103.68(28)
O(1)-P-O(3)	107.12(15)	C(3)-C(6)-C(4)	110.11(29)
O(2)-P-O(3)	106.36(15)	C(3)-C(6)-C(5)	115.12(29)
P-O(1)-C(1)	121.09(23)	C(4)-C(6)-C(5)	110.56(27)
P-O(2)-C(2)	119.46(21)	C(5)-C(6)-C(7)	102.25(27)
P-O(3)-C(3)	119.42(22)	C(6)-C(7)-C(8)	104.65(32)
O(1)-C(1)-C(5)	110.97(29)	C(7)-C(8)-C(9)	106.38(34)
O(2)-C(2)-C(5)	112.48(29)	C(5)-C(90-C(8)	107.28(31)
O(3)-C(3)-C(6)	113.32(30)	C(1)-C(5)-C(6)	115.24(28)
O(4)-C(4)-C(6)	109.89(30)	C(2)-C(5)-C(6)	112.35(28)
C(1)-C(5)-C(2)	107.71(29)		

Table 15. Selected bond distances and angles in 25,[a] 26,[b] 27[c]

Bond Distances (Å)

Bond	25	26[d]	27
P-O(1)	1.445(2)	1.464(16)	
P-O(2)	1.594(2)	1.576(17)	1.60(2)
P-O(3)	1.577(2)	1.567(12)	1.59(2)
P-O(4)	1.577	1.567(12)	1.56(2)
O(2)-C(1)	1.492(4)	1.456(23)	1.47(4)
O(3)-C(2)	1.478(2)	1.453(17)	1.48(4)
O(4)-C(3)	1.478(2)	1.453(17)	1.52(4)

Bond Angles (°)

Angle	25	26[d]	27
O(1)-P-O(2)	121.9(1)	115.4(10)	
O(1)-P-O(3)	115.8(1)	114.6(6)	
O(1)-P-O(4)	115.8(1)	114.6(6)	
O(2)-P-O(3)	97.4(1)	103.2(6)	105(11)
O(2)-P-O(4)	97.4(1)	103.2(6)	103(11)
S-P-O(2)			113(1)
S-P-O(3)			114(1)

---

[a] See reference 55.

[b] See reference 56.

[c] See reference 57.

[d] Distances are are average values of two orientations in the crystal.

Table 15. Continued

Angle	25	26[d]	27
S-P-O(4)			114(1)
O(3)-P-O(4)	105.1(1)	104.2	106(0)
P-O(2)-C(1)	95.3(2)	115.2(12)	114(17)
P-O(3)-C(2)	105.8(1)	115.3(9)	112(17)
P-O(3)-C(2)	105.8(1)	115.3(9)	114(17)

REFERENCES

1. Holmes, R. R. Prog. Inorg. Chem. 1984, 32, 119.
2. Bentrude, W. G.; Del Alley, W.; Johnson, N. A.; Murakami, M.; Nishikida, K.; Tan, H. W. J. Am. Chem. Soc. 1977, 99, 4383.
3. Westheimer, H. F. Acc. Chem. Res. 1968, 1, 70.
4. Hamerlinck, J. H. H.; Schipper, P.; Buck, H. M. J. Am. Chem. Soc. 1983, 105, 385.
5. Berry, R. S. J. Chem. Phys. 1960, 32, 933.
6. a) Holmes, R. R.; Deiters, J. A. J. Am. Chem. Soc. 1977, 99, 3318.
   b) Dennis, L. W.; Bartuska, V. J.; Maciel, G. E. J. Am. Chem. Soc. 1982, 104, 230.
7. Abdov, W. M.; Denney, D. B.; Denney, D. Z.; Pator, S. D. Phosphorus and Sulfur 1985, 22, 99.
8. a) Marsi, K. L. J. Org. Chem. 1975, 40, 1779.
   b) Marsi, K. L. J. Am. Chem. Soc. 1969, 91, 4724.
   c) Egan, W.; Chauviere, G.; Mislow, K.; Clark, R. T.; Marsi, K. L. Chem. Commun. 1970, 733.
   d) Marsi, K. L.; Burns, F. B.; Clark, R. T. J. Org. Chem. 1972, 37, 238.
   e) DeBruin, K. E.; Padilla, A. G.; Campbell, M.-T. J. Am. Chem. Soc. 1973, 95, 4681.

9. Corriu, R. J. P. *Phosphorus and Sulfur* 1986, *27*, 1. Deiters, J. A.; Holmes, R. R. *J. Am. Chem. Soc.* 1987, *108*, 1686.

10. Corriu, R. J. P.; Guerin, C. *J. Organomet. Chem.* 1980, *198*, 231.

11. a) Howard, J. A.; Russel, D. R.; Trippett, S. *J. Chem. Soc., Chem. Commun.* 1973, 856.
    b) Althoff, W.; Day, R. O.; Brown, R. K.; Holmes, R. R. *J. Am. Chem. Soc.* 1977, *99*, 3332.
    c) Clark, T. E.; Day, R. O. Holmes, R. R. *Inorg. Chem.* 1979, *18*, 1660.
    d) Sarma, R.; Ramirez, F.; Marecek, J. F. *J. Org. Chem.* 1976, *41*, 473.
    e) Clark, T. E.; Day, R. O.; Holmes, R. R. *Inorg. Chem.* 1979, *18*, 1668.
    f) Day, R. O.; Holmes, R. R. *Inorg. Chem.* 1983, *22*, 1771.

12. Holmes, R. R. *J. Am. Chem. Soc.* 1975, *97*, 5379.

13. Brown, R. K.; Day, R. O.; Husebye, S.; Holmes, R. R. *Inorg. Chem.* 1978, *17*, 3276.

14. a) Goldwhite, H.; Teller, R. G. *J. Am. Chem. Soc.* 1978, *100*, 5357.
    b) Holmes, R. R.; Day, R. O.; Sau, A. C. *Organometallics* 1985, *4*, 714.

c) Poutasse, C. A.; Day, R. O.; Holmes, J. M.; Holmes, R. R. Organometallics 1985, 4, 708.

15. a) Holmes, R. R.; Day, R. O.; Chandrasekhar, V.; Holmes, J. M. Inorg. Chem. 1987, 26, 157.

b) Holmes, R. R.; Day, R. O.; Chandrasekhar, V.; Holmes, J. M. Inorg. Chem. 1987, 26, 163.

16. a) Boer, F. P.; Flynn, J. J.; Turley, J. W. J. Am. Chem. Soc. 1968, 90, 6973.

b) Holmes, R. R.; Day, R. O.; Harland, J. J.; Sau, A. C.; Holmes, J. M. Organometallics 1984, 3, 341.

c) Holmes, R. R.; Day, R. O.; Harland, J. J.; Holmes, J. M. Organometallics 1984, 3, 347.

d) Holmes, R. R.; Day, R. O.; Chandrasekhar, V.; Holmes, J. M. Inorg. Chem. 1985, 24, 2009.

e) Holmes, R. R.; Day, R. O.; Chandrasekhar, V.; Harland, J. J.; Holmes, J. M. Inorg. Chem. 1985, 24, 2016.

17. a) Holmes, R. R.; Day, R. O.; Sau, A. C.; Poutasse, C. A.; Holmes, J. M. Inorg. Chem. 1985, 24, 193.

b) Holmes, R. R.; Day, R. O.; Sau, A. C.; Holmes, J. M. Inorg. Chem. 1986, 25, 600.

c) Holmes, R. R.; Day, R. O.; Sau, A. C.; Poutasse, C. A.; Holmes, J. M. Inorg. Chem. 1986, 25, 607.

18. a) Holmes, R. R.; Shafieezad, S.; Chandrasekhar, V.; Sau, A. C.; Holmes, J. M.; Day, R. O. J. Am. Chem. Soc. 1988, 110, 1168.

  b) Holmes, R. R.; Shafieezad, S.; Holmes, J. M.; Day, R. O. Inorg. Chem. 1988, 27, 1232.

  c) Day, R. O.; Holmes, J. M.; Shafieezad, S.; Chandrasekhar, V.; Holmes, R. R. J. Am. Chem. Soc. 1988, 110, 5377.

19. Clark, T. E.; Day, R. O.; Holmes, R. R. Inorg. Chem. 1979, 18, 1653.

20. Bernard, D.; Laurenco, C.; Burgada, R. J. Organomet. Chem. 1973, 47, 113.

21. a) Burgada, R. Phosphorus and Sulfur 1976, 2, 237.

  b) Koenig, M.; Munoz, A.; Garrigues, B.; Wolf, R. Phosphorus and Sulfur 1979, 6, 435.

  c) Garrigues, B.; Munoz, A.; Koenig, M.; Sanchez, M.; Wolf, R. Tetrahedron 1977, 33, 635.

22. Burgada, R.; Laurenco, C. J. Organomet. Chem. 1974, 66, 255.

23. Van Lier, J. J. C.; Hermans, R. J. M.; Buck, H. M. Phosphorus and Sulfur 1984, 19, 173.

24. Bohlen, R.; Hacklin, H.; Heine, J.; Offermann, W.; Roschenthaler, G. Phosphorus and Sulfur 1986, 27, 321.

25. Verkade, J. G. Phosphorus and Sulfur 1976, 2, 251.

26. Taira, K.; Mock, W. L.; Gorenstein, D. G. J. Am. Chem. Soc. 1984, 106, 7831.

27. Mason, M. Iowa State University Chemistry Department, personal communication, 1987.

28. a) Weinges, K.; Klessing, K.; Kolb, R. Chem. Ber. 1973, 106, 2298.
    b) Buchta, E.; Droeniger, A. Chimia 1968, 22, 430. Eberson, L. Acta Chem. Scand. 1958, 12, 731.
    c) Bailey, W. J.; Sorenson, W. R. J. Am. Chem. Soc. 1954, 76, 5421.

29. Sheldrick, G. M. In "Computing in Crystallography"; Schenk, H.; Olthof-Hazekamp, R.; Van Koningsveld, H.; Bassi, G. C.; Eds.; Delft University: Delft, 1978.

30. Cromer, D. T.; Waber, J. T. "International Tables for X-ray Crystallography"; Kynoch: Birmingham, England, 1974; Vol. IV.

31. Westheimer, F. H.; Huang, S.; Coritz, F. J. Am. Chem. Soc. 1988, 110, 181.

32. Bertrand, R. D.; Verkade, J. G.; White, D. W.; Gagnaire, D.; Robert, J. B.; Verrier, J. J. Magn. Reson. 1970, 3, 494.

33. Derome, A. E. In "Modern NMR Techniques for Chemistry Research"; Baldwin, J. E.; Ed., Pergamon: Elmsford, New York, 1987; p. 197.

34. Silverstein, R. M.; Bassler, G. C.; Morrill, T. C. "Spectrometric Identification of Organic Compounds", 4th Ed.; John Wiley & Sons: New York, 1981; p. 209.

35. Rutar, V.; Wong, T. C.; Guo, W. J. Magn. Reson. 1985, 64, 849.

36. Rutar, V.; Wong, T. C. J. Magn. Reson. 1984, 60, 333.

37. Derome, A. E. In "Modern NMR Techniques for Chemistry Research"; Baldwin, J. E., Ed.; Pergamon: Elmsford, New York, 1987; p. 245.

38. Guimaraes, A. C.; Robert, J. B.; Taib, C.; Tabony, J. Org. Magn. Reson. 1978, 11, 411.

39. Derome, A. E. In "Modern NMR Techniques for Chemistry Research"; Baldwin, J. E., Ed.; Pergamon: Elmsford, New York, 1987; p. 234.

40. Jameson, C. J. In "Phosphorus-31 NMR spectroscopy In Stereochemical Analysis"; Verkade, J. G.; Quin, L. D.; Eds.; VCR: Deerfield Beach, Florida, 1987; p. 215.

41. Tebby, J. C. In "Phosphorus-31 NMR Spectroscopy in Stereochemical Analysis"; Verkade, J. G.; Quin, L. D.; Eds.; VCR: Deerfield Beach, Florida, 1987; pp 1-12.

42. Kroshefsky, R. D.; Weiss, R.; Verkade, J. G. Inorg. Chem. 1979, 18, 469.

43. Verkade, J. G. Pure and Appl. Chem. 1980, 52, 1131.

44. Vainshtein, B. K.; Fridkin, V. M.; Indenbom, V. L. In "Modern Crystallography II"; Cardona, M.; Fulde, P.; Queisser, H.-J., Eds.; Springer-Verlag; New York, 1982; p. 56.

45. Whalon, M. R.; Bushweller, C. H.; Anderson, W. G. J. Org. Chem. 1984, 49, 1185.

46. Boyd, R. H. J. Am. Chem. Soc. 1975, 97, 5353.

47. Dodziuk, H. J. Comput. Chem. 1984, 5, 571.

48. Clardy, J. C.; Milbrath, D. S.; Verkade, J. G. J. Am. Chem. Soc. 1977, 99, 631.

49. Clardy, J. C.; Milbrath, D. S.; Verkade, J. G. Inorg. Chem. 1977, 16, 2135.

50. a) Corbridge, D. E. C. In "Top Phosphorus Chem."; Griffith, E. J.; Grayson, M., Eds.; John Wiley & Sons: New York, New York, 1966; Vol. III, pp. 211-212.

    b) Verkade, J. G. Bioinorg. Chem. 1974, 3, 165.

    c) Newton, M. G.; Campbell, B. S. J. Am. Chem. Soc. 1974, 96, 7790.

    d) Finocchiaro, P.; Recca, A.; Bentrude, W. G.; Tan, H. W.; Yee, K. C. J. Am. Chem. Soc. 1976, 98, 3537.

    e) Jones, P. G.; Sheldrick, G. M.; Kirby, A. J.; Briggs, A. J. Acta Crystallogr., Sect. B.: Cryst. Struct. Commun. 1984, C40, 1061.

51. Milbrath, D. S.; Verkade, J. G.; Kenyon, G. L.; Eargle, D. H. J. Am. Chem. Soc. 1978, 100, 3167.

52. Nimrod, D. M.; Fitzwater, D. R.; Verkade, J. G. J. Am. Chem. Soc. 1968, 90, 2780.

53. Andersen, P.; Hjortaas, K. E. Acta Chem. Scand. 1960, 14, 829.

54. Taira, K.; Gorenstein, D. G. J. Am. Chem. Soc. 1984, 106, 7825.

55. de Ruiter, B.; Benson, J. E.; Jacobson, R. A.; Verkade, J. G., accepted for publication in Inorg. Chem.

56. Grand, A.; Robert, J. B. Acta Crystallogr., Sect. B.: Struct. Sci. 1978, 38, 199.

57. Coulter, C. L. J. Am. Chem. Soc. 1975, 97, 4085.

58. a) Hendrickson, J. B. J. Am. Chem. Soc. 1967, 89, 7036.

    b) Hendrickson, J. B.; Boeckman, R. K.; Glickson, J. D.; Grunwald, E. J. Am. Chem. Soc. 1973, 95, 494.

SECTION III. DEPROTONATION OF PNICTOGEN ESTERS CONTAINING PENDANT ALCOHOL GROUPS

INTRODUCTION

Although the trigonal bipyramidal (TBP) geometry is the most common in isolable pentacoordinate pnictogen compounds, the square pyramidal (SP) geometry is believed to be present as an intermediate in many reactions. The small energy increase in the SP geometry relative to the TBP represents an excited state in pentacoordinate pnictogen compounds that undergo Berry pseudorotation (see below)1 and, therefore, an intermediate state in many of their reactions. Even in reactions of species such as phosphoranyl radicals and phosphoranide anions, which contain one and two electrons, respectively, in the fifth ligand site, SP intermediates are believed to be present[2] as a result of Berry pseudorotation.[3] Because of the role of these SP species in the reactions of pnictogen compounds, knowledge of their properties and reactivity is desirable. Recently a number of SP phosphorus, arsenic and antimony compounds, stablized in relation to the TBP geometry by both steric and electronic factors of the ligands, have been prepared by Holmes.[4] While X-ray structure determinations have elucidated some of the structural properties of these

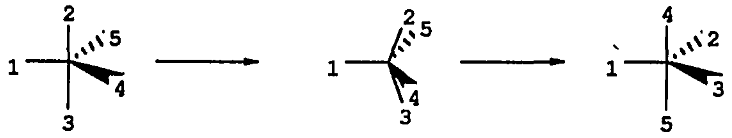

compounds, their inherent stability has precluded the investigation of their reactivity.

The deprotonation of phosphites containing pendant alcohol groups has been reported to yield stable phosphoranide anions which are in equilibrium with the phosphite species as shown in reaction 1.[5] This equilibrium is present in a number of deprotonated phosphite compounds,[6]

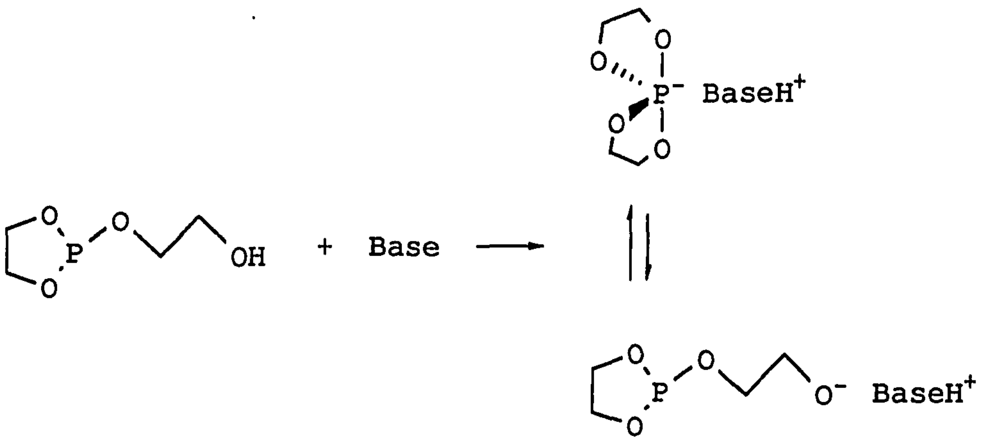

(1)

and in one instance the anion has been structurally characterized.[7] Though in this case the phosphoranide anion has a TBP geometry, studies of similar phosphoranide systems suggest that the energy barrier between the TBP and the SP geometries is small.[8] The equilibrium between tricoordinate and pentacoordinate forms of hydrospiroarsoranes can be observed in the ^{1}H NMR spectrum of 1, although in compounds

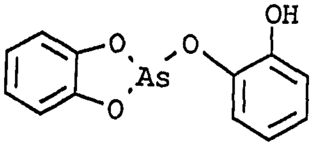

1

containing saturated five-membered rings only the tricoordinate form is detectable.[9] Reaction of the equilibrium mixture with base yields the arsoranide anion in reaction 2. The chalcogenide derivatives of the

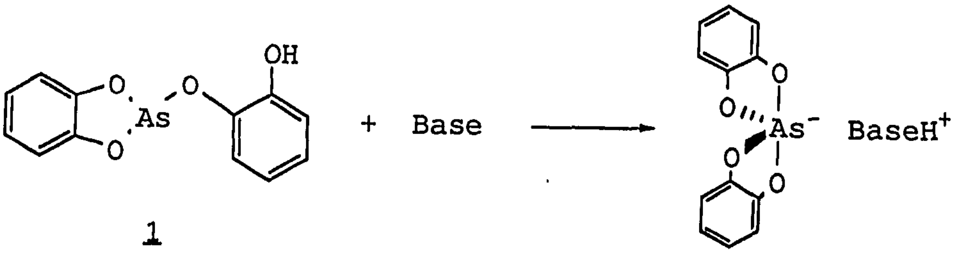

(2)

phosphoranide anions, 2-5, can be prepared and also exhibit

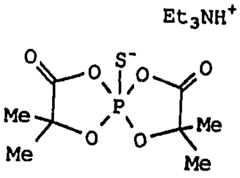

2

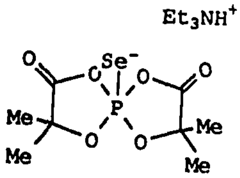

3

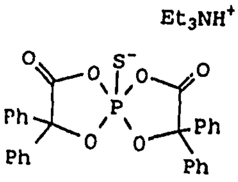

4

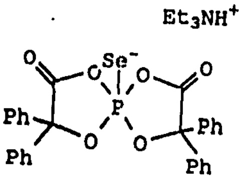

5

such equilibria.[10] In these compounds the position of their equilibria should be affected by the presence of electron withdrawing substituents on phosphorus making the pentacoordinate form more favorable. Gamayurova et al. have recently reported the preparation of compounds 6-9 which are in the tetracoordinate form in the solid state.[11] In

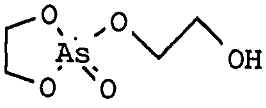

6

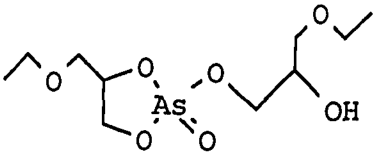

7

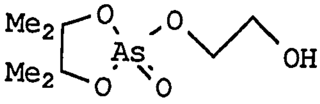

8

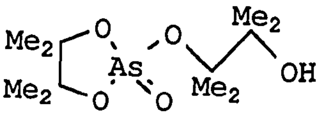

9

solution, however, these compounds rapidly undergo conversion to the pentacoordinate form. Unlike the tricoordinate systems described above, the transformations in the tetracoordinate cases do not involve an equilibrium and indeed, the pentacoordinate species could not be converted back to the tetracoordinate form. Presumably this is due to the presence of the more electronegative oxygen on the arsenic, making the arsenic more susceptible to nucleophilic attack by the pendent alcohol group. In addition, the arsoryl oxygen probably has more affinity for the proton than the arsenic lone electron pair present in the tricoordinate form. In 6-9 the pentacoordinate form is stabilized to such an extent, that it is preferred in compounds containing saturated rings.

We recently described our attempts to prepare square pyramidal phosphorus species using the alcohols 10a-e to synthesize 11-15.[12] Although the equilibrium between tricoordinate and pentacoordinate tautomers in reaction 3 is known for dioxaphospholanes[13] and dioxaphosphorinanes[14] containing pendant alcohol groups, phosphites 11a-e and

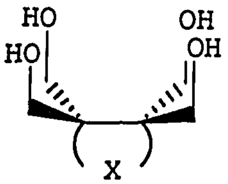

10a-e

	X
10a	H_2
10b	CH_2
10c	$(CH_2)_2$
10d	$(CH_2)_3$
10e	$(CH_2)_4$

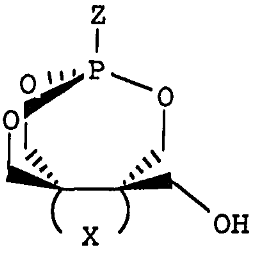

	Z
11a-e	lp
12a-e	O
13a-c	S
14a-e	Se
15a-e	Ph_3C^+

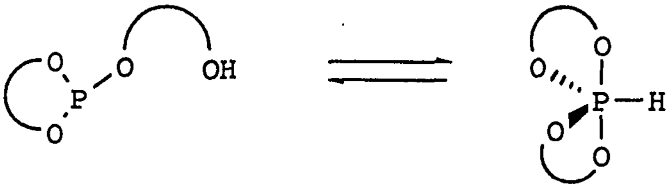

(3)

their derivatives 12a-e, 13a-e, 14a-e and 15a-e show no sign of such tautomeric equilibria. Furthermore, these compounds have base properties, coupling constants and NMR resonances comparable to the model phosphites 16, 17 and their derivatives with corresponding Z groups.

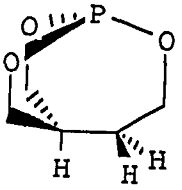
16

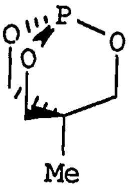
17

We report here the preparation of several metal complexes of 11a-e and an investigation of these compounds to determine whether they exhibit a tautomeric equilibrium between tetracoordinate and SP pentacoordinate phosphorus forms. The reactions of phosphites 11a-e and their derivatives with a base have also been studied in an attempt to prepare SP phosphoranide anions. The reactions of the new metal complexes of 11a-e with base are discussed. In addition, we report the preparation and

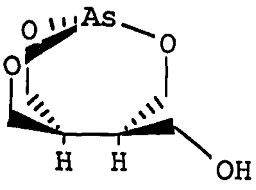
18a

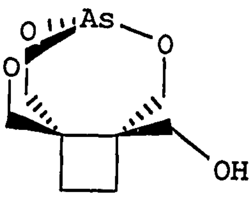
18b

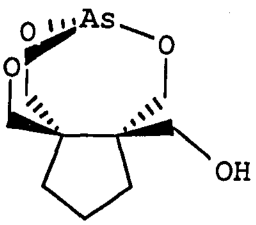
18c

characterization of the arsenic compounds 18a-c. We show that these compounds react with base to give fluxional arsoranide anions.

EXPERIMENTAL SECTION

Physical Measurements

NMR spectra were obtained on Nicolet NT-300 (^{1}H), Bruker WM-200 (^{13}C) and Bruker WM-300 (^{31}P) instruments at room temperature. The ^{1}H, ^{13}C and ^{31}P NMR data of the compounds described in this paper are presented in Tables 1, 2 and 3, respectively. Variable temperature NMR measurements were recorded on a Bruker WM-200 instrument. These spectra were recorded in d_3-acetonitrile solutions over the temperature range 223 to 350K. Chemical shifts are given in ppm (positive downfield) relative to internal Me_4Si (^{1}H, ^{13}C) and external 85% H_3PO_4 (^{31}P) standards.

Preparation of Compounds

Compounds 11-16,[15] 17,[16] $W(CO)_5(THF)$,[17] $Mn(CO)_5Br$,[18] $Fe_3(CO)_{12}$,[19] $[CpFe(CO)_2(THF)][BF_4]$,[20] $CpCo(CO)I_2$,[21] $As(NMe_2)_3$,[22] and $N[CH_2CH_2N(Me)]_3P$ (19)[23] were prepared as previously described. All reactions were performed with the strict exclusion of moisture unless otherwise described. Solvents were dried by standard methods and distilled before use. All other chemicals were used as received.

$W(CO)_5$(16), (20)

To a sample of 16 (0.1699 g, 1.147 mmole) in a 250 mL round bottomed flask was added a solution of $W(CO)_5(THF)$ in 150 mL of THF prepared from $W(CO)_6$ (0.4220 g, 1.199 mmole).

This solution was stirred for three hours at room temperature and the solvent removed under vacuum. The resulting white solid was purified by silica-gel chromatography using ethyl acetate as the eluent. After unreacted $W(CO)_6$ was collected the product eluted and removal of the solvent under vacuum gave pure 20 (yield 0.3945 g, 0.8358 mmole, 72.9%).

$W(CO)_5$(11a), (21a)

A solution of $W(CO)_5$(THF) in 150 mL of THF, prepared from $W(CO)_6$ (0.2629 g, 0.7471 mmole), was added to a 250 mL round bottomed flask containing 11a (0.1262 g, 0.7085 mmole). This reaction mixture was stirred for three hours at room temperature and the solvent removed under vacuum to give a white solid. The solid was then dissolved in ethyl acetate and chromatographed on silica-gel using ethyl acetate as the eluent. The product was collected after the elution of unreacted $W(CO)_6$, and removal of the solvent under vacuum gave pure 21a (yield 0.2433 g, 0.4824 mmole, 68.1%).

$W(CO)_5$(11b), (21b)

To a sample of 11b (0.2258 g, 1.187 mmole) in a 250 mL round bottomed flask was added a solution of $W(CO)_5$(THF), prepared from $W(CO)_6$ (0.4334 g, 1.231 mmole), in 150 mL of THF. The reaction mixture was stirred for three hours at room temperature and the solvent removed under vacuum to give impure white 21b. The product was then purified by silica-gel chromatography using ethyl acetate as the eluent to give pure 21b (yield 0.3128 g, 0.6085 mmole, 51.2%).

$W(CO)_5$(11c), (21c)

A solution of $W(CO)_5$(THF) in 150 mL of THF, prepared from $W(CO)_6$ (0.6232 g, 1.771 mmole), was added to a sample of 11c (0.3556 g, 1.742 mmole) in a 250 mL round bottomed flask. After stirring for three hours at room temperature the solvent was removed under vacuum and the residue dissolved in ethyl acetate. The residue was then subjected to silica-gel chromatography with ethyl acetate to give pure 21c (yield 0.6472 g, 1.226 mmole, 70.4%).

$W(CO)_5$(11d), (21d)

To a 250 mL round bottomed flask containing 11d (0.2147 g, 0.9840 mmole) was added a solution of $W(CO)_5$(THF) prepared from $W(CO)_6$ (0.3620 g, 1.031 mmole). After stirring for three hours at room temperature, the solvent was removed under vacuum and the resulting residue subjected to silica-gel chromatography using ethyl acetate as the eluent. After unreacted $W(CO)_6$ eluted, the product was collected and removal of the solvent under vacuum gave pure 21d (yield 0.3736 g, 0.6892 mmole, 70.0%).

$Mn(CO)_4Br$(11a), (22)

To a 50 mL round bottomed flask containing $Mn(CO)_5Br$ (0.4313 g, 1.569 mmole) and 11a (0.2754 g, 1.546 mmole) was added 25 mL of THF. The resulting solution was stirred for three hours at room temperature and the solvent removed under vacuum to give a pale yellow solid. The product was purified by silica-gel chromatography using ethyl acetate as the eluent giving pure 22 (yield 0.3480 g, 0.8188 mmole, 53.0%).

$Fe(CO)_4$(11a), (23a)

A mixture of $Fe_3(CO)_{12}$ (0.4419 g, 0.8774 mmole) and 11a (0.4655 g, 2.613 mmole) in 50 mL of benzene was heated to reflux for three hours. The solvent was then removed under vacuum and the solid residue extracted with three 25 mL portions of hot hexane. The hexane extracts were combined and the solvent removed under vacuum to give pure 23a (yield 0.4480 g, 1.295 mmole, 49.5%).

$Fe(CO)_4$(11b), (23b)

A mixture of $Fe_3(CO)_{12}$ (0.1220 g, 0.2422 mmole) and 11b (0.1332 g, 0.7005 mmole) in 50 mL of benzene was heated to reflux for three hours. The solvent was then removed under vacuum and the residue extracted with three 25 mL portions of hot hexane. Solvent removal from the extracts under vacuum gave 23b (yield 0.0853 g, 0.2382 mmole, 34.0%).

$Fe(CO)_4$(11c), (23c)

A mixture of $Fe_3(CO)_{12}$ (0.3016 g, 0.5988 mmole) and 11c (0.3625 g, 1.775 mmole) in 50 mL benzene was refluxed for three hours and the solvent removed under vacuum. The resulting solid residue was extracted three times with 25 mL portions of hot hexane and the hexane fractions combined. Solvent removal from the hexane extracts under vacuum gave 23c (yield 0.3401 g, 0.9141 mmole, 51.5%).

$[CpFe(CO)_2$(16)]$[BF_4]$, (24)

To a 50 mL round bottomed flask containing $[CpFe(CO)_2(THF)][BF_4]$ (0.3368 g, 1.003 mmole) and 16 (0.1483 g, 1.001 mmole) was added 25 mL of THF. The solution was then stirred for 30 minutes and hexane added to precipitate the product. Filtration of the cream colored solid gave pure 24 (yield 0.3821 g, 0.9277 mmole, 92.6%).

$[CpFe(CO)_2$(11a)]$[BF_4]$, (25a)

A solution containing $[CpFe(CO)_2(THF)][BF_4]$ (1.2908 g, 3.843 mmole) and 11a (0.6841 g, 3.840 mmole) in 25 mL of THF was stirred for 30 minutes. Hexane was then added to the solution to precipitate the product and upon filtration pure cream colored 25a was obtained (yield 1.4787 g, 3.346 mmole, 87.3%).

[CpFe(CO)$_2$(11b)][BF$_4$], (25b)

A solution containing [CpFe(CO)$_2$(THF)][BF$_4$] (0.2896 g, 0.8622 mmole) and 11b (0.1633 g, 0.8589 mmole) in 25 mL THF was stirred for 30 minutes. Hexane was then added to the solution to precipitate the cream colored product. Filtration gave 25b (yield 0.3017 g, 0.6647 mmole, 77.4%).

[CpFe(CO)$_2$(11c)][BF$_4$], (25c)

To a 50 mL round bottomed flask containing [CpFe(CO)$_2$(THF)][BF$_4$] (1.129 g, 3.363 mmole) and 11c (0.6860 g, 3.360 mmole) was added 25 mL of THF. The resulting solution was stirred for 30 minutes and hexane added to precipitated the product. Filtration gave cream colored 25c (yield 1.4173 g, 3.029 mmole, 90.1%).

[CpFe(CO)$_2$(11d)][BF$_4$], (25d)

To a 50 mL round bottomed flask containing [CpFe(CO)$_2$(THF)][BF$_4$] (0.3854 g, 1.147 mmole) and 11d (0.2499 g, 1.145 mmole) was added 25 mL of THF. The solution was stirred for 30 minutes and hexane added to precipitate the product. Filtration gave cream colored 25d (yield 0.5053 g, 1.048 mmole, 91.5%).

[CpFe(CO)$_2$(11e)][BF$_4$], (25e)

A solution containing [CpFe(CO)$_2$(THF)][BF$_4$] (0.6280 g, 1.870 mmole) and 11e (0.4338 g, 1.868 mmole) in 25 mL THF was stirred for 30 minutes and hexane added to precipitate the product. Filtration gave cream colored 25e (yield 0.7909 g, 1.595 mmole, 85.4%).

CpCo(17)I_2, (26)

To a solution of CpCo(CO)I_2 (0.7914 g, 1.950 mmole) in 10 mL CH_2Cl_2 was added dropwise a solution of 17 (0.2883 g, 1.947 mmole) in 5 mL CH_2Cl_2 over a period of three hours. The solution was stirred an additional hour and the solvent removed under vacuum. The crude product was then purified by silica-gel chromatography using ethyl acetate as the eluent and the purple product band collected. Removal of the solvent gave pure 26 (yield 0.8451 g, 1.607 mmole, 82.5%).

CpCo(11a)I_2, (27a)

To a solution of CpCo(CO)I_2 (0.8354 g, 2.058 mmole) in 10 mL CH_2Cl_2 was added dropwise a solution of 11a (0.3661 g, 2.055 mmole) in 5 mL CH_2Cl_2 over a period of three hours. The solution was then stirred an additional hour and the solvent removed under vacuum. Silica-gel chromatography of the solid residue using ethyl acetate as the eluent gave a solution containing the purple product. Solvent removal gave pure purple solid 27a (yield 0.9063 g, 1.630 mmole, 79.3%).

CpCo(11b)I_2, (27b)

To a solution of CpCo(CO)I_2 (0.7261 g, 1.789 mmole) in 10 mL CH_2Cl_2 was added dropwise a solution of 11b (0.3396 g, 1.786 mmole) in 5 mL CH_2Cl_2 over a period of three hours. The solution was then stirred an additional hour and the solvent removed under vacuum. Silica-gel chromatography of the solid residue with ethyl acetate gave a solution containing the purple product. Solvent removal gave pure solid 27b (yield 0.7308 g, 1.287 mmole, 72.0%).

CpCo(11c)I_2, (27c)

A solution of 11c (0.4021 g, 1.969 mmole) in 5 mL CH_2Cl_2 was added dropwise over a period of three hours to a solution of CpCo(CO)I_2 (0.8002 g, 1.972 mmole) in 10 mL CH_2Cl_2. After an additional hour the solvent was removed under vacuum and the resulting solid subjected to silica-gel chromatography using ethyl acetate as the eluent. The purple band was collected and removal of the solvent gave pure 27c (yield 0.8593 g, 1.476 mmole, 75.0%).

CpCo(11d)I_2, (27d)

A solution of 11d (0.3701 g, 1.696 mmole) in 5 mL CH_2Cl_2 was added dropwise over a period of three hours to a solution of CpCo(CO)I_2 (0.6900 g, 1.700 mmole) in 10 mL CH_2Cl_2. The solution was stirred an additional hour and the solvent removed under vacuum. The crude product was then purified by silica-gel chromatography using ethyl acetate as the eluent. Solvent removal from the purple product band gave 27d (yield 0.7359 g, 1.235 mmole, 72.8%).

CpCo(11e)I_2, (27e)

To a solution of CpCo(CO)I_2 (0.2129 g, 0.5246 mmole) in 10 mL CH_2Cl_2 was added dropwise a solution of 11e (0.1211 g, 0.5215 mmole) in 5 mL of CH_2Cl_2 over a period of three hours. The solution was stirred an additional hour and the solvent removed under vacuum. The resulting solid was subjected to silica-gel chromatography using ethyl acetate as the eluent and the purple product band collected. Solvent removal from this band gave pure 27e (yield 0.2235 g, 0.3664 mmole, 70.2%).

$Ni(CO)_3$(16), (28)

To a solution of 16 (0.1674 g, 1.130 mmole) in 20 mL $CHCl_3$ was added $Ni(CO)_4$ (0.1992 g, 1.167 mmole) in one portion by syringe. The solution was stirred for 16 hours and the solvent reduced to ca. 3 mL. Addition of hexane to precipitate the product followed by filtration gave white solid 28 (yield 0.1323 g, 0.4549 mmole, 40.2%).

$Ni(CO)_3$(11a), (29a)

To a solution of 11a (0.2995 g, 1.681 mmole) in 20 mL $CHCl_3$ was added $Ni(CO)_4$ (0.2952 g, 1.729 mmole) in one portion by syringe. The solution was stirred for 16 hours and the solvent reduced to ca. 3 mL. Addition of hexane to precipitate the product followed by filtration gave white solid 29a (yield 0.2027 g, 0.6317 mmole, 37.6%).

$Ni(CO)_3$(11b), (29b)

In one portion $Ni(CO)_4$ (0.1444 g, 0.8457 mmole) was added by syringe to a solution of 11b (0.1535 g, 0.8073 mmole) in 20 mL $CHCl_3$. The solution was stirred for 16 hours and the solvent reduced to ca. 3 mL. Hexane was then added and the precipitate collected by filtration to give 29b (yield 0.0785 g, 0.2358 mmole, 29.2%).

$Ni(CO)_3$(11c), (29c)

To a solution of 11c (0.5594 g, 2.740 mmole) in 20 mL $CHCl_3$ was added $Ni(CO)_4$ (0.4721 g, 2.765 mmole) in one portion by syringe. The solution was stirred for 16 hours and the solvent reduced to ca. 3 mL. Hexane was then added to precipitate the product and the solid collected by filtration to give pure 29c (yield 0.3636 g, 1.048 mmole, 38.2%).

$Ni(CO)_3$(11d), (29d)

To a solution of 11d (0.4012 g, 1.839 mmole) in 20 mL $CHCl_3$ was added $Ni(CO)_4$ (0.3214 g, 1.882 mmole) in one portion by syringe. The solution was stirred for 16 hours and the solvent reduced to ca. 3 mL. Hexane was then added and the precipitate collected by filtration to give 29d (yield 0.2548 g, 0.7060 mmole, 38.4%).

$Ni(CO)_3$(11e), (29e)

In one portion $Ni(CO)_4$ (0.0774 g, 0.4533 mmole) was added by syringe to a solution of 11e (0.1022 g, 0.4401 mmole) in 20 mL $CHCl_3$. The solution was stirred for 16 hours and the solvent reduced to ca. 3 mL. Hexane was the added and the precipitate collected by filtration to give 29e (yield 0.0515 g, 0.1373 mmole, 31.2%).

4-Hydroxymethyl-1-arsa-2,7,8-trioxatricyclo[3.2.2.$0^{1,5}$]-nonane, (18a)

To a suspension of 10a (0.6346 g, 4.226 mmole) in 25 mL THF was added in one portion $As(NMe_2)_3$ (0.8762 g, 4.230 mmole). The reaction mixture was then heated to 65°C for three hours. Upon cooling to room temperature the solvent was removed under vacuum and the crude solid produce purified by silica-gel chromatography using ethyl acetate as the eluent. Removal of the solvent from the product fraction gave pure white solid 18a (yield 0.3175 g, 1.430 mmole, 33.8%).

4-Hydroxymethyl-1-arsa-2,9,10-trioxatricyclo[5.2.2.$0^{4,7}$]-undecane, (18b)

To a suspension of 10c (0.4705 g, 2.670 mmole) in 25 mL THF was added in one portion $As(NMe_2)_3$ (0.5539 g, 2.674

mmole). The mixture was heated to 65°C for three hours and then allowed to cool to room temperature. The solvent was then removed under vacuum and the crude product subjected to silica-gel chromatography using ethyl acetate as the eluent. Removal of the solvent from the product fraction gave pure 18b as a white solid (yield 0.3016 g, 1.215 mmole, 45.5%).

4-Hydroxymethyl-1-arsa-2,10,11-trioxatricyclo[6.2.2.$0^{4,8}$]-dodecane, (18c).

To a suspension of 10d (0.6706 g, 3.525 mmole) in 25 mL THF was added in one portion $As(NMe_2)_3$ (0.7313 g, 3.530 mmole). The reaction mixture was then heated to 65°C for three hours and allowed to cool to room temperature. The solvent was then removed under vacuum and the crude product purified by silica-gel chromatography using ethyl acetate as the eluent. Removal of the solvent from the product containing fraction gave pure 18c as a white solid (yield 0.4072 g, 1.553 mmole, 44.1%).

Deprotonation Reactions

A number of different bases were used in the deprotonation of the compounds described above and four procedures were followed depending on the base: 1) In the case of Et_3N, 1,8-diazabicyclo[5.4.0]undec-7-ene (DBU) and pyridine, a solution containing a large (20-fold) excess of base in d_6-benzene was syringed into an NMR tube, under nitrogen, containing a weighed amount of the reagent to be deprotonated. The resulting mixture was then analyzed using ^{1}H and ^{31}P NMR spectroscopy. 2) For the bases NaH and KH a 2-fold excess of the base was placed in a 20 ml round bottom flask containing a weighed amount of the reagent to be deprotonated. All manipulations were carried out in an argon flushed glove bag. THF (10 mL) was then added and the mixture stirred for one hour. The mixture was filtered and the filtrate placed in an NMR tube containing a small amount of d_6-benzene. This solution was then analyzed by ^{1}H and ^{31}P NMR spectroscopy. 3) Deprotonation using n-BuLi was accomplished by syringing three equivalents of a 22% solution of n-BuLi in hexane into an NMR tube containing ca. 0.1 mmoles of the reactant to be deprotonated dissolved in ca. 1 ml THF/d_6-benzene mixture (90/10) at -78°C under argon. The resulting products were then analyzed by ^{1}H and ^{31}P NMR spectroscopy. 4) In the case of base 19, one equivalent of the base and one equivalent of the reagent to be deprotonated were placed in an NMR tube and 2 mL of d_3-acetonitrile added to dissolve the mixture. The products of the deprotonation were analyzed by ^{1}H and ^{31}P NMR spectroscopy.

X-ray Diffraction Data

The same general procedure was used for both structure determinations described herein. A crystal of 26 or 27d, grown by slow evaporation of solvent from saturated CH_2Cl_2 solutions, was mounted on a glass fiber and centered on an Enraf-Nonuis CAD4 diffractometer. Cell dimensions and the orientation matrix were obtained from least-squares refinement using setting angles of 25 reflections in the range 25 < two-theta < 34°. During data collection, three representative reflections were checked every 60 min. as orientation and intensity standards. Since the change in intensity was less than the error in the measurements, no decay correction was applied. Lorentz and polarization corrections were applied to the data, and empirical absorbtion corrections, based on a series of psi-scans, were initially applied to the data. Refinement of the structure was carried out using the SHELX76 package.[24] Scattering factors were obtained from the usual sources.[25]

In both structures, 25 reflections chosen from a rotation photograph were indexed to give the appropriate unit cell which subsequent solution of the structure showed to be of a specific symmetry. The structure was solved with the use of over 3000 unique reflections in both cases with $I > 2s(I)$.

Structure Solution and Refinement

Both structures were solved by direct methods. All iodine, cobalt and phosphorus atoms were located from a direct methods E-map. The remainder of the nonhydrogen atoms were located by alternate least-squares and difference Fourier procedures. Hydrogen atoms were then used in calculated positions for structure factor calculations only. Isotropic thermal parameters for the hydrogen atoms were set at 1.30 times the value of the isotropic equivalent of the thermal parameter for the attached carbon atom. Following least-squares convergence (all atoms with isotropic thermal parameters) a numerical absorbtion correction was applied giving correction factors ranging from 0.696 to 1.287. The crystal data for both structures are summarized in Table 4. The positional parameters are given in Tables 5 and 6 for 26 and 27d, respectively. Selected bond lengths and angles for these respective compounds are given in Tables 7 and 8. The ORTEP diagrams of 26 and 27d are presented in Figures 1 and 2, respectively.

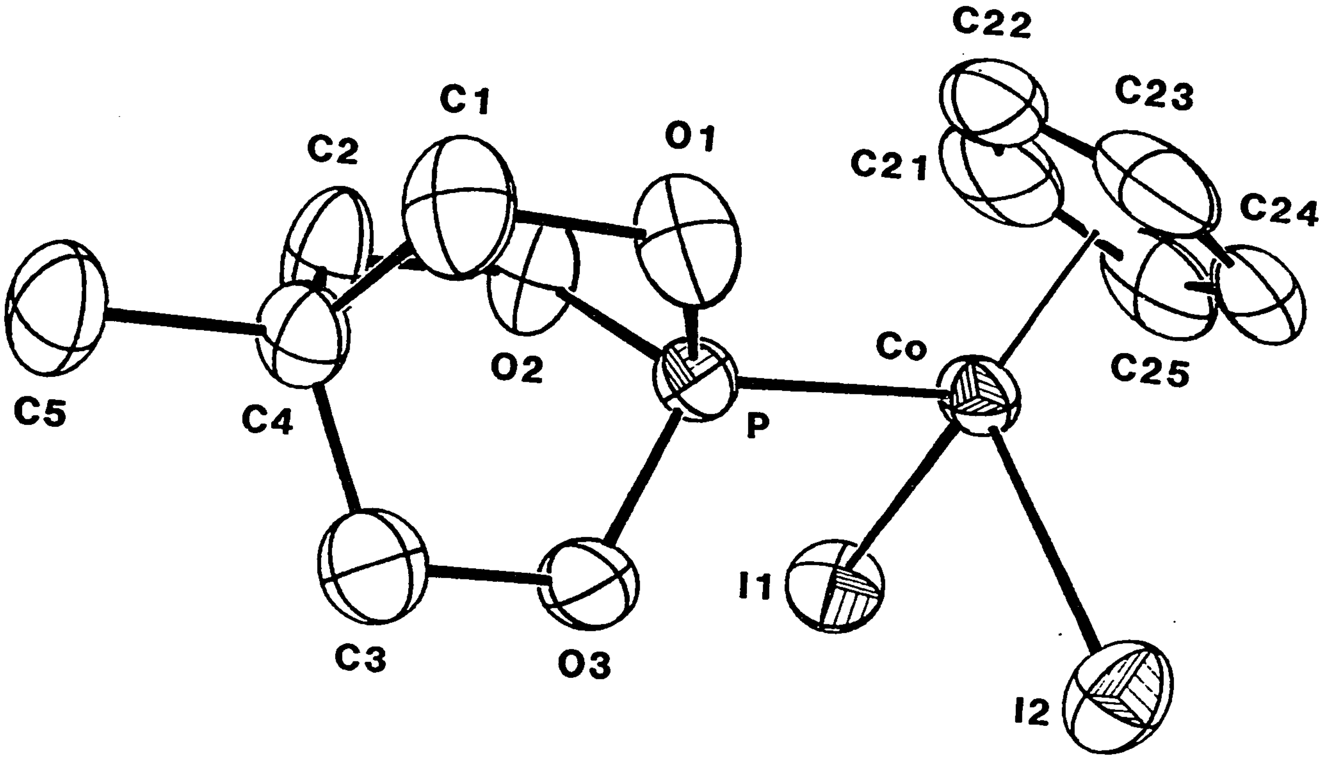

Figure 1. ORTEP drawing of <u>26</u>, with ellipsoids at the 50% probability level

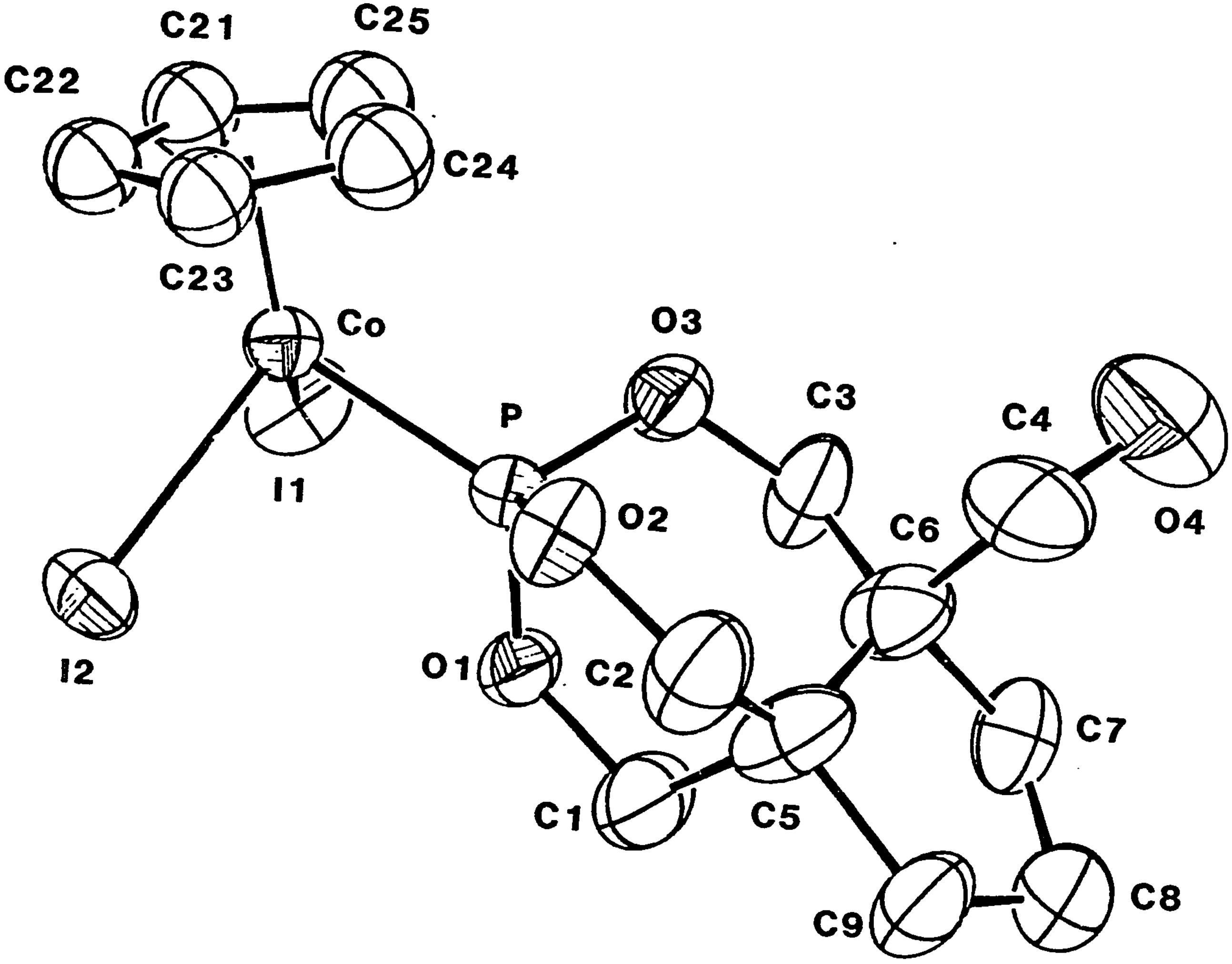

Figure 2. ORTEP drawing of <u>27d</u>, with ellipsoids at the 50% probability level

RESULTS AND DISCUSSION

Synthetic Pathways

As an extension of our earlier work, a number of metal complexes of phosphites 11a-e, shown below, were prepared in

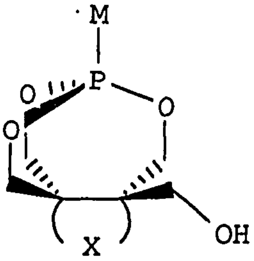

	M
21a-d	$W(CO)_5$
22	$Mn(CO)_4Br$
23a-c	$Fe(CO)_4$
25a-c	$CpFe(CO)_2^+$
27a-e	$CpCoI_2$
29a-e	$Ni(CO)_3$

the hope that the presence of the electron withdrawing metal fragments would make the phosphorus more susceptible to nucleophilic attack by the pendant hydroxymethyl group and form SP species. Complexes of 16 with the metal fragments $W(CO)_5$, $[CpFe(CO)_2]^+$ and $Ni(CO)_3$ were prepared as a control since 16 contains no pendant alcohol arm and, therefore, cannot form SP species similar to ligands 11a-e. The reactions used to prepare these complexes are shown below (reactions 4-9).

$$W(CO)_5(THF) + L \xrightarrow{THF} W(CO)_5(L) \qquad (4)$$

$$Mn(CO)_5Br + L \longrightarrow Mn(CO)_4(L)Br + CO \qquad (5)$$

$$Fe_3(CO)_{12} + 3L \longrightarrow 3Fe(CO)_4(L) \qquad (6)$$

$$[CpFe(CO)_2(THF)][BF_4] + L \longrightarrow [CpFe(CO)_2(L)][BF_4] \qquad (7)$$

$$CpCo(CO)I_2 + L \longrightarrow CpCo(L)I_2 + CO \qquad (8)$$

$$Ni(CO)_4 + L \longrightarrow Ni(CO)_3(L) + CO \qquad (9)$$

$$L = \underline{11a}\text{-}\underline{e},\ \underline{16}$$

Reaction of the appropriate alcohol with $As(NMe_2)_3$ (reaction 10) gave 18a-c, which are the arsenic analogs of 11a, 11c and 11d.

$$\underline{10a},\ \underline{10c},\ \underline{10d} + As(NMe_2)_3 \longrightarrow \underline{11a}\text{-}\underline{c} + 3HNMe_2 \qquad (10)$$

Spectroscopic Results

The ^1H NMR data, ^{13}C NMR data and ^{31}P NMR data of compounds 20-29 are summarized in Tables 1, 2 and 3, respectively. The major differences expected in the ^1H and ^{13}C NMR spectra of the tricoordinate and pentacoordinate forms of 11a-e and their derivatives stem from the differences in the symmetries of these two tautomers shown in Figure 3. These differences are present in all of the derivatives of 11a-e. In the pentacoordinate form (a) the higher symmetry of this tautomer results in three types of protons and two types of carbon atoms in the carbon backbone displayed in Figure 3. In the tri- or tetracoordinate form (b), however, all of the protons and carbon atoms shown are

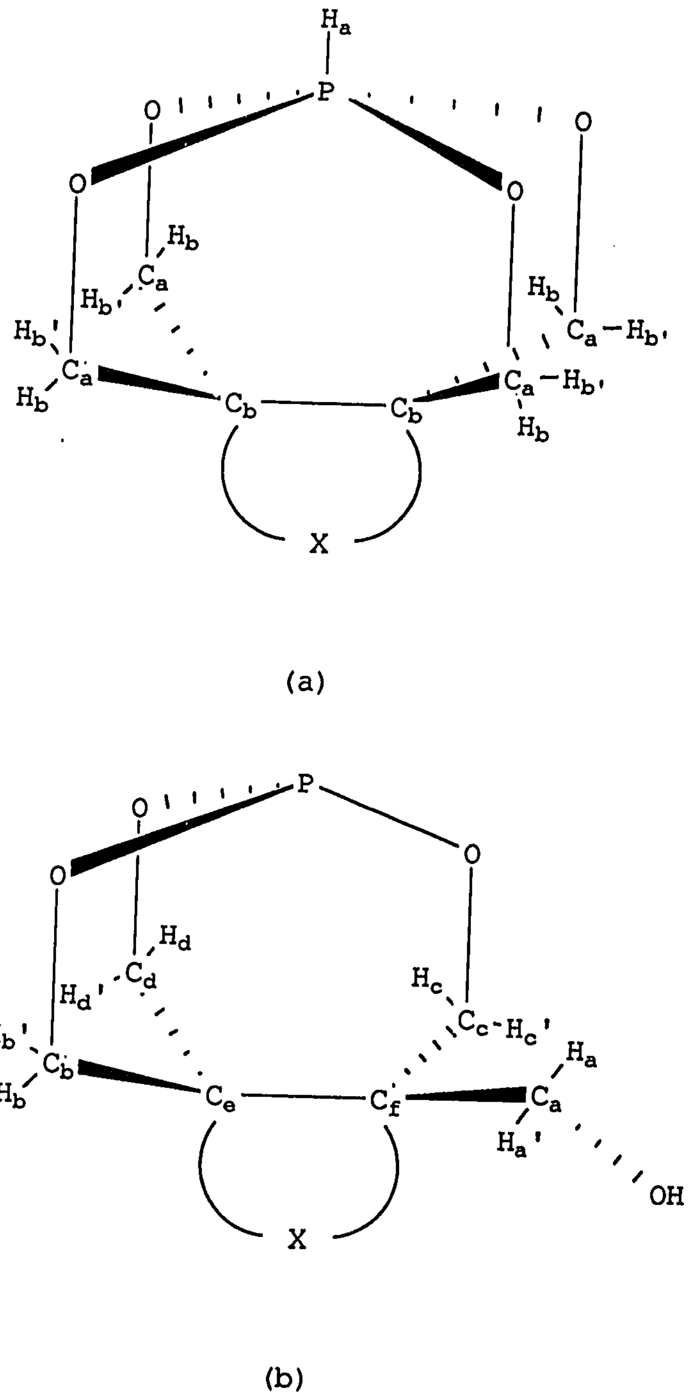

Figure 3. Pentacoordinate (a) and tricoordinate (b) forms of 11a-e

inequivalent. In addition, in (b) the protons and carbon atoms present in the X group are also inequivalent. The latter chemical inequivalencies are observed in the ^{1}H and ^{13}C NMR spectra of 11a-e, 12a-e, 13a-e, 14a-e and 15a-e.

All of the metal complexes of 11a-e give rise to ^{1}H and ^{13}C NMR spectra consistent with form (b) (Tables 1 and 2). In the spectrum of each of the metal complexes, all of the signals in the ^{1}H NMR and ^{13}C NMR spectra could be assigned to the tricoordinate form (b) and in no instance were additional signals due to the SP pentacoordinate tautomer observed. Variable temperature NMR spectra were obtained for several of these complexes; however in no instance was any change observed in the proton resonances over the range of 223 to 350K.

Several trends in the proton coupling constants and chemical shifts of the metal complexes of 11a-e are found in Table 1. Although there is some variation in the ^{3}J(POCH) values between complexes containing different metal groups, ^{3}J(POCH) values are very similar among compounds containing the same metal functionality. As in other derivatives of 11a-e, there is also a great deal of similarity among the geminal proton-proton coupling constants of equivalent phosphite ligands. Indeed, little change occurs in the ^{2}J(HCH) values upon complexation to the metal as evidenced by the similarity in these values and their counterparts in free 11a-e.[15] The methyne proton signals of 11a and the ring proton signals of 11b-e are influenced only slightly by the derivatization of the phosphorus atom, clearly indicating that little change in the geometry of the carbon backbone of 11a-e takes place upon coordination to the metal fragments. Comparison of the phosphorus-hydrogen coupling constants derived from the ^{1}H NMR spectra of the metal complexes of 11a-e with the analogous values of complexes of phosphite 16 supports the tetracoordinate structure in these complexes. As in other derivatives of 11a-e, the chemical shift of proton b in metal complexes of 11a-e appears significantly downfield from the other seven methylene protons in this region of the spectrum in complexes of 11b-e. In complex 11a, though, the proton b signal is within the range of the other methylene protons. This phenomenon is probably due to the higher degree of freedom present in derivatives of 11a which can adopt two different orientations around their methyne carbons as shown below.

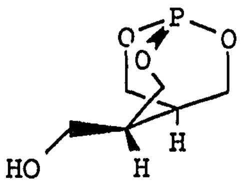

(a)

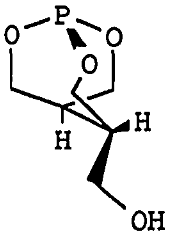

(b)

In 11b-e the presence of the carbocyclic rings inhibits twisting about this carbon-carbon bond. This restriction may place the alcoholic arm of 11b-e and its derivatives in close proximity to proton b in solution, thus causing its slight downfield shift.

The similarities between the ^{13}C NMR spectra of 11a-e and their corresponding metal complexes indicate that these compounds contain a tetracoordinate geometry around phosphorus. Variable temperature NMR spectra were obtained for a number of these complexes and no change was observed over the range of 223 to 350K. The chemical shifts of the inequivalent carbon atoms shown in Table 2 appear to be nearly independent of the metal fragment. The magnitude of $^{2}J(POC)$, though, does show some variation with different metals. The chemical shift of carbon b appeared further downfield than the other methylene carbon signals in complexes 11a-e, presumably due to the interaction of the alcoholic arm with proton b, and thereby with carbon b, described above. As expected, this downfield shift was not observed in complexes of 11a. Also as expected, the value of $^{3}J(POCC)$ for carbon e was, in all cases, greater than that of f which has fewer bond pathways through which coupling can occur.

Perhaps the best technique for determining the coordination of the phosphorus in the metal complexes of

11a-e is ^{31}P NMR spectroscopy, since the chemical shift of a phosphorus compound is very dependent on the oxidation state of the phosphorus, the charge on the phosphorus, and on the number of substituents bound to the phosphorus atom.[26] Typically, ^{31}P shifts for complexes containing pentacoordinate phosphorus appear much further upfield than their tetracoordinate counterparts.[27] In the cases of 30 and 31, prepared by Lattman,[28] the ^{31}P NMR signals appeared at 67 and 73 ppm, respectively, while typical $Mn(CO)_5$ and $Co(CO)_3(PPh_3)$ phosphite complexes resonate at ca. 130 and ca. 120 ppm, respectively. Similar trends are found in complexes of 32, which also contain pentacoordinate phosphorus.[29] With this in mind the ^{31}P NMR spectra of the metal complexes of 11a-e were obtained and compared with spectra of known tetracoordinate complexes.[30] In all of the complexes of 11a-e, the chemical shifts were in the typical range of tetracoordinate phosphite complexes. In addition, derivatives of 11a-e compared well with the resonances

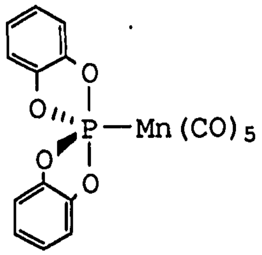

30

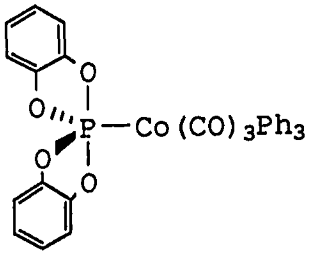

31

32

observed in complexes of 16, which cannot form pentacoordinate species.

Compounds 18a-c yield ^1H NMR spectra which are very similar to those of 11a, 11c, and 11d. Variable temperature experiments performed on these compounds yielded no evidence of a tricoordinate-pentacoordinate tautomeric equilibrium. No changes in the ^1H NMR spectra were observed over the range of 223 to 350K. The lack of couplings due to the substitution of phosphorus by arsenic in these esters greatly simplifies the splitting patterns of 18a-c with respect to the corresponding phosphites and allowed facile assignment of the proton spectrum. As in 11a, c, d and their derivatives, comparison of the proton-proton coupling constants of 18a with those of 18b and 18c indicates that little change takes place in the carbon backbone in going from one arsenic derivative to another. All of the coupling constants compare well with one another and are consistent with a tricoordinate structure. Compounds 18b and 18c contain b proton resonances that appear far downfield with respect to their other methylene protons. In 18a this proton resonance is well within the range defined by the other seven methylene protons, thus suggesting that, as in 11a-e, this phenomenon is probably due to the twist about the methyne-methyne C-C bond present in 18a, which would preclude interaction between the alcohol arm and the b proton which could be present in relatively rigid 18b and 18c.

The ^{13}C NMR spectra of 18a-c are very similar to those of 11a, 11c and 11d, respectively. As in their phosphorus analogs, the inequivalence of all of the carbon atoms in these three arsenites indicates the tricoordinate nature of these compounds. No signals assignable to pentacoordinate species were detected. Variable temperature NMR spectra were recorded in the range of 223 to 350K and no change in the ^{13}C resonances were observed for any of the three arsenites. Little change in the chemical shifts of the carbon resonances occurs in going from 18a to 18c, although carbon b exhibits a downfield shift in 18b and 18c which is not present in 18a. Again, this is probably due to interaction of the alcoholic arm of 18b and 18c with proton b, thereby shifting the b carbon resonance to lower field in solution.

Deprotonation Studies

In an attempt to prepare SP pentacoordinate phosphoranide anions, deprotonation reactions of 11a-e and their derivatives using the bases pyridine, Et_3N, DBU, NaH, KH, n-BuLi and 19 were studied using ^{1}H, ^{13}C and ^{31}P NMR spectroscopy (reaction 11). In the case of pyridine, Et_3N

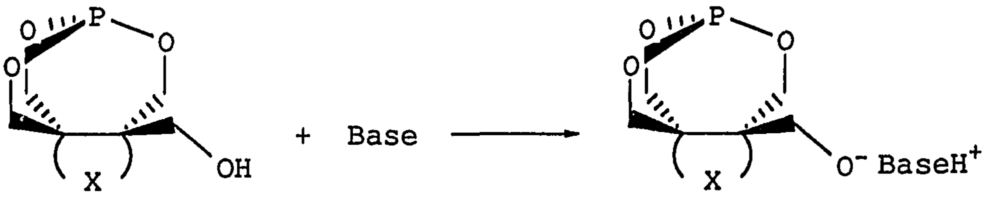

11a-e

(11)

and DBU, the reaction mixture showed no change in the ^1H, ^{13}C and ^{31}P NMR signals of the starting material. When metal complexes containing carbonyl ligands were reacted with these reagents, evidence of CO ligand displacement was detected while the ligand resonances remained largely unchanged. The evolution of gas in these reactions, and the appearance of multiple cyclopentadienyl ^1H and ^{13}C NMR resonances in the case of 19a-e and 20a-e, suggest that loss of CO is occurring in these complexes. Similarly, ^1H, ^{13}C and ^{31}P NMR spectra consistent with tri- or tetracoordinate anions were obtained from reactions of 11a-e, 12a-e, 13a-e, 14a-e and 15a-e with NaH and KH. The reactions of these bases with the metal complexes, however, resulted in the decomposition of the complexes. The ^1H NMR spectra of these reaction mixtures, however, proved that the phosphite ligands remained intact. In none of the reactions of the strong base n-BuLi did the 11a-e framework remain intact. Nucleophilic attack on phosphorus by the n-Bu^- anion was found to occur. Thus in the reactions of n-BuLi with 11a-e, n-Bu_3P could be detected in both the ^1H and ^{31}P NMR spectra and small amounts of 10a-e were observed in the ^{1}H NMR spectra of the reaction mixtures. This reaction is similar to that of PhLi with $P(OEt)_3$, which gives PPh_3 in 80% yield.[31] Reaction of 11a-e and its derivatives with the strong base 19 confirmed the deprotonation of these samples. In reactions of this base, the driving force is the formation of a transannular bond between the phosphorus and the nitrogen upon protonation. This change in the structure produces large differences between the ^{1}H, ^{13}C and ^{31}P NMR spectra of 19 and 33,[23] and these changes can be used as an

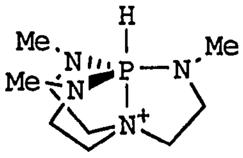

33

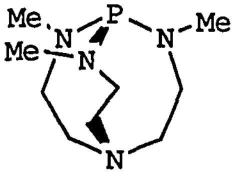

24

indication of the protonation of 19. In all of the deprotonation reactions performed using 19 as the base, both 19 and 33 are detected in the ^{1}H, ^{13}C and ^{31}P NMR spectra. No significant changes are observed, however, in the spectral regions containing the signals of 11a-e and their derivatives, indicating that these species remain tri- or tetracoordinate upon deprotonation. In reactions of 19 with the metal complexes of 11a-e, displacement of CO was observed in addition to deprotonation. The evolution of gas and the appearance of $^{2}J(PMP)$ coupling accompanied by new downfield signals in the ^{31}P NMR spectra confirmed the displacement of CO ligands by 19. In addition, the displacement by 19 of 11a-e from the metal fragments was observed, resulting in the appearance of free phosphite ligand signals in the 120-111 ppm region in the ^{31}P NMR spectra of these reaction mixtures. Variable temperature ^{1}H and ^{31}P NMR studies of deprotonation reactions using the bases pyridine, DBU and 19 showed no change relative to the spectra of 11a-e and their derivatives from 223 to 350K. In no case did the deprotonation of 11a-e or their derivatives lead to the formation of any detectable pentacoordinate phosphorus species or to detectable exchange of the alcohol arm with the other alkoxy groups of the system.

Deprotonations of the arsenic compounds 18a-c were also accomplished using several of the bases used above. In reactions in which the bases pyridine and DBU were used, no change was observed in the room temperature ^{1}H NMR spectra of 18a-c. In variable temperature ^{1}H NMR experiments performed on DBU containing solutions of 18a, however, the resonances of the eight methylene protons a-d began to broaden as the temperature was raised, eventually forming one broad resonance at 350K. However, similar experiments performed on 18b and 18c showed no detectable change in the ^{1}H NMR spectrum. The ^{31}P NMR spectra of reaction mixtures containing 19 and 18a-c contained resonances due to both the starting material 19, and the protonated form 33 confirming that deprotonation of the arsenic species had occurred. The ^1H NMR spectrum of the reaction mixture containing 18c and 19 was very similar to the ^1H NMR spectrum of the starting arsenite 18c, except for the addition of signals due to 19 and 33. No change in the splitting pattern of the protons of 18c was detected from 223 to 350K in variable temperature NMR studies of this reaction mixture. The room temperature ^1H NMR spectrum of the reaction of 18a with 19, however, contained a single broad resonance in the methylene proton region of 18a and a single resonance for the methyne protons. Variable temperature ^1H NMR experiments failed to cause any change in the spectrum of this reaction mixture over the range of 223 to 350K. Analysis of the reaction mixture using ^{13}C NMR failed to show the six carbon signals characteristic of the tricoordinate form of 18a. Rather, only two broad resonances at 65 and 25 ppm due to the methylene and methyne carbons, respectively, appeared. These data are consistent with a fluxional system in which the deprotonated alcoholic arm is exchanging with the remaining alkoxy arms which are bound to the arsenic. The reaction of 18b with 19 also resulted in broad resonances for the a-d protons of the methylene arms and for the ring methylene protons at room temperature. Variable temperature ^1H NMR spectroscopy performed on this reaction mixture yielded signals similar to the starting tricoordinate form of 18b at 223K, while at room temperature and above the sample contained single broad signals for protons a-d and for the protons of the cyclobutane ring. At room temperature the ^{13}C NMR spectrum of this reaction mixture displayed eight carbon signals characteristic of the tricoordinate form of 18b. These signals, however, are much broader than those of the starting material, although the signals due to 19 and 33 are relatively sharp. Variable temperature ^{13}C NMR studies performed on this reaction mixture yielded eight sharp $O\underline{C}H_2$ signals for the deprotonated form of 18b at 223K, and a single broad resonance (ca. 65 ppm) for these methylene carbon atoms at 350K. As with 18a, these data are consistent with a fluxional anionic species in which the four alkoxy arms are exchanging. As the temperature is lowered this exchange becomes slow and the ^1H NMR spectrum resembles that of the tricoordinate starting material. The deprotonations of 18a and 18b by 19 have been shown to be reversible by the addition of a small amount of water to these samples. Upon protonation, the ^1H NMR spectra of these reaction mixtures match those of the starting arsenites. Addition of more 19 to these samples again yields ^1H NMR spectra similar to those of the deprotonated arsenites discussed above.

The differences in the spectra obtained from the reactions of 18a, 18b and 18c with 19 are probably due to the different X groups present in these systems. For any of these compounds to exhibit exchange of their arsenic-bound and unbound alkoxy arms they must proceed through a transition state in which carbons a and f are in an eclipsed conformation. In the case of 18c, the preference of the cyclopentane ring to be puckered prevents the formation of such an eclipsed conformation of these two carbons. For 18b, on the other hand, the relatively low energy difference between the puckered and planar forms of cyclobutane allow the exchange of the alkoxy arms. At reduced temperature, however, the puckered form is favored and the exchange is slow relative to the NMR time scale. Compound 18a, which contains no carbocyclic ring, has the lowest barrier to the eclipsed conformation of all of these compounds and exchange of the alkoxy arms is observed over the entire temperature range studied. It should be noted that in no instance was the exchange rapid enough to yield the simple AB pattern expected for a rapidly exchanging 18b, or an ABX pattern expected for a rapidly exchanging 18a.

Description of the Structures

The structure of complex 26 is shown in Figure 1 and contains a single ligand 17 bound to a $CpCoI_2$ metal fragment. The effect of the coordination of the phosphite ligand to the metal fragment on its P-O bond lengths is roughly equivalent to the effect caused by the presence of a P==O in the structure of 34.[32] The P-O distances in 26, shown in Table 7, compare well with those of 34 shown in Table 9. In the similar phosphite 35, these distances are

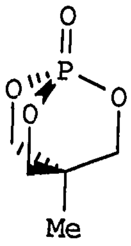

34

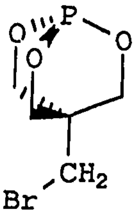

35

ca. 1.615 A,[33] as shown in Table 9. Comparison of the remaining bond lengths of the ligand in 26 with those of 34 and 35 indicates that within experimental error, little change occurs in the carbon backbone upon coordination of the phosphite to the metal. Likewise the bond angles within 26, 34 and 35 are all equivalent within experimental error. These results parallel those found in other structurally characterized complexes of 17, in which little change in the ligand bond lengths is seen upon coordination to a metal.

Examination of the Co-P-O bond angles in 26 shows that the complex contains two equivalent angles (114.0(1) A) and one slightly larger angle (118.6(1) A) indicating that the ligand is tilting slightly away from the two large iodine atoms of the molecule. In the X-ray structure of 36, which we have recently reported,[34] this effect is also

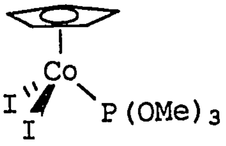

36

observed. In 26 the geometry around the cobalt atom can be considered pseudooctahedral with the cyclopentadienyl ring occupying one face of the octahedron. Accordingly, the I-Co-I (96.17(2) A) and I-Co-P angles (93.11(4) and 93.12(3) A) are all nearly 90°. The Co-P bond length (2.140(1) is slightly shorter than that of 36 (2.160(1) A) and this shortening of the Co-P bond is accompanied by a slight lengthening of one of the Co-I bonds (2.5762(6) A) with respect to those of 36 (2.5704(6) and 2.5717(6) A).

Complex 27d, shown in Figure 2, contains a single ligand 11d bound to a $CpCoI_2$ metal fragment. As in the case of 26, the carbon backbone of the phosphite ligand in 27d remains largely unchanged upon coordination to the metal and the structure of the phosphite ligand in 27d is similar to the structure of the phosphate 12d within experimental error.[15] The effect of the phosphate oxygen on the P-O bond lengths is nearly the same as coordination of the phosphorus to the metal fragment as shown by comparison of the P-O distances in 27d, presented in Table 8, with those of 12d, presented in Table 10. Further comparison of the remaining C-O and C-C bond lengths shows that they too are equivalent within experimental error. Comparison of the bond angles of 27d with those of 12d indicates significant differences between the two structures. Examination of the O-P-O angles of the two structures shows 27d to contain slightly smaller angles (103.6(4)°, 104.6(5)° and 104.5(4)°) in comparison with the analogous angles of 12d (105.9(1)°, 107.1(2)° and 106.4(2)°). In light of the fact that the increase in the O-P-O bond angles in going from 35 to 34 is believed to be due to a rehybridization of the P and O orbitals, the difference between these angles in 27d and 12d is probably due to greater phosphite character present in the ligand of 27d. This decrease in the O-P-O angles is accompanied by an increase in the C(2)-C(5)-C(6) and C(3)-C(6)-C(5) angles in 27d (122.(1)° and 120.(1)°, respectively) in comparison with those of 12d (115.1(3)° and 115.2(3)°, respectively). The remaining bond angles of the two structures, however, are all the equivalent within experimental error.

Comparison of the structure of 27d with the structures of 26 and 36 indicates that the geometry around the phosphorus in 27d contains few of the structural characteristics of a bicyclicphosphite and is more similar to an acyclic phosphite. Perhaps the best measure of this can be found in the P-O-C bond angles of these three structures. In free phosphites these values are typically ca. 120° for acyclic phosphites and ca. 115° for bicyclic phosphites. On coordination to the metal fragment these values are ca. 120° in 27d (120.3(8)°, 121.1(7)° and 120.2(7)°), ca. 115° in 26 (114.4(3)°, 115.3(3)° and 115.5(3)°) and ca. 122° in 36 (125.(1)°, 124.9(4)° and 119.4(5)°). Clearly 27d is structurally more similar to 36 than 26. Experiments described elsewhere,[15] however, show that in terms of reactivity and base properties 11a-e are similar to 17. In 27d the angles about the cobalt(III) are ca. 90° (95.86(5)°, 90.70(9)° and 91.59(9)°) indicating a pseudooctahedral geometry around the metal center. The Co-I bond distances (2.563(2) / and 2.566(2) /) are somewhat shorter than both of those in 26 (2.5676(7) / and 2.5762(6) /) and 36 (2.5704(6) / and 2.5717(6) /). The Co-P bond distance (2.140(3) /) is the same within experimental error as that in 26 (2.140(1) /) and slightly shorter than that in 36 (2.160(1) /).

CONCLUSIONS

It has been demonstrated that the metal complexes of 11a-e do not exhibit a tautomeric equilibrium between tetracoordinate and SP pentacoordinate forms in solution. The deprotonation of 11a-e and their derivatives has been accomplished using several different bases including 19. In all cases the deprotonation of these compounds causes no significant change in their ^{1}H, ^{13}C and ^{31}P NMR spectra. In no instance has any evidence of a SP pentacoordinate species been obtained. To extend these investigations to arsenic, compounds 18a-c were prepared. Although in solution these compounds yield NMR spectra characteristic of tricoordinate species, deprotonation of 18a and 18b result in ^{1}H and ^{13}C NMR data consistent with a fluxional anion in which all of the alkoxy arms are exchanging rapidly. Since 18c does not exhibit this fluxionality, it has been proposed that the energy difference between the puckered and boat forms of cyclopentane is sufficient to inhibit the formation of the fluxional species.

Table 1. ^{1}H NMR spectral data (chemical shifts (ppm) and coupling constants (Hz)) for compounds 18, 20-29

Compound	18a[a]	18b[a]	18c[a]	20[b]	21a[b]	21b[b]
H_a	3.39	3.94	4.35		3.38	3.87m
$[^2J(H_aCH_{a'})]$	10.63	10.09	10.58		10.78	
$[^3J(H_aCOH)]$	5.25	5.30	5.30			
$[^3J(H_aCCH_f)]$	6.82				6.91	
$H_{a'}$	3.34	3.84	3.84		3.32	
$[^2J(H_{a'}CH_a)]$	10.63	10.09	10.58		10.78	
$[^3J(H_{a'}COH)]$	5.25	5.30	5.30			
$[^3J(H_{a'}CCH_f)]$	7.30				6.55	
H_b	4.20	4.61	4.39		4.12	
$[^2J(H_bCH_{b'})]$	10.72	10.55	10.43		10.25	
$[^3J(H_bCOP)]$					8.38	
$[^4J(H_bCCCH_d)]$	2.86	3.37	3.52		3.31	
$[^3J(H_bCCH_e)]$	1.93				1.74	

---

[a] DMSO.

[b] $CDCl_3$.

[c] Detailed NMR analyses were not carried out for this compound. The value given includes the resonances for H_a, $H_{a'}$, H_b, $H_{b'}$, H_c, $H_{c'}$, H_d and $H_{d'}$.

Table 1. Continued

Compound	$\underline{18a}^a$	$\underline{18b}^a$	$\underline{18c}^a$	$\underline{20}^b$	$\underline{21a}^b$	$\underline{21b}^b$
$H_{b'}$	4.14	3.98	3.82		4.01	
[$^2J(H_{b'}CH_b)$]	10.72	10.55	10.43		10.25	
[$^3J(H_{b'}COP)$]					10.25	
[$^3J(H_{b'}CCH_e)$]	4.67				3.28	
H_c	4.05	4.00	4.11	4.02	3.95	
[$^2J(H_cCH_{c'})$]	11.73	11.12	11.59		11.31	
[$^3J(H_cCOP)$]				14.21	28.06	
[$^3J(H_cCCH_f)$]	4.67			6.59	6.96	
$H_{c'}$	3.85	4.09	4.57		3.75	
[$^2J(H_{c'}CH_c)$]	11.73	11.12	11.59		11.31	
[$^3J(H_{c'}COP)$]					8.12	
[$^3J(H_{c'}CCH_f)$]	9.56				8.79	
H_d	3.89	3.86	3.99	4.51	3.79	
[$^2J(H_dCH_{d'})$]	10.36	10.17	10.80	10.04	10.14	
[$^3J(H_dCOP)$]				6.30	7.99	
[$^4J(H_dCCCH_b)$]	2.86	3.37	3.52		3.31	
[$^3J(H_dCCH_e)$]	1.92			2.52	3.40	

Table 1. Continued

Compound	18a[a]	18b[a]	18c[a]	20[b]	21a[b]	21b[b]
$H_{d'}$	4.31	3.77	3.89	4.37	4.20	
$[^2J(H_{d'},CH_d)]$	10.36	10.17	10.80	10.04	10.14	
$[^3J(H_{d'},COP)]$				6.47	1.92	
$[^3J(H_{d'},CCH_e)]$	3.57			2.09	3.44	
H_e	2.15			2.41	2.27	
$[^3J(H_eCCH_f)]$				4.69		
$[^3J(H_eCCH_b)]$	1.93				1.74	
$[^3J(H_eCCH_{b'})]$	4.67				3.28	
$[^3J(H_eCCH_d)]$	1.92			2.52	3.40	
$[^3J(H_eCCH_{d'})]$	3.57			2.09	3.44	
H_f	2.12			2.29	2.03	
$[^3J(H_fCCH_e)]$				4.69		
$[^3J(H_fCCH_a)]$	6.82				6.91	
$[^3J(H_fCCH_{a'})]$	7.30				6.55	
$[^3J(H_fCCH_c)]$	4.67			6.59	6.96	
$[^3J(H_fCCH_{c'})]$	9.56				8.79	
H						
$[^3J(HOCH_a)]$	5.25	5.30	5.30			
$[^3J(HOCH_{a'})]$	5.25	5.30	5.30			
ring		1.60m	1.93m			2.27m

Table 1. Continued

Compounds	21c^b	21d^b	22^b	23a^b	23b^b	23c^b
H_a	3.91	3.53		3.46	3.91m^c	3.46
[$^2J(H_aCH_{a'})$]	10.41	10.34		11.12		10.61
[$^3J(H_aCOH)$]						
[$^3J(H_aCCH_f)$]				6.57		
$H_{a'}$	4.46	3.89		3.39		4.10
[$^2J(H_{a'}CH_a)$]	10.41	10.34		11.12		10.61
[$^3J(H_{a'}COH)$]						
[$^3J(H_{a'}CCH_f)$]				6.62		
H_b	4.79	4.25		4.25		4.57
[$^2J(H_bCH_{b'})$]	10.78	10.77		10.65		10.70
[$^3J(H_bCOP)$]	8.17	8.23		9.32		7.15
[$^4J(H_bCCCH_d)$]	3.41	3.36		3.34		3.38
[$^3J(H_bCCH_e)$]				1.58		
$H_{b'}$	4.07	3.71		4.18		4.03
[$^2J(H_{b'}CH_b)$]	10.78	10.77		10.65		10.70
[$^3J(H_{b'}COP)$]	9.76	9.82		10.15		10.49
[$^3J(H_{b'}CCH_e)$]				3.22		

Table 1. Continued

Compounds	$\underline{\text{21c}}^{b}$	$\underline{\text{21d}}^{b}$	$\underline{\text{22}}^{b}$	$\underline{\text{23a}}^{b}$	$\underline{\text{23b}}^{b}$	$\underline{\text{23c}}^{b}$
H_c	4.26	3.87		4.05		4.09
$[^2J(H_cCH_{c'})]$	11.29	11.74		11.35		11.49
$[^3J(H_cCOP)]$	3.57	3.43		26.18		3.30
$[^3J(H_cCCH_f)]$				5.56		
$H_{c'}$	4.29	3.98		3.88		4.12
$[^2J(H_{c'}CH_c)]$	11.29	11.74		11.35		11.49
$[^3J(H_{c'}COP)]$	8.20	7.98		9.66		8.79
$[^3J(H_{c'}CCH_f)]$						
H_d	4.11	3.77		3.89		3.97
$[^2J(H_dCH_{d'})]$	10.55	10.81		10.60		10.70
$[^3J(H_dCOP)]$	10.30	10.81		8.58		10.61
$[^4J(H_dCCCH_b)]$	3.41	3.36		3.34		3.38
$[^3J(H_dCCH_e)]$				3.34		
$H_{d'}$	3.96	3.79		4.31		3.86
$[^2J(H_{d'}CH_d)]$	10.55	10.81		10.60		10.70
$[^3J(H_{d'}COP)]$	6.63	6.81		1.94		6.53
$[^3J(H_{d'}CCH_e)]$				3.43		

Table 1. Continued

Compounds	21c^b	21d^b	22^b	23a^b	23b^b	23c^b
H_e				1.92		
$[^3J(H_eCCH_f)]$						
$[^3J(H_eCCH_b)]$				1.58		
$[^3J(H_eCCH_{b'})]$				3.22		
$[^3J(H_eCCH_d)]$				3.34		
$[^3J(H_eCCH_{d'})]$				3.43		
H_f				1.71		
$[^3J(H_fCCH_e)]$						
$[^3J(H_fCCH_a)]$				6.57		
$[^3J(H_fCCH_{a'})]$				6.62		
$[^3J(H_fCCH_c)]$				5.56		
$[^3J(H_fCCH_{c'})]$				9.66		
H						
$[^3J(HOCH_a)]$						
$[^3J(HOCH_{a'})]$						
ring	1.98m	2.00m			2.23m	2.17m

Table 1. Continued

Compound	$\underline{24}^{d}$	$\underline{25a}^{d}$	$\underline{25b}^{d}$	$\underline{25c}^{d}$	$\underline{25d}^{d}$	$\underline{25e}^{d}$
H_a		3.49	3.65	4.19	3.57	3.52
[$^2J(H_aCH_{a'})$]		11.32	10.65	10.59	10.66	10.31
[$^3J(H_aCOH)$]						
[$^3J(H_aCCH_f)$]		6.25				
$H_{a'}$		3.42	4.31	4.27	3.75	3.91
[$^2J(H_{a'}CH_a)$]		11.32	10.65	10.59	10.66	10.31
[$^3J(H_{a'}COH)$]						
[$^3J(H_{a'}CCH_f)$]		6.76				
H_b		4.15	4.82	5.24	4.54	4.32
[$^2J(H_bCH_{b'})$]		10.14	10.71	10.61	10.67	10.55
[$^3J(H_bCOP)$]		9.43	9.24	5.89	7.21	7.9
[$^4J(H_bCCCH_d)$]		3.30	3.60	3.46	3.48	3.51
[$^3J(H_bCCH_e)$]		1.61				
$H_{b'}$	4.10	4.08	4.15	4.39	3.91	3.95
[$^2J(H_{b'}CH_b)$]		12.00	11.84	11.50	11.83	11.82
[$^3J(H_{b'}COP)$]	15.38	26.71	22.51	3.29	3.29	3.35
[$^3J(H_{b'}CCH_e)$]	6.09	5.54				

$^{d}CD_2Cl_2$.

Table 1. Continued

Compound	$\underline{24}^{d}$	$\underline{25a}^{d}$	$\underline{25b}^{d}$	$\underline{25c}^{d}$	$\underline{25d}^{d}$	$\underline{25e}^{d}$
H_{c}	4.10	4.08	4.15	4.39	3.91	3.95
$[^{2}J(H_{c}CH_{c}')]$		12.00	11.84	11.50	11.83	11.82
$[^{3}J(H_{c}COP)]$	15.38	26.71	22.51	3.29	3.29	3.35
$[^{3}J(H_{c}CCH_{f})]$	6.09	5.54				
$H_{c'}$		3.96	4.22	4.48	4.20	4.07
$[^{2}J(H_{c'}CH_{c})]$		12.00	11.84	11.50	11.83	11.82
$[^{3}J(H_{c'}COP)]$		9.63	8.92	8.75	25.33	27.36
$[^{3}J(H_{c'}CCH_{f})]$		9.85				
H_{d}	4.47	4.53	3.96	4.46	4.11	3.89
$[^{2}J(H_{d}CH_{d'})]$	9.73	9.70	10.46	10.69	10.71	11.22
$[^{3}J(H_{d}COP)]$	6.50	8.57	10.46	10.69	10.71	11.22
$[^{4}J(H_{d}CCCH_{b})]$		3.30	3.60	3.46	3.48	3.51
$[^{3}J(H_{d}CCH_{e})]$	2.77	3.34				
$H_{d'}$	4.21	4.61	3.99	4.60	4.23	4.12
$[^{2}J(H_{d'}CH_{d})]$	9.73	9.70	10.46	10.69	10.71	11.22
$[^{3}J(H_{d'}COP)]$	6.69	1.92	5.97	6.19	6.83	6.83
$[^{3}J(H_{d'}CCH_{e})]$	2.11	3.42				

Table 1. Continued

Compound	24^d	$25a^d$	$25b^d$	$25c^d$	$25d^d$	$25e^d$
H_e	2.37	2.43				
$[{}^3J(H_eCCH_f)]$	4.67					
$[{}^3J(H_eCCH_b)]$		1.61				
$[{}^3J(H_eCCH_{b'})]$		3.18				
$[{}^3J(H_eCCH_d)]$	2.77	3.34				
$[{}^3J(H_eCCH_{d'})]$	2.11	3.42				
H_f	2.25	2.36				
$[{}^3J(H_fCCH_e)]$	4.67					
$[{}^3J(H_fCCH_a)]$		6.25				
$[{}^3J(H_fCCH_{a'})]$		6.76				
$[{}^3J(H_fCCH_c)]$	6.09	5.54				
$[{}^3J(H_fCCH_{c'})]$		9.85				
H						
$[{}^3J(HOCH_a)]$						
$[{}^3J(HOCH_{a'})]$						
ring			2.29m	2.33m	2.10m	2.19m
Cp	5.61	5.65	5.64	5.65	5.64	5.61

Table 1. Continued

Compound	26[b]	27a[b]	27b[b]	27c[b]	27d[b]	27e[b]
H_a		3.59	3.42	4.20	3.58	3.51
$[{}^2J(H_aCH_{a'})]$		11.09	10.62	10.60	10.69	10.35
$[{}^3J(H_aCOH)]$						
$[{}^3J(H_aCCH_f)]$		6.49				
$H_{a'}$		3.53	4.07	4.31	3.76	3.83
$[{}^2J(H_{a'}CH_a)]$		11.09	10.62	10.60	10.69	10.35
$[{}^3J(H_{a'}COH)]$						
$[{}^3J(H_{a'}CCH_f)]$		6.74				
H_b		4.23	4.58	5.19	4.58	4.29
$[{}^2J(H_bCH_{b'})]$		10.24	10.68	10.61	10.70	10.60
$[{}^3J(H_bCOP)]$		9.26	9.32	5.15	7.23	7.20
$[{}^4J(H_bCCCH_d)]$		3.32	3.51	3.40	3.38	3.46
$[{}^3J(H_bCCH_e)]$		1.62				
$H_{b'}$		4.57	3.82	4.72	4.26	3.71
$[{}^2J(H_{b'}CH_b)]$		10.24	10.68	10.61	10.70	10.60
$[{}^3J(H_{b'}COP)]$		10.24	10.68	10.61	10.11	10.00
$[{}^3J(H_{b'}CCH_e)]$		3.20				

Table 1. Continued

Compound	26[b]	27a[b]	27b[b]	27c[b]	27d[b]	27e[b]
H_c	3.96	4.21	3.95	4.42	3.95	3.86
$[^2J(H_cCH_{c'})]$		11.86	11.83	11.68	11.83	11.83
$[^3J(H_cCOP)]$	12.92	25.60	25.27	3.15	3.19	3.20
$[^3J(H_cCCH_f)]$		5.48				
$H_{c'}$		4.02	4.01	4.49	4.25	4.03
$[^2J(H_{c'}CH_c)]$		11.86	11.83	11.68	11.83	11.83
$[^3J(H_{c'}COP)]$		9.75	8.51	8.69	25.87	25.51
$[^3J(H_{c'}CCH_f)]$		9.85				
H_d		4.57	3.72	4.45	4.07	3.79
$[^2J(H_dCH_{d'})]$		9.76	10.48	10.70	10.74	11.17
$[^3J(H_dCOP)]$		8.61	10.48	10.70	10.74	11.17
$[^4J(H_dCCCH_b)]$		3.32	3.51	3.40	3.38	3.46
$[^3J(H_dCCH_e)]$		3.32				
$H_{d'}$		4.66	3.96	4.56	4.26	3.84
$[^2J(H_{d'}CH_d)]$		9.76	10.48	10.74	10.74	11.17
$[^3J(H_{d'}COP)]$		1.89	6.01	6.12	6.73	6.79
$[^3J(H_{d'}CCH_e)]$		3.39				

Table 1. Continued

Compound	26[b]	27a[b]	27b[b]	27c[b]	27d[b]	27e[b]
H_e		2.62				
$[^3J(H_eCCH_f)]$						
$[^3J(H_eCCH_b)]$		1.62				
$[^3J(H_eCCH_{b'})]$		3.20				
$[^3J(H_eCCH_d)]$		3.32				
$[^3J(H_eCCH_{d'})]$		3.39				
H_f		2.40				
$[^3J(H_fCCH_e)]$						
$[^3J(H_fCCH_a)]$		6.49				
$[^3J(H_fCCH_{a'})]$		6.74				
$[^3J(H_fCCH_c)]$		5.48				
$[^3J(H_fCCH_{c'})]$		9.85				
H						
$[^3J(HOCH_a)]$						
$[^3J(HOCH_{a'})]$						
ring			2.32m	2.34m	2.01m	2.16m
Cp	5.25	5.24	5.22	5.24	5.25	5.29
Me	1.25					

Table 1. Continued

Compound	$\underline{28}^b$	$\underline{29a}^b$	$\underline{29b}^b$	$\underline{29c}^b$	$\underline{29d}^b$	$\underline{29e}^b$
H_a		4.48	3.92m^c	4.19	3.61	3.78m^c
$[^2J(H_aCH_{a'})]$		11.09		10.60	10.65	
$[^3J(H_aCOH)]$						
$[^3J(H_aCCH_f)]$		5.99				
$H_{a'}$		4.05		4.22	4.28	
$[^2J(H_{a'}CH_a)]$		11.09		10.60	10.65	
$[^3J(H_{a'}COH)]$						
$[^3J(H_{a'}CCH_f)]$		1.74				
H_b		4.52		5.04	4.76	
$[^2J(H_bCH_{b'})]$		10.23		10.69	10.73	
$[^3J(H_bCOP)]$		9.59		5.75	7.25	
$[^4J(H_bCCCH_d)]$		3.34		3.40	3.43	
$[^3J(H_bCCH_e)]$		1.74				
$H_{b'}$		3.97		4.70	3.93	
$[^2J(H_{b'}CH_b)]$		10.23		10.69	10.73	
$[^3J(H_{b'}COP)]$		10.23		10.69	10.73	
$[^3J(H_{b'}CCH_e)]$		3.21				

Table 1. Continued

Compound	$\underline{28}^{b}$	$\underline{29a}^{b}$	$\underline{29b}^{b}$	$\underline{29c}^{b}$	$\underline{29d}^{b}$	$\underline{29e}^{b}$
H_c	4.14	4.06		4.35	4.15	
$[^2J(H_cCH_{c'})]$		11.82		11.46	11.80	
$[^3J(H_cCOP)]$	6.33	25.91				
$[^3J(H_cCCH_f)]$	16.02	5.54				
$H_{c'}$		4.11		4.39	4.28	
$[^2J(H_{c'}CH_c)]$		11.82		11.46	11.80	
$[^3J(H_{c'}COP)]$		9.57		3.31	3.29	
$[^3J(H_{c'}CCH_f)]$		9.69				
H_d	4.51	3.95		4.36	3.92	
$[^2J(H_dCH_{d'})]$	9.85	10.21		10.76	10.78	
$[^3J(H_dCOP)]$	6.53	10.21		10.29	10.78	
$[^4J(H_dCCCH_b)]$		3.34				
$[^3J(H_dCCH_e)]$	2.81	3.34				
$H_{d'}$	4.37	3.81		4.51	3.99	
$[^2J(H_{d'}CH_d)]$	9.85	10.21		10.76	10.78	
$[^3J(H_{d'}COP)]$	6.74	2.00		6.32	6.91	
$[^3J(H_{d'}CCH_e)]$	2.20	3.41				

Table 1. Continued

Compound	28^b	29a^b	29b^b	29c^b	29d^b	29e^b
H_e	2.33	2.47				
[$^3J(H_eCCH_f)$]	4.61					
[$^3J(H_eCCH_b)$]		1.74				
[$^3J(H_eCCH_{b'})$]		3.21				
[$^3J(H_eCCH_d)$]	2.81	3.34				
[$^3J(H_eCCH_{d'})$]	2.20	3.41				
H_f	2.08	2.31				
[$^3J(H_fCCH_e)$]	4.61					
[$^3J(H_fCCH_a)$]		5.99				
[$^3J(H_fCCH_{a'})$]		6.21				
[$^3J(H_fCCH_c)$]	16.02	5.54				
[$^3J(H_fCCH_{c'})$]		9.69				
H						
[$^3J(HOCH_a)$]						
[$^3J(HOCH_{a'})$]						
ring			2.26m	2.31m	2.01m	2.24m

Table 2. ^{13}C NMR spectral data (chemical shifts (ppm) and coupling constants (Hz)) for compounds 18, 20-29

Compound	18a[a]	18b[a]	18c[a]
Carbon			
a	62.611	62.94	60.682
b	70.409	73.16	73.804
c	65.546	69.53	68.720
d	64.195	68.18	66.826
e	38.262	46.23	50.186
f	49.688	49.16	56.430
g		22.36	34.564
h		22.25	30.933
i			21.200
j			

---

[a] DMSO.

[b] $CDCl_3$.

[c] CD_2Cl_2.

Table 2. Continued

	20[b]	21a[b]	21b[b]	21c[b]	21d[b]	22[b]
Carbon						
a		61.22	62.18	63.14	61.01	62.29
b		70.09	72.93	73.11	73.74	71.43
c	63.62	65.86	66.82	69.05	68.49	65.85
d	62.17	64.38	64.41	67.93	66.82	64.79
e	35.86	38.06	42.18	45.99	49.91	39.27
f	48.29	45.36	49.21	55.89	46.59	
g			22.15	22.21	36.87	
h				21.94	30.87	
i					21.63	
j						

Table 2. Continued

	23a[b]	23b[b]	23c[b]
Carbon			
a	60.87	61.65	63.20
b	69.92	72.11	73.75
c	64.84	66.35	69.80
d	63.28	64.77	67.37
e	37.82	42.91	45.29
f	48.00	45.05	49.17
g		22.42	22.62
h			22.91
i			
j			

Table 2. Continued

	24^c	25a^c	25b^c	25c^c	25d^c	25e^c
Carbon						
a		61.86	62.57	62.09	61.68	62.29
b		70.02	72.75	72.17	73.21	71.43
c	63.94	65.13	66.20	68.66	68.53	65.85
d	62.81	64.80	64.12	67.15	66.62	64.79
e	36.77	38.41	42.30	44.94	49.19	42.31
f	48.43	47.43	45.55	49.16	54.36	44.22
g			23.01	22.58	34.34	34.28
h				22.28	30.04	29.12
i					22.40	21.25
j						20.77

Table 2. Continued

	26[b]	27a[b]	27b[b]	27c[b]	27d[b]	27c[b]
Carbon						
a		61.06	62.32	62.24	61.26	62.07
b		71.42	73.43	72.52	73.51	72.48
c	63.19	66.35	66.36	68.20	68.23	65.94
d	41.88	64.99	64.26	66.01	66.29	64.87
e		39.91	43.00	44.74	49.63	42.73
f		48.48	45.59	49.87	55.13	45.25
g	17.53		22.84	22.31	35.33	34.53
h				21.08	30.02	30.76
i					22.27	22.69
j						22.37

Table 2. Continued

	28[b]	29a[b]	29b[b]	29c[b]	29d[b]	29e[b]
Carbon						
a		61.25	62.39	62.07	63.49	62.51
b		70.64	72.21	73.53	73.54	72.13
c	64.12	65.13	66.84	68.92	68.39	65.92
d	62.55	64.18	64.91	66.26	67.48	64.32
e	36.01	39.03	42.49	45.58	49.42	43.77
f	48.31	47.51	45.32	49.14	55.71	45.10
g			22.71	22.37	35.06	34.64
h				21.98	31.18	29.72
i					22.95	22.11
j						22.30

Table 3. ^{31}PNMR spectral data (chemical shifts (ppm) and coupling constants (Hz)) for compounds 20-29

Compound		a	b	c	d	e
20[a]	128					
[J(P-W)]	[417]					
21a-d[a]		129	130	131	130	
[J(P-W)]		[419]	[401]	[405]	[413]	
22[a]	157					
23a-c[a]		165	165	167		
24[b]	162					
25a-e[b]		159	160	161	162	160
26a-e[a]		136	138	137	140	137
27a-e[a]		136	138	137	140	137
28[a]	157					
29a-e[a]		165	163	159	162	163

[a] $CDCl_3$.

[b] Acetonitrile.

Table 4. Crystallographic data for (26) and (27)

Compound	26	27d
mol. wt	525.9	596.03
Space group	$P2_1/n$	$P2_1/c$
a, Å	9.474(2)	7.758(3)
b, Å	8.346(3)	19.327(4)
c, Å	19.416(5)	11.958(2)
b,deg	102.81(2)	97.28(2)
Vol, $Å^3$	1497(1)	177((1)
d_{calcd}, g/cm^3	2.33	2.23
Z	4	4
Lambda	MoK α	MoKα
mu,cm^{-1}	53.26	45.0
cryst. size, mm	0.20x0.20x0.22	0.20x0.20x0.15
refl. coll.	±h, ± k, ± l	±h, ± K, ± l
no. of refl. coll.	3413	2323
unique data with $F^2>2^{\sigma}(F^2)$	2420	1419
range, deg.	0-55	0-45
final R, %	2.85	3.41
final Rw, %	3.74	4.29
GOF[a]	0.913	0.929
no. of var.	154	168
temp., °C	22±1	22±1

Table 4. Continued

Compound	26	27d
mode	ω-20	ω-scans
max. trans factor	1.287	1.0
min. trans factor	0.696	0.869

[a] The goodness of fit is defined as $[w(F_o - F_c)^2/(n_o-n_u)]1/2$, where n_o and n_u denote the number of data and variables, respectively.

Table 5. Positional parameters for CpCo[17]I_2, 26, and their estimated standard deviations[a]

Atom	x	y	z	B($Å^2$)
I(1)[a]	0.2047(1)	0.17365(4)	0.17052(6)	5.35(2)
I(2)	-0.17097(9)	0.08977(4)	0.29632(7)	4.52(2)
Co	0.1588(2)	0.10230(7)	0.3453(1)	3.12(3)
P	0.2036(4)	0.0085(1)	0.2584(2)	3.10(7)
O(1)	0.105(1)	-0.0034(3)	0.1353(6)	4.1(2)
O(2)	0.153(1)	-0.0578(4)	0.3262(6)	4.4(2)
O(3)	0.4027(9)	-0.0024(4)	0.2454(7)	4.4(2)
O(4)	0.674(1)	-0.1617(6)	0.222(1)	9.4(4)
C(1)	0.085(2)	-0.0728(7)	0.088(1)	7.5(5)
C(2)	0.137(2)	-0.1257(6)	0.273(1)	5.7(4)
C(3)	0.452(2)	-0.0428(6)	0.153(1)	5.5(4)
C(4)	0.492(2)	-0.1609(8)	0.248(1)	7.8(5)
C(5)	0.199(2)	-0.1273(7)	0.162(1)	5.6(4)
C(6)	0.385(2)	-0.1140(7)	0.147(1)	5.5(4)
C(7)	0.407(2)	-0.1480(7)	0.030(1)	6.3(4)
C(8)	0.287(2)	-0.2095(8)	0.021(1)	7.6(5)
C(9)	0.153(2)	-0.1989(6)	0.106(1)	5.7(4)

---

[a] Starred atoms were refined isotropically. Anisotropically refined atoms are given in the form of the isotropic equivalent displacement parameter defined as: (4/3) * [a^2*B(1,1) + b^2B(2,2) + c^2*B(3,3) + ab(cos gamma)*B(1,2) + ac(cos beta)*B(1,3) = bc(cos alpha)*B(2,3)].

Table 5. Continued

Atom	x	y	z	B(Å^2)
C(21)	0.278(1)	0.1805(3)	0.4480(8)	4.8(3)*
C(22)	0.130(1)	0.1565(3)	0.4954(8)	4.4(2)*
C(23)	0.152(1)	0.0845(3)	0.5168(8)	4.2(2)*
C(24)	0.313(1)	0.0641(3)	0.4828(8)	5.1(3)*
C(25)	0.391(1)	0.1233(3)	0.4402(8)	5.4(3)*

Table 6. Positional parameters for CpCo(11d)I_2, 27d, and their estimated standard deviations[a]

Atom	x	y	z	B($Å^2$)
I(1)	-0.04076(4)	0.14468(4)	0.36216(2)	3.732(6)
I(2)	0.23066(4)	-0.18899(5)	0.43169(2)	4.118(7)
Co	-0.03433(6)	-0.16287(7)	0.36324(3)	2.60(1)
P	0.0229(1)	-0.1671(1)	0.26264(5)	2.44(2)
O(1)	0.0417(4)	-0.3424(4)	0.2338(2)	4.08(7)
O(2)	-0.0962(3)	-0.0926(4)	0.2005(2)	3.60(6)
O(3)	0.1659(3)	-0.0796(5)	0.2547(2)	4.56(8)
C(1)	0.0687(6)	-0.3469(6)	0.1618(3)	4.4(1)
C(2)	-0.0605(5)	-0.0934(8)	0.1315(2)	4.5(1)
C(3)	0.1998(6)	-0.0912(9)	0.1851(3)	5.4(1)
C(4)	0.080(5)	-0.1797(6)	0.1341(2)	3.03(8)
C(5)	0.1156(6)	-0.1873(8)	0.0614(2)	4.3(1)
C(21)	-0.2543(6)	-0.1854(8)	0.3498(4)	5.9(1)
C(22)	-0.1958(6)	-0.3226(7)	0.3246(3)	5.1(1)
C(23)	-0.0965(7)	-0.3896(6)	0.3813(3)	5.2(1)
C(24)	-0.0990(7)	-0.2963(8)	0.4413(3)	5.7(1)
C(25)	-0.1934(6)	-0.1718(7)	0.4224(3)	5.4(1)

---

[a] Starred atoms were used in calculated positions for structure factor calculations only.

Anisotropically refined atoms are given in the form of the isotropic equivalent displacement parameter defined as: $(4/3) * [a^2*B(1,1) + b^2B(2,2) + c^2*B(3,3) + ab(\cos \gamma)*B(1,2) + ac(\cos \beta)*B(1,3) = bc(\cos \alpha)*B(2,3)]$.

Table 6. Continued

Atom	x	y	z	B(Å^2)
H(1)	-0.0090	-0.4009	0.1313	5*
H(2)	0.1564	-0.4028	0.1627	5*
H(3)	-0.0520	0.0139	0.1167	5*
H(4)	-0.1354	-0.1459	0.0987	5*
H(5)	0.2884	-0.1474	0.1891	7*
H(6)	0.2091	0.0136	0.1675	7*
H(7)	0.0405	-0.2429	0.0298	5*
H(8)	0.1233	-0.0817	0.0443	5*
H(9)	0.2046	-0.2421	0.0645	5*
H(10)	-0.3230	-0.1144	0.3235	7*
H(11)	-0.2194	-0.3623	0.2775	6*
H(12)	-0.0379	-0.4813	0.3796	6*
H(13)	-0.0438	-0.3166	0.4876	7*
H(14)	-0.2140	-0.0904	0.4529	7*

Table 7. Selected bond distances and angles in CpCo(17)I$_2$, 26[a]

Bond Distances (Å)

Co	I(1)	2.5676(7)	O(2)	C(2)	1.452(6)
Co	I(2)	2.5762(6)	O(3)	C(3)	1.459(7)
Co	P	2.140(1)	C(1)	O(4)	1.508(7)
Co	C(21)	2.051(5)	C(2)	C(4)	1.510(7)
Co	C(22)	2.042(6)	C(3)	C(4)	1.518(7)
Co	C(23)	2.035(6)	C(4)	C(5)	1.522(7)
Co	C(24)	2.080(6)	C(21)	C(22)	1.407(9)
Co	C(25)	2.089(6)	C(21)	C(25)	1.404(8)
P	O(1)	1.590(3)	C(22)	C(23)	1.497(8)
P	O(2)	1.585(3)	C(23)	C(24)	1.406(9)
P	O(3)	1.577(4)	C(24)	C(25)	1.367(9)

Bond Angles (°)

I(1)	Co	I(2)	96.17(2)	O(2)	C(2)	C(4)	111.0(4)
I(1)	Co	P	91.11(4)	O(3)	C(3)	C(4)	110.6(4)
I(2)	Co	P	93.12(3)	C(1)	C(4)	C(2)	108.5(4)
Co	P	O(1)	114.0(1)	C(1)	C(4)	C(3)	108.8(4)
Co	P	O(2)	114.0(1)	C(1)	C(4)	C(5)	109.9(4)
Co	P	O(3)	118.6(1)	C(2)	C(4)	C(3)	108.3(4)
O(1)	P	O(2)	102.1(2)	C(2)	C(4)	C(5)	111.2(4)

---

[a] Numbers in parentheses are estimated standard deviations in the least significant digits.

Table 7. Continued

Bond Angles (°)							
O(1)	P	O(3)	103.0(2)	C(3)	C(4)	C(5)	110.0(4)
O(2)	P	O(3)	103.1(2)	C(22)	C(21)	C(25)	108.0(5)
P	O(1)	C(1)	114.4(3)	C(21)	C(22)	C(23)	107.4(5)
P	O(2)	C(2)	115.3(3)	C(22)	C(23)	C(24)	107.4(5)
P	O(3)	C(3)	115.5(3)	C(23)	C(24)	C(25)	109.2(5)
O(1)	C(1)	C(4)	110.9(4)	C(21)	C(25)	C(24)	107.8(5)

Table 8. Selected bond distances and angles in CpCo(11d)I_2, 27d[a]

Bond Distances (Å)

I(1)	Co	2.566(2)	C(1)	C(5)	1.57(2)
I(2)	Co	2.563(2)	C(2)	C(5)	1.47(2)
Co	P	2.140(3)	C(3)	C(6)	1.47(2)
Co	C(21)	2.089(7)	C(4)	C(6)	1.64(2)
Co	C(22)	2.113(9)	C(5)	C(6)	1.50(2)
Co	C(23)	2.087(9)	C(5)	C(9)	1.56(2)
Co	C(24)	2.046(8)	C(6)	C(7)	1.58(2)
Co	C(25)	2.047(8)	C(7)	C(8)	1.51(2)
P	O(1)	1.589(7)	C(8)	C(9)	1.56(2)
P	O(2)	1.591(8)	C(21)	C(22)	1.42(1)
P	O(3)	1.586(8)	C(21)	C(25)	1.42(1)
O(1)	C(1)	1.45(1)	C(22)	C(23)	1.420(9)
O(2)	C(2)	1.45(1)	C(23)	C(24)	1.42(1)
O(3)	C(3)	1.45(2)	C(24)	C(25)	1.42(1)
O(4)	C(4)	1.48(2)			

Bond Angles (°)

I(1)	Co	I(2)	95.86(5)	C(1)	C(5)	C(9)	106.(1)
I(1)	Co	P	90.70(9)	C(2)	C(5)	C(6)	122.(1)
I(2)	Co	P	91.59(9)	C(2)	C(5)	C(9)	109.(1)

---

[a] Numbers in parentheses are estimated standard deviations in the least significant digits.

Table 8. Continued

Bond Angles (°)

Co	P	O(1)	118.9(2)	C(6)	C(5)	C(9)	106.(1)
Co	P	O(2)	111.7(3)	C(3)	C(6)	C(4)	110.(1)
Co	P	O(3)	112.3(3)	C(3)	C(6)	C(5)	120.(1)
O(1)	P	O(2)	103.6(4)	C(3)	C(6)	C(7)	111.(1)
O(1)	P	O(3)	104.6(5)	C(4)	C(6)	C(5)	103.(1)
O(2)	P	O(3)	104.5(4)	C(4)	C(6)	C(7)	109.(1)
P	O(1)	C(1)	120.3(8)	C(5)	C(6)	C(7)	104.(1)
P	O(2)	C(2)	121.1(7)	C(6)	C(7)	C(8)	105.(1)
P	O(3)	C(3)	120.2(7)	C(7)	C(8)	C(9)	108.(1)
O(1)	C(1)	C(5)	112.(1)	C(5)	C(9)	C(8)	105.(1)
O(2)	C(2)	C(5)	113.(1)	C(22)	C(21)	C(25)	108.0(6)
O(3)	C(3)	C(6)	114.(1)	C(21)	C(22)	C(23)	108.0(8)
O(4)	C(4)	C(6)	105.(1)	C(22)	C(23)	C(24)	108.0(8)
C(1)	C(5)	C(2)	106.(1)	C(23)	C(24)	C(25)	108.0(6)
C(1)	C(5)	C(6)	108.(1)	C(21)	C(25)	C(24)	108.0(7)

Table 9. Selected distances and angles in 34[a], 35[b] and 36[c]

compound	34	35	36
Distances (Å)			
P-O(1)	1.576(17)	1.613(4)	1.54(2)
P-O(2)	1.567(12)	1.616(5)	1.555(4)
P-O(3)	1.567(17)	1.616(5)	1.663(6)
P-O(4)	1.464(16)		
O(1)-C(1)	1.456(23)	1.446(7)	1.45(2)
O(2)-C(2)	1.453(17)	1.454(8)	1.46(1)
O(3)-C(3)	1.453(17)	1.440(7)	1.402(9)
Co-P			2.160(1)
Co-I(1)			2.5704(6)
Co-I(2)			2.5717(6)
Angles (°)			
O(1)-P-O(2)	103.2(6)	100.8(2)	108.5(7)
O(1)-P-O(3)	103.2(6)	99.9(2)	97.4(3)
O(2)-P-O(3)	104.2(6)	99.6(3)	97.4(3)
P-O(1)-C(1)	115.2(12)	117.6(3)	125.(1)
P-O(2)-C(2)	115.3(9)	117.2(4)	124.((4)
P-O(3)-C(3)	115.3(9)	117.7(3)	119.4(5)
P-Co-I(1)			93.18(4)
P-Co-I(2)			92.43(4)
I(1)-Co-I(2)			96.26(2)

[a] See reference 31.

[b] See reference 32.

[c] See reference 33.

Table 10. Selected distances and angles in 12d[a]

Bond Distances (Å)			
P-O(1)	1.5448(29)	C(2)-C(5)	1.5130(5)
P-O(2)	1.5571(26)	C(3)-C(6)	1.5123(50)
P-O(3)	1.5605(27)	C(4)-C(6)	1.5390(49)
P-O(5)	1.4599(30)	C(5)-C(6)	1.5630(47)
O(1)-C(1)	1.4626(46)	C(5)-C(9)	1.5580(52)
O(2)-C(2)	1.4719(45)	C(6)-C(7)	1.5422(52)
O(3)-C(3)	1.4652(49)	C(7)-C(8)	1.5220(59)
O(4)-C(4)	1.4220(48)	C(8)-C(9)	1.5196(66)
C(1)-C(5)	1.5242(53)		

Bond Angles (°)			
O(1)-P-O(2)	105.87(14)	C(6)-C(5)-C(9)	103.68(28)
O(1)-P-O(3)	107.12(15)	C(3)-C(6)-C(4)	110.11(29)
O(2)-P-O(3)	106.36(15)	C(3)-C(6)-C(5)	115.12(29)
P-O(1)-C(1)	121.09(23)	C(4)-C(6)-C(5)	110.56(27)
P-O(2)-C(2)	119.46(21)	C(5)-C(6)-C(7)	102.25(27)
P-O(3)-C(3)	119.42(22)	C(6)-C(7)-C(8)	104.65(32)
O(1)-C(1)-C(5)	110.97(29)	C(7)-C(8)-C(9)	106.38(34)
O(2)-C(2)-C(5)	112.48(29)	C(5)-C(9)-C(8)	108.28(31)
O(3)-C(3)-C(6)	113.32(30)		

---

[a] See reference 34.

Table 10. Continued

Bond Angles (°)	
O(4)-C(4)-C(6)	109.89(30)
C(1)-C(5)-C(2)	107.71(29)
C(1)-C(5)-C(6)	115.24(28)
C(2)-C(5)-C(6)	112.35(28)

REFERENCES

1. Holmes, R. R. J. Am. Chem. Soc. **1975**, 97, 5379.
2. Hamerlink, J. H. H.; Schipper, P.; Buck, H. M. J. Am. Chem. Soc. **1983**, 105, 385.
3. Berry, R. S. J. Chem. Phys. **1960**, 32, 933.
4. a) Day, R. O.; Holmes, R. R. Inorg. Chem. **1983**, 22, 1771.
    b) Clark, T. E.; Day, R. O.; Holmes, R. R. Inorg. Chem. **1979**, 18, 1668.
    c) Clark, T. E.; Day, R. O.; Holmes, R. R. Inorg. Chem. **1979**, 18, 1668.
    d) Althoff, W.; Day, R. O; Brown, R. K.; Holmes, R. R. Inorg. Chem. **1977**, 99, 3332.
    e) Holmes, R. R. Day, R. O.; Sau, A. C. Organometallics **1985**, 4, 714.
    f) Poutasse, C. A.; Day, R. O.; Holmes, J. M.; Holmes, R. R. Organometallics **1985**, 4, 704.
    g) Holmes, R. R.; Day, R. O.; Chandreasekhar, V.; Holmes, J. M. Inorg. Chem. **1987**, 26, 163.
    h) Holmes, R. R.; Day, R. O.; Chandrasekhar, V.; Holmes, J. M. Inorg. Chem. **1987**, 26, 157.
5. Granoth, I.; Martin, J. C. J. Am. Chem. Soc. **1978**, 100, 7434.
6. a) Garrigues, B.; Koenig, M.; Munoz, A. Tetrahedron Lett. **1979**, 43, 4205.

b) Garrigues, B.; Boyer, D.; Munoz, A. *Can. J. Chem.* **1984**, *62*, 2170.

c) Garrigues, B.; Munoz, A. *Can. J. Chem.* **1984**, *62*, 2179.

7. Schomburg, D.; Storzer, W.; Bohlen, R.; Kuhn, W.; Roschenthaler, G. *Chem. Ber.* **1983**, *116*, 3301.

8. Lattman, M.; Olmstead, M. M.; Power, P. O.; Rankin, D. W. H.; Robertson, H. E. *Inorg. Chem.* **1988**, *27*, 3012.

9. Gamayurova, V. S.; Niyazov, N. A. *J. Chem. Soc. U. S. S. R., Eng. Trans.* **1985**, *55*, 2210.

10. Lamande, L.; Munoz, A.; Garrigues, B. *Phosphorus and Sulfur* **1987**, *30*, 181.

11. Gamayurova, V. S.; Niyazov, N. A.; Khalitov, F. G.; Arkhipov, V. P. *J. Chem. Soc. U. S. S. R., Eng. Trans.* **1987**, *57*, 1567.

12. a) Weinges, K.; Klessing, K.; Kolb, R. *Chem. Ber.* **1973**, *106*, 2298.

    b) Buchta, E.; Kroeniger, A. *Chimica* **1968**, *22*, 430.

    c) Eberson, L. *Acta Chem. Scand.* **1958**, *12*, 731.

    d) Bailey, W. J.; Sorenson, W. R. *J. Am. Chem. Soc.* **1954**, *76*, 5421.

13. a) Bernard, D.; Laurenco, C.; Burgada, R. *J. Organomet. Chem.* **1973**, *47*, 113.

    b) Burgada, R. *Phosphorus and Sulfur* **1976**, *2*, 237.

c) Koenig, M.; Munoz, A.; Garrigues, B.; Wolf, R. Phosphorus and Sulfur **1979**, 6, 435.

d) Burgada, R.; Laurenco, C. J. Organomet. Chem. **1974**, 66, 255.

14. a) Bohlen, R.; Hacklin, H.; Heine, J.; Offerman, W.; Roschenthaler, G. Phosphorus and Sulfur **1986**, 27, 321.

b) Van Lier, J. J. C.; Hermans, R. J. M.; Buck, H. M. Phosphorus and Sulfur **1984**, 19, 173.

15. Davis, R. V. Synthetic Approaches to Rigid Spuare Pyramidal Pnictogens and Synthesis of New trinuclear Cobalt(II) Complexes, PhD dissertation, Iowa State University, Ames, IA, 1989; Section II.

16. Verkade, J. G.; Reynolds, L. T. J. Org. Chem. **1960**, 25, 663.

17. Petz, W. J. Organomet. Chem. **1977**, 125, C33.

18. Quick, M. H.; Angelici, R. J. "Inorg. Syn."; Shriver, D. F., Ed.; John Wiley & Sons: New York, New York, 1979; Vol. XIX, p. 160.

19. King, R. B. "Organometallic Synthesis"; King, R. B.; Eish, J. J., Eds.; Academic: New York, New York, 1965; Vol. E, p. 95.

20. Reger, D. L.; Coleman, C. J. Organomet. Chem. **1977**, 131, 153.

21. King, R. B. Inorg. Chem. **1966**, 5, 82.

22. Von Hirsch, H. Chem. Ber. **1967**, 100, 1289.

23. Schmidt, H.; Lensink, C.; Xi, S. K.; Verkade, J. G. Z. Anorg. Chem. in press.

24. Sheldrick, G. M. In "Computing in Crystallography"; Schenk, H.; Olthof-Hazekamp, R.; Van Koningsveld, H.; Bassi, G. C., Eds.; Delft University: Delft, 1978.

25. Cromer, D. T.; Weber, J. T. "International Tables for X-ray Crystallography"; Kynoch: Birmingham, England, 1974; Vol. IV.

26. "NMR and the Periodic Table"; Harris, R. K.; Mann, B. E.; Eds.; Academic: New York, New York, 1978.

27. Fluck, E.; Heckmann, G. In "Phosphorus-31 NMR Spectroscopy in Stereochemical Analysis"; Verkade, J. G.; Quin, L. D., Eds.; VCH: Deerfield Beach, Florida, 1987.

28. a) Lattman, M.; Anand, B. N.; Garrett, D. R.; Whitener, M. A. Inorg. Chem. Acta **1983**, 76, L139.
    b) Lattman, M.; Anand, B. N.; Chu, S. S. C.; Rosenstein, R. R. Phosphorus and Sulfur **1983**, 18, 303.

29. a) Lattman, M.; Chopra, S. K.; Cowley, A. H.; Arif, A. M. Organometallics **1986**, 5, 677.
    b) Lattman, M.; Burns, E. G.; Chopra, S. K.; Cowley, A. H.; Arif, A. M. Inorg. Chem. **1987**, 26, 1926.

c) Lattman, M.; Chopra, S. K.; Burns, E. G. *Phosphorus and Sulfur* **1987**, *30*, 185.

d) de Meester, P.; Lattman, M.; Chu S. S. C. *Acta Crystallogr., Sect. C. Cryst. Struct. Commun.* **1987**, *C43*, 162.

30. Verkade, J. G.; Coskran, K. J. in "Organic Phosphorus Compounds"; Kosolapoff, G. M.; Maier, L., Eds.; John Wiley & Sons: New York, New York, 1976; Vol. II.

31. Williams, J. L. *Chem. Ind.* **1957**, 235.

32. Nimrod, D. M.; Fitzwater, D. R.; Verkade, J. G. *J. Am. Chem. Soc.* **1968**, *90*, 2780.

33. Milbrath, D. S.; Verkade, J. G.; Kenyon, G. L.; Eargle, D. H. *J. Am. Chem. Soc.* **1978**, *100*, 3167.

34. Davis, R. V. Synthetic Approaches to Rigid Square Pyramidal Pnictogens and Synthesis of New Trinuclear Cobalt(II) Complexes, PhD dissertation, Iowa State University, Ames, IA, 1989; Section I.

GENERAL SUMMARY

This dissertation demonstrates that $CpCo[P(OMe)_3]I_2$ and $CpCo[P(O)(OMe)_2][P(OMe)_3]I$ undergo a novel decomposition forming the trinuclear complex $[CpCo[P(O)(OMe)_2]_2I]_2Co$. This compound can exist as either octahedral or tetrahedral cobalt(II) isomers, thus representing the first structurally-characterized example of true octahedral-tetrahedral isomerism of cobalt(II). Similar results are obtained for $[Cp^*Co[P(O)(OMe)_2]_2I]_2Co$.

The research described in this dissertation also shows that pnictogen derivatives of 1 form tricoordinate compounds containing pendant alcohol groups rather than pentacoordinate species. Heating these compounds in the presence of acid results in a rearrangement to phosphonate compounds containing cyclic ether functions. This is the first example of a rearrangement of phosphorus compounds in which ethers are formed. Further derivatization of the phosphorus in the derivatives of 1, which should make the pentacoordinate form more favorable, leads only to tetracoordinate species.

Finally, it has also been demonstrated that deprotonation of the above mentioned compounds, producing a nucleophilic RO^- group, results in no detectable change in the geometry about the phosphorus atom. In the case of the arsenic derivatives of 1, however, deprotonation yields fluxional anions in which the rate of exchange of the alkoxy arms is dependent on the carbocyclic ring present in the compound. Although no pentacoordinate species were isolated from the latter reactions, the transition state of the fluxional intermediate probably contains a square pyramidal geometry.

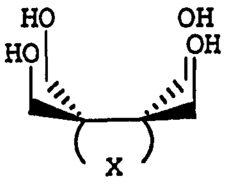

1

	X
1a	H_2
1b	CH_2
1c	$(CH_2)_2$
1d	$(CH_2)_3$
1e	$(CH_2)_4$